Doctoral thesis

Studies on electrochemical immobilization of Prussian blue on carbon fiber and the adsorption behavior of cesium ions with the adsorbent

(プルシアンブルーのカーボンファイバー上への電気化学的固定化
およびセシウムイオンの吸着挙動に関する研究)

Ayano Yamashita

Division of Environmental Materials Science
Graduate School of Environmental Science
Hokkaido University

2018

CONTENTS

Chapter 3

Chapter 4

Chapter 1

General Introduction

1.1. Pollutions with Cesium

By the nuclear tests conducted in the 1950s and 1960s and the accidents at the Chernobyl Nuclear Power Plant (CNPP) in 1986 and at the Fukushima Daiichi Nuclear Power Plant (FNPP) in 2011 due to the Great East Japan Earthquake, various radioactive substances were released into the environment. The main radionuclides include ^{134}Cs, ^{137}Cs, ^{131}I, ^{89}Sr and ^{90}Sr. Among them, the long-term effect of radioactive ^{137}Cs having a relatively long half-life of about 30.2 years is concerned. Cs is one of the major fission products and therefore was released in large quantities by the accidents of CNPP and FNPP [1-3]. In addition, Cs exists as a monovalent cation in water and then has high solubility and mobility [4,5]. Due to these characteristics, it is known that Cs^+ diffuses widely into the environment and adversely affects the environment and human health. The amount of radionuclide released into the atmosphere due to the accident of FNPP and CNPP is shown in Table 1. The radioactive Cs emission was estimated to be approximately 85 PBq in CNPP and 36.6 PBq at FNPP at a maximum by a number of studies.

Although Cs shows a high mobility in the aqueous environment, it is known to strongly interact with clay minerals having negative charges in the soil environment. The affinity of these clay minerals with Cs^+ is different depending on the composition and the components. Especially 2:1 layered mica clay minerals such as illite and vermiculite show the high affinity for Cs^+ [6,7]. At the same time, these clay minerals have the adsorption affinity for other monovalent cations such as K^+, NH_4^+, and Rb^+. From this characteristic, it was reported that a small amount of radioactive Cs^+

adsorbed in clay minerals was released into water by the ion exchange with NH_4^+ [8]. Therefore, the rapid removal of Cs^+ existing in the aqueous environments is necessary.

Table 1. The estimated amount of released radionuclides into atmosphere. [9-12]

Radionuclide	Half-life	Released amounts into atmosphere/PBq	
		Chernobyl	Fukushima Daiici
^{131}I	8.0 day	<1760	150-500
^{90}Sr	28.8 year	<10	0.09-0.9
^{134}Cs	2.1 year	<54	10-18
^{137}Cs	30.2 year	<85	6.1-36.6

(PBq: 10^{15} Bq)

1.2. Treatment method for Cs^+

After the FNPP accident, many kinds of the remediation methods have been attempted for decontamination of soil polluted with Cs, including physical methods and chemical methods using an adsorbents, phytoremediation, soil washing, and electrochemical method. Particularly, the physical methods such as topsoil stripping showed the high efficiency of 86 to 91% reduction rate of the radioactive Cs [13]. On the other hand, the decontamination processing of a plenty of collected topsoil is now a major issue in Fukushima area. For elution of Cs in the soil into an aqueous solution, the extraction with some reagents has been performed. Water, nitric acid, sulfuric acid, sodium hydroxide, organic acids, and ammonium salts were used as eluents [14,15].

However, the removal efficiency was greatly different depending on the soil type, and the high elution rate has not been obtained except under high temperature or pressure conditions. In addition, high level contaminated water with radionuclides has been generated still now near the nuclear plant due to the inflow of groundwater into the plant and the addition of a large amount of seawater to the nuclear reactor as a core coolant. In order to prevent the contaminated water from flowing into the soil and the ocean, the treatment system for the high level contaminated water was constructed immediately after the accident. This system consists of an oil separator, a radioactive material treatment system and a desalination system. Water containing radioactive species was passed through an adsorption device comprising of zeolite and ion exchange resin. Although this system allowed to treat a large amount of contaminated water, large scale equipment for pumping and piping is necessary. In addition, leakage of contaminated water due to corrosion of the pipe and clogging of the filter has occurred often.

Various studies have been conducted for the removal of Cs in radioactive wastes. Among them, solvent extraction and adsorption have been reported as a removal method of Cs^+ in aqueous solution [16-20]. The solvent extraction method could separate and concentrate Cs^+ from contaminated water by using calix-crown derivatives and crown ethers as extractants for Cs^+. In recent years, the separation technology of cesium with these extractants has been improved to enhance the selectivity for Cs^+ by improvement of synthesis method and extraction conditions. However, these solvent extraction methods require mixing organic solvents with

contaminated water vigorously. As a result, it is difficult to apply them directly to treat plenty volume of contamination water.

The adsorption method can concentrate Cs^+ in adsorbents having selective adsorption property. Zeolite and Prussian blue (PB) are widely used as an adsorbent for Cs^+. Zeolite is a type of clay mineral which can catch cations in the structure by the ion exchange mechanism. The selectivity for alkali metal and alkali earth metal ions is different from the type of zeolite. Especially, the mordenite type of zeolite has a highly selective adsorption property for Cs^+ and shows a high distribution coefficient even in the presence of coexisting cations [19]. PB is an inorganic coordination compound composed of iron and cyanide, and it is used for a long time as a pigment for blue color. This crystal structure is a cubic lattice shape, and it can selectively adsorb Cs^+ inside the lattice. The advantage of the removal method using these adsorbents is able to remove contaminants very quickly and at low cost without any special equipment. It is not easy and high cost to transfer a plenty of environmental water or contaminated wastewater to the treatment facilities. Therefore, in-situ treatment systems, which the treatment is carried out in the vicinity of the contaminated site, are required. Adsorption is one of the methods which satisfy the requirement.

1.3. Prussian blue and analogs

Prussian blue can be synthesized easily and it is known to maintain high Cs^+ adsorption ability even in the presence of other monovalent cations. Not only PB but also other hexacyanide complexes such as nickel, copper and cobalt hexacyanoferrate

have the similar crystal structure. These PB analogs also exhibit the adsorption ability to alkali metal ions, especially Cs^+, and then are often used for sensing of alkali metal and the removal of Cs^+ [22-24]. The typical structure of PB and its analogs is shown in Fig. 1. PB consists of a structure in which divalent and trivalent iron ions are alternately coordinated and a cyanide ion is connected between ferric and ferrous ions (Fig. 2) [25,26]. The cell constant and the channel diameter of PB are about 10.2 Å and 3.2 Å, respectively. Therefore, hydrated monovalent cations such as K^+, NH_4^+, Rb^+, and Cs^+ can be absorbed into the PB lattice. In addition, it is known that Cs^+ ions intercalate inside the crystal lattice or a channel entrance of PB surface with a dehydrated state [27]. The PB analogs have a structure in which the iron ion and another transition metal ion are alternately coordinated. PB and its analogs are colored on the basis of the electron transfer between metal ions. The iron, nickel, copper and cobalt hexacyanoferrate exhibit blue, yellow, red and brown, respectively. From this characteristic, PB and its analogs are also used as an electrochromic material [28-30].

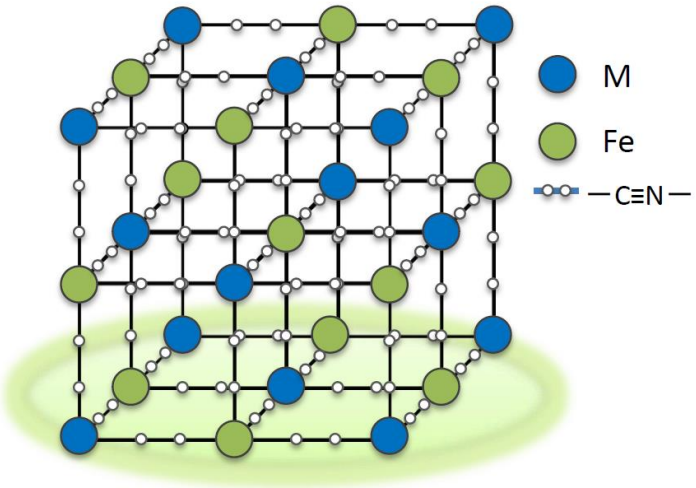

Fig. 1. Schematic structure of PB analogs (metal hexacyanoferrates).

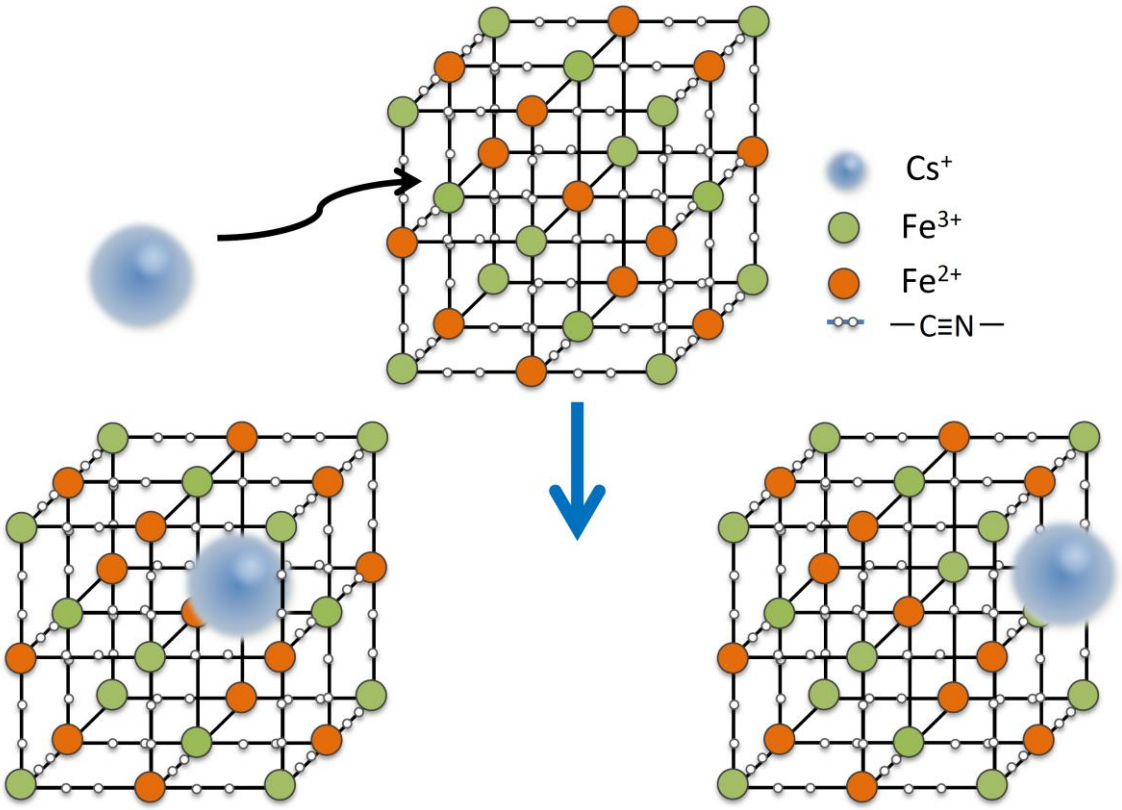

Fig. 2. Unit cell of the Prussian blue and adsorption of Cs^+.

When these hexacyanoferrates are used for removal of Cs, it is necessary to choose a hexacyanoferrate among them according to the operating environment and the features. Although nickel hexacyanoferrate has a high cation adsorption capacity and stability, it is relatively expensive. Copper hexacyanoferrate is stable in a wide pH range [31], however, the toxicity to human health by the elution of copper ion is concerned as well as nickel. Even though iron hexacyanoferrate has a low stability at high pH, iron has the lower toxicity compared with other metals. Therefore, in this study, iron hexacyanoferrate (PB) was selected as an adsorbent for Cs^+.

1.4. Preparation method of Prussian blue

The most basic method of the synthesis of PB is the mixing ferrous or ferric ions with ferricyanide or ferrocyanide ions, respectively. When Fe^{3+} exists in excess, PB precipitate is formed rapidly, but mixing iron and hexacyanoferrate in equimolar produced a colloidal dispersion PB solution. PB can exist in two forms which are “insoluble” and “soluble”. In addition, PB can change to Prussian white (PW), a reduced form, and to Berlin Green (BG), an oxidized form, as accompanied by the color change. The two reactions, the oxidation of PB to Berlin green, and the reduction to Prussian white proposed by Itaya *et al*. were represented by the equation (1) – (4). [32,33]

$$KFe^{III}Fe^{II}(CN)_6 \leftrightarrow Fe^{III}Fe^{III}(CN)_6 + K^+ + e^- \quad (1)$$

Prussian blue Berlin green

$$KFe^{III}Fe^{II}(CN)_6 + K^+ + e^- \leftrightarrow K_2Fe^{II}Fe^{II}(CN)_6 \quad (2)$$

Prussian blue Prussian white

$$Fe_4^{III}[Fe^{II}(CN)_6]_3 + 3A^- \leftrightarrow Fe_4^{III}[Fe^{III}(CN)_6A]_3 + 3e^- \quad (3)$$

Prussian blue Berlin green

$$Fe_4^{III}[Fe^{II}(CN)_6]_3 + 4K^+ + 4e^- \leftrightarrow K_4Fe_4^{II}[Fe^{II}(CN)_6]_3 \quad (4)$$

Prussian blue Prussian white

The equations (1) and (2) are the redox reactions of soluble PB, and the equations (3) and (4) are those of insoluble PB. Although the ideal crystal structure of PB is the cubic lattice structure as shown in Fig. 1, in the case of insoluble PB, a part of $Fe(CN)_6$ is partially defecting, and water molecules are coordinated in the defective parts. The adsorption capacity of Cs^+ becomes higher when the deficiency occurred, and Cs^+ is introduced by the ion exchange with the protons of the coordinated water in the crystals [34]. As described above, PB has a high Cs^+ adsorption property derived from its crystalline structure. However, PB ordinarily exists as fine particles, and it is difficult to collect them after use as an adsorbent. Therefore, the immobilization of PB on the substrate is necessary to be collected easily.

1.5. Modification method for Prussian blue

When PB and its analogs are used in the environment as an adsorbent, the easily collectable property is indispensable. For this reason, many researches to develop the materials in which PB and its analogs are immobilized on various substrates have been reported. Both PB and its analogs can be formed basically by the reaction of transition metal ions with ferricyanide or ferrocyanide. Therefore, when metal ions are eluted from the surface of transition metal, and then reacted with ferricyanide or ferrocyanide at the surface, PB and its analogs can be formed on the metal surface [35,36]. It has been reported that magnetite particles are added to an acidic solution containing ferrocyanide, and then PB is formed on the surface of magnetite particles by reacting ferrocyanide with eluted iron ions. In another method, a

PB analog is prepared as a liquid like an ink by mixing Cu^{2+} with ferricyanide and then the electrode surface was coated with the ink [37]. In this method, PB analog was coated on the metal electrode using spin coating. Since a precious metal was often used as the electrode substrate, it was high cost, and took a long time to hydrophilize the PB analog ink to enhance the water dispersibility.

In order to immobilize the PB or its analogs on a cloth, a piece of cloth was immersed in the PB or its analogs solution and dried [38,39]. However, these methods have some disadvantages, e.g., it takes a long time until the sufficient amounts of PB analogs are immobilized. In addition, these chemical modification methods are difficult to control the amount of PB modified on the surface.

The immobilization of PB by electrolysis has been reported on the surface of Pt [39,32], glassy carbon (GC) [30,32], and carbon fiber (CF) [40]. By applying a potential at these electrode in the mixed solution of ferrocyanide and trivalent iron ions, iron ions were reduced to divalent ions to form PB on the electrode surface. By the electrochemical method, the immobilized amount of PB can be controlled relative easily by the choice of the potential.

1.6. Sensing method for Cs^+

The concentration and deposition condition of the Cs^+ released into the environment vary largely depending on the topography of the environment and the wind direction when Cs^+ is released. Therefore, it is necessary to detect Cs exactly in contaminated sites in order to remediate the environments contaminated with Cs. For

this purpose, some instrumental analyses of Cs^+ have been generally used. Especially, atomic absorption photometer (AAS) or inductively coupled plasma mass spectrometer (ICP-MS) are known as a sensitive and selective analysis method. However, these methods sometimes need the complicated pretreatment of the sample and the equipments are very expensive. The fluorescence detection method using a squaraine or a fluoroionophore as a fluorescent probe is one of the detection methods not based on the instrumental analysis [41]. Furthermore, an electrochemical method for Cs^+ using calixarene has been reported [42]. According to this report, the concentration of Cs^+ affects largely the impedance at low frequencies, and the linearity was found by plotting the impedance change at a single layer electrode against the concentration of Cs^+ in solution. Moreover, the electrochemical detection methods using nickel hexacyanoferrate have also been reported [43]. In this report, the peak potential of hexacyanoferrate redox couple was shifted in the presence of Cs^+ when the potential was swept using the electrode modified with the nickel hexacyanoferrate, and the linearity was obtained from the plot of the half wave potential against the logarithm of the Cs^+ concentration.

The purpose of this research is to develop an adsorbent on the basis of electrochemical synthesis of PB on carbon fiber (CF) to remove Cs^+ from aqueous environment. PB was immobilized on CF electrochemically in a short time, and the adsorption behavior for Cs^+ was investigated. In addition, a simple detection method for Cs^+ was developed by the adsorption ability of PB for Cs^+. This thesis consists of

five chapters including a general introduction of this chapter.

In chapter 2, the modification conditions were examined for PB immobilized on CF electrochemically. The modification of PB from potassium ferricyanide and trivalent iron ion was carried out by controlling the applied potential and time. The coloration of the solution and the weight change of CF were observed. The mixed solution of Fe^{3+} and $[Fe(CN)_6]^{3-}$ was used for the formation of PB layer on CF electrochemically. And then the adsorption behavior of the PB immobilized CF (PB-CF) for Cs^+ in water was investigated.

In chapter 3, Cs^+ adsorption behavior on PB-CF prepared in Chapter 2 was examined in detail. The adsorption performance of PB-CF was estimated by using the pseudo first order and pseudo second order kinetic equation. In order to improve the durability of PB-CF, a polyaniline film was synthesized on the surface of PB-CF by the electrochemical polymerization. The stability of the PB-CF coated with polyaniline was estimated in the presence of oxalic acid.

In Chapter 4, a simple Cs^+ detection method was developed on the basis of the findings of the study on removal of Cs^+ by using PB. In the experiments of Chapter 2 and 3, the stability of PB in the basic solution was different in the presence and absence of Cs^+. In the presence of Cs^+, the decomposition of PB and the color change were suppressed depending on the concentration of Cs^+. Therefore, by the observation of the color changes of PB in the presence of Cs^+ in detail, a simple detection method of Cs^+ was developed.

In Chapter 5, the contents of each chapter are summarized and the usability of

PB modified CF as an adsorbent for Cs^+ and a simple detection method of Cs^+ using colloidal PB solution is discussed as a general conclusion.

References

[1] S.V. Fesenko, R.M. Alexakhin, M.I. Balonov, I.M. Bogdevitch, B.J. Howard, V.A. Kashparov, N.I. Sanzharova, A.V. Panov, G. Voigt, Y.M. Zhuchenka, An extended critical review of twenty years of countermeasures used in agriculture after the Chernobyl accident, *Sci. Total. Environ*. 383 (2007) 1–24.

[2] T. Nakajima, S. Misawa, Y. Morino, H. Tsuruta, D. Goto, J. Uchida, T. Takemura, T. Ohara, Y. Oura, M. Ebihara, M. Satoh, Model depiction of the atmospheric flows of radioactive cesium emitted from the Fukushima Daiichi Nuclear Power Station accident, *Prog. Earth. Planet. Sci*. 4 (2017) 2.

[3] M. Chino, H. Nakayama, H. Nagai, H. Terada, G. Katata, H. Yamazawa, Preliminary estimation of release amounts of ^{131}I and ^{137}Cs accidentally discharged from the Fukushima Daiichi Nuclear Power Plant into atmosphere, *J. Nucl. Sci. Technol.* 48 (2011) 1129–1134.

[4] N.L. Hakem, I. Al Mahamid, J.A. Apps, G.J. Moridis, Sorption of Cesium and Strontium on Hanford Soil, *J. Radioanal. Nucl. Chem.* 246 (2000) 275–278.

[5] M.M. Hamed, M. Holiel, I.M. Ahmed, Sorption behavior of cesium, cobalt and europium radionuclides onto hydroxyl magnesium silicate, *Radiochim. Acta*. 104 (2016) 873–890.

[6] C.A. Sikalidis, P. Misaelides, C.A. Alexiades, Cesium selectivity and fixation of vermiculite in the presence of competing cations, *Environ. Pollut*. 52 (1988) 67–79.

[7] R.N.J. Comans, M. Haller, P. De Preter, Sorption of cesium on illite: Non-equilibrium behaviour and reversibility, *Geochim. Cosmochim. Acta*. 55 (1991) 433–440.

[8] D.W. Evans, J. J. Alberts, R.A. Clark, Reversible ion-exchange fixation of cesium-137 leading to mobilization from reservoir sediments, *Geochim. Cosmochim. Acta*. 41 (1983) 1041–1049.

[9] Tokyo Electric Power Company, Japan (2012) Estimation of Radioactive Material Released to the Atmosphere during the Fukushima Daiichi NPS Accident, Available at: http://www.tepco.co.jp/en/press/corp-com/release/betu12_e/images/120524e0205.pdf. Accessed on 24 November 2017.

[10] M. Dreicer, A. Aarkrog, R. Alexakhin, L. Anspaugh, N.P. Arkhipov, K.J. johansson, Consequences of the Chernobyl accident for the natural and human environments, In: One Decade after Chernobyl. Summing up the Consequences of the Accident. Austria Centre Vienna, Austria, 8–12 April (1996) 319–361.

[11] A. Stohl, P. Seibert, G. Wotawa, D. Arnold, J.F. Burkhart, S. Eckhardt, C. Tapia, A. Vargas, T.J. Yasunari, Xenon-133 and caesium-137 releases into the atmosphere from the Fukushima Dai-ichi nuclear power plant: determination of the source term, atmospheric dispersion, and deposition, *Atmos. Chem. Phys*. 12 (2012) 2313–2343.

[12] N. Casacuberta, P. Masque, J. Garcia-Orellana, R. Garcia-Tenorio, K.O. Buesseler, ^{90}Sr and ^{89}Sr in seawater off Japan as a consequence of the Fukushima Dai-ichi nuclear accident, *Biogeosciences*, 10 (2013) 3649–3659.

[13] Ministry of Agriculture, Forestry and Fisheries (2013) Result of agricultural land decontamination measure projects, Available at: http://www.maff.go.jp/j/nousin/seko/josen/pdf/kekka.pdf. Accessed on 8 December 2017. (in Japanese)

[14] G.N. Kim, W.K. Choi, C.H. Jung, J.K. Moon, Development of a Washing System for Soil Contaminated with Radionuclides Around TRIGA Reactors, *J. Ind. Eng. Chem.* 3 (2007) 406–413.

[15] D. Parajuli, A. Takahashi, H. Tanaka, M. Sato, S. Fukuda, R. Kamimura, T. Kawamoto, Variation in available cesium concentration with parameters during temperature induced extraction of cesium from soil, *J. Environ. Radioact*. 140 (2015) 78–83.

[16] H. Luo, S. Dai, P.V. Bonnesen, Solvent Extraction of Sr^{2+} and Cs^{+} Based on Room-Temperature Ionic Liquids Containing Monoaza-Substituted Crown Ethers, *Anal. Chem.* 76 (2004) 2773–2779.

[17] L.H. Delmau, P.V. Bonnesen, B.A. Moyer, A solution to stripping problems caused by organophilic anion impurities in crown-ether-based solvent extraction systems: a case study of cesium removal from radioactive wastes, *hydrometallurgy.* 72 (2004) 9–19.

[18] D.R. Raut, P.K. Mohapatra, M.K. Choudhary, S.K. Nayak, Evaluation of two calix-crown-6 ligands for the recovery of radio cesium from nuclear waste solutions: Solvent extraction and liquid membrane studies, *J. Membr. Sci*. 429 (2013) 197–205.

[19] R.R. Sheha, E. Metwally, Equilibrium isotherm modeling of cesium adsorption onto magnetic materials, *J. Hazard. Mater*. 143 (2007) 354–361.

[20] M.R. Awual, S. Suzuki, T. Taguchi, H. Shiwaku, Y. Okamoto, T. Yaita, Radioactive cesium removal from nuclear wastewater by novel inorganic and conjugate adsorbents, *Chem. Eng. J.* 242 (2014) 127–135.

[21] K.Y. Lee, M. Park, J. Kim, M. Oh, E.H. Lee, K.W. Kim, D.Y. Chung, J.K. Moon, Equilibrium, kinetic and thermodynamic study of cesium adsorption onto nanocrystalline mordenite from high-salt solution, *Chemosphere.* 150 (2016) 765–771.

[22] A.A. Karyakin, Prussian Blue and its analogues: electrochemistry and analytical applications, *Electroanalysis*. 13 (2001) 813–819.

[23] T. Ikeshoji, Separation of Alkali Metal Ions by Intercalation into a Prussian Blue Electrode, *J. Electrochem. Soc.* 133 (1986) 2108–2109.

[24] H. Mimura, J. Lehto, R. Harjula, Ion Exchange of Cesium on Potassium Nickel Hexacyanoferrate(II)s, *J. Nucl. Sci. Technol*. 34 (1997) 484–489.

[25] J.F. Keggin, F.D. Miles, Structures and Formulæ of the Prussian Blues and Related Compounds, *Nature.* 137 (1936) 577–578.

[26] H.J. Buser, D. Schwarzenbach, W. Petter, A. Ludi, The crystal structure of Prussian Blue: $Fe_4[Fe(CN)_6]_3.xH_2O$, *Inorg. Chem.* 16 (1977) 2704–2710.

[27] N. Ruankaew, N. Yoshida, Y. Watanabe, H. Nakano, S. Phongphanphanee, Size-dependent adsorption sites in a Prussian blue nanoparticle: A 3D-RISM study, *Chem. Phys. Lett.* 684 (2017) 117–125.

[28] M. Isizaki, K. Kanaizuka, M. Abe, Y. Hoshi, M. Sakamoto, T. kawamoto, H. Tanaka, M. Kurihara, Preparation of electrochromic Prussian blue nanoparticles dispersible into various solvents for realisation of printed electronics, *Green. Chem*. 14 (2012) 1537–1544.

[29] S. Hara, H. Shiozaki, A. Omura, H. Tanaka, T. Kawamoto, M. Tokumoto, M. Yamada, A. Gotoh, M. Kurihara, M. Sakamoto, Color-Switchable Glass and Display Devices Fabricated by Liquid Processes with Electrochromic Nanoparticle "Ink", *Appl. Phis. Express*. 1 (2008) 104002.

[30] K. Itaya, K. Shibayama, H. Akahoshi, S. Toshima, Prussian-blue-modified electrodes: An application for a stable electrochromic display device, *J. Appl. Phys*. 53 (1982) 804–805.

[31] H. Mimura, J. Lehto, R. Harjula, Ion Exchange of Cesium on Potassium Nickel Hexacyanoferrate (II)s, *J. Nucl. Sci. Technol*. 34 (2000) 484–489.

[32] K. Itaya, H. Akahoshi, S. Toshima, Electrochemistry of Prussian Blue modified electrodes: an electrochemical preparation method, *J. Electrochem. Soc.* 129 (1982) 1498–1500.

[33] V.D. Neff, Electrochemical Oxidation and Reduction of Thin Films of Prussian Blue, *J. Electrochem. Soc*. 125 (1978) 886–887.

[34] M. Ishizaki, S. Akiba, A. Ohtani, Y. Hoshi, K. Ono, M. Matsuba, T. Togashi, K. Kananizuka, M. Sakamoto, A. Takahashi, T. Kawamoto, H. Tanaka, M. Watanabe, M. Arisaka, T. Nankawad, M. Kurihara, Proton-exchange mechanism of specific Cs^+ adsorption via lattice defect sites of Prussian blue filled with coordination and crystal water molecules, *Dalton. Trans*. 42 (2013) 16049–16055.

[35] M.A. Lilga, R.J. Orth, J.P.H. Sukamto, S.M. Haight, D.T. Schwartz, Metal ion separations using electrically switched ion exchange, *Sep. Purif. Technol*. 11 (1997) 147–158.

[36] B.F.Y.Yon Hin, C.R. Lowe, Catalytic Oxidation of Reduced Nicotinamide Adenine Dinucleotide at Hexacyanoferrate-Modified Nickel Electrodes, *Anal. Chem*. 59 (1987) 2111–2115.

[37] R. Chen, H. Tanaka, T. Kawamoto, M. Asai, C. Fukushima, H. Na, M. Kurihara, M. Watanabe, M. Arisaka, T. Nankawa, Selective removal of cesium ions from wastewater using copper hexacyanoferrate nanofilms in an electrochemical system, *Electrochimica Acta*, 87 (2013) 119–125.

[38] P. Nie, L. Shen, G. Pang, Y. Zhu, G. Xu, Y. Qing, H. Dou, X. Zhang, Flexible metal–organic frameworks as superior cathodes for rechargeable sodium-ion batteries, *J. Mater. Chem. A*. 3 (2015) 16590–16597.

[39] B. Sun, X.G. Hao, Z.D. Wang, G.Q. Guan, Z.L. Zhang, Y.B. Li, S.B. Liu, Separation of low concentration of cesium ion from wastewater by electrochemically switched ion exchange method: experimental adsorption kinetics analysis, *J. Hazard. Mater*. 233-234 (2012) 177–183

[40] X. Zhang, J. Wang, B. Ogorevc, U.S. Spichiger, Glucose nanosensor based on Prussian-Blue modified carbon-fiber cone nanoelectrode and an integrated reference electrode, *Electroanalysis*. 11 (1999) 945–949.

[41] B. Radaram, T. Mako, M. Levine, Sensitive and selective detection of cesium via fluorescence quenching, *Dalton. Trans.* 42 (2013) 16276–16278.

[42] V. Souchon, I. Leray, B. Valeur, Selective detection of cesium by a water-soluble fluorescent molecular sensor based on a calix[4]arene-bis(crown-6-ether), *Chem. Commun*. (2006) 4224–4226.

[43] C.Y. Chang, L.K. Chau, W.P. Hu, C.Y. Wang, J.H Liao, Nickel hexacyanoferrate multilayers on functionalized mesoporous silica supports for selective sorption and sensing of cesium, *Micropor. Mesopor. Mater*. 109 (2008) 505–512.

Chapter 2

Electrochemical Synthesis and Immobilization of a Beadwork-Like Prussian Blue on Carbon Fiber and the Removal of Cesium

2.1. Introduction

In order to prepare PB immobilized adsorbent, the electrochemical method has some advantages; for example, the PB modification can be controlled by the potential without adding any specific chemicals.

In this chapter, electrochemical immobilization of PB on a sheet of CF was investigated for the removal of Cs^+ in aqueous environments. Some papers have reported the electrochemical modification of PB on Pt, carbon, SnO_2, and indium tin oxide electrodes [1-3]. PB could be electrochemically modified on carbon materials, such as a grassy carbon and one strand of carbon fiber (CF) [4-7]. However, these studies focused on the development of biosensors. Therefore, the surface area of the electrode was very small and the amount of PB modified on the electrode was not enough to remove Cs^+ in aquatic environments. CF has a large surface area, conductivity, and chemical stability. From these properties, CF cloth is suited for the electrode material to remove of pollutants [8-10]. The immobilized amounts of PB can be significantly increased using a sheet of CF cloth as a modification substance for PB. The chemical properties and stabilities of PB-modified carbon fiber sheets (PB-CF) were investigated by controlling the modification potentials and scanning potential in aqueous solution of several pH values. The removal of Cs^+ in water was also investigated using the electrochemically prepared PB-CF.

2.2. Materials and methods

2.2.1. Materials

Iron(III) chloride hexahydrate and potassium hexacyanoferrate(III) were used for the preparation of PB-CF and were purchased from Wako Pure Chemical Industries, Ltd. (Osaka, Japan). Sodium dihydrogen phosphate was purchased from Wako Pure Chemical Industries, Ltd., and disodium hydrogen phosphate dodecahydrate and ethanol were purchased from Junsei Chemical Co., Ltd. (Tokyo, Japan). The alkali metal salts used for the adsorption experiment, a cesium standard solution (1000 mg/L) and cesium chloride were purchased from Junsei Chemical Co., Ltd. Hydrochloric acid and sodium hydroxide for pH adjustment were purchased from Kanto Chemical Co., Inc. (Tokyo, Japan) and Junsei Chemical Co., Ltd., respectively. Potassium chloride for Cs analysis by atomic absorption spectroscopy (AAS) was purchased from Junsei Chemical Co., Ltd. Oxalic acid was purchased from Wako Pure Chemical Industries, Ltd. All reagents were of analytical grade and used without any prior treatment. Ion exchange water was prepared by water purifying apparatus (Autostill WA73, Yamato scientific Co., Ltd. Japan) and ultra-pure water for pretreatment of CF was prepared by Milli-Q Advantage A10 (Millipore, USA).

2.2.2. Modification of Prussian blue on carbon fiber

The modification of CF with PB was performed using an electrochemical redox reaction in a three-electrode system. A potentiostat-galvanostat HA-301 (Hokuto Denko Ltd., Japan) was used to apply a constant potential. A CF (0.5-mm diameter;

Hokuto Denko Ltd. Tokyo, Japan) were used as the working electrode. A platinum wire and Ag/AgCl/Saturated KCl (International Chemistry Co., Ltd., Japan) were used as a counter and a reference electrodes, respectively. Before use, the CF was dipped in ethanol and then sonicated in ultra-pure water for 15 min; the ultra-pure water was changed every 5 min during the sonication.

The pretreatment of CF and electrochemical modification of PB were performed according to the procedure shown by Ricci *et al*. [11] and Karyakin *et al*. [12]. For the electrochemical pretreatment of the CF, a constant potential of 1.7 V vs. Ag/AgCl was applied for 3 min in 0.1 M KCl and 0.1 M phosphate buffer (pH 6.8). After the pretreatment, a constant potential vs Ag/AgCl was applied in the mixed solution of 2 mM $K_3[Fe(CN)_6]$, 2 mM $FeCl_3$, 0.1 M KCl, and 3 mM HCl. Then, the potential scan between -0.05 V and 0.35 V with a sweep rate of 50 mV/s was repeated for 10 cycles in a solution of 0.1 M KCl, and 3 mM HCl, and the PB-CF was washed with ultra-pure water. The prepared PB-CF was dried at 80 °C for 30 min and stored in the dark at room temperature. The chemical modification of PB on CF was performed according to the report by Sun et al. [13]. First, a CF sheet (1 cm × 5 cm) was immersed in ethanol overnight. After that, the CF was placed in a solution of 50 mM $K_3[Fe(CN)_6]$ containing ethanol. Then, the CF was transferred into a 50 mM $FeCl_2$ solution containing 2.3 M ethanol. After modification, PB-CF was dried at 80 °C in air.

2.2.3. Effect of the modification potential

In order to examine the stable immobilization conditions of PB, a constant

potential between -0.2 V and 0.8 V was applied for 10 min in the mixed solution of 2 mM $K_3[Fe(CN)_6]$, 2 mM $FeCl_3$, 0.1 M KCl, and 3 mM HCl. Then, the solution after applying the potential was used to measure the absorbance at 710 nm, which is proportional to the amount of PB produced in the solution. The solution after applying the potential was filtered and measured the absorbance at 420 nm, which is proportional to the amount of $FeCl_3$ and $K_3[Fe(CN)_6]$. Ultraviolet-visible spectrophotometry was carried out by UV-Vis spectrophotometer (V-550 and V-650DS, JASCO, Japan). The absorbance at 710 nm of solution and absorbance ratio at 420 nm of filtered solution was plotted against the potential.

2.2.4. Amount of PB on the CF

The amount of modified PB on the CF was estimated by measuring the weight of PB-CF before and after elution of PB from CF. The elution of PB was carried out by immersing a 1 cm × 1 cm piece of PB-CF in a 0.1 M oxalic acid solution and slowly stirring; then, the piece of CF was washed with deionized water and dried at 80 °C overnight. The weight measurement was performed after cooling to the room temperature.

2.2.5. Characterization of PB-CF

The characterization of PB-CF was carried out by cyclic voltammetry (CV), scanning electron microscopy (SEM), and energy dispersive X-ray spectroscopy (EDS). A CV-50W voltammetric analyzer (BAS, USA) was used for CV analysis. The

morphological structure of the modified CF with PB using SEM and EDS were observed by a low vacuum-SEM (JSM-6360LA, JEOL, Japan).

2.2.6. Influence of pH on the stability of PB-CF

A 2-cm long thread of PB-CF as a working electrode was immersed in 15 mL of 0.1 M KCl; the solution pH was adjusted from 1 to 11, and the CVs were measured after a constant interval using the thread. The stability of PB on the CF surface was estimated by measuring the decrement of the oxidation peak current and the observation of the surface of the PB-CF.

2.2.7. Adsorption of cesium on PB-CF

Adsorption experiments were performed using the batch method with 10 mL of a 5 ppm Cs^+ solution (prepared by CsCl solution); the pH and concentration of the solution were adjusted to obtain adequate conditions for Cs^+ removal. An electrochemically prepared PB-CF sheet (1 cm × 1 cm) was immersed in the Cs^+ solution for a constant time at room temperature. Then, the PB-CF was removed from the solution. The remaining Cs^+ in the solution was measured by AAS (A-2000 HITACHI, Japan) at 852.11 nm with air-acetylene gas. Distribution coefficients (K_d, mL/g) of Cs^+ were measured in batch tests with 5-100 ppm Cs^+ concentrations. A 1 cm × 1 cm PB-CF sheet prepared by applying 0.35 V for 10 min was immersed in the 10 mL of the Cs^+ solution, and slowly shaken for 72 h at room temperature.

2.3. Results and discussion

2.3.1. Modification of Prussian blue on carbon materials

2.3.1.1. Modification potential

The simplest method to modify PB on a piece of CF sheet was chemical modification by immersing it in a solution containing the ingredients of PB [13,14]. However, the modification of PB on CF by this method required a lot of time to immerse in the solution or to repeat the cycle of dipping to immobilize sufficient PB on the CF surface. On the other hand, the electrochemical modification is an excellent method to obtain stable PB on CF in a short time. The process of electrochemical modification of PB on CF in a $FeCl_3$ and $K_3[Fe(CN)_6]$ mixed solution is shown in Scheme 1. It is based on the reactions of $[Fe(CN)_6]^{3-}$ with Fe^{2+} produced by the reduction of Fe^{3+} on the electrode. That is, Fe^{3+} in the solution is firstly reduced to Fe^{2+} by applying a reductive potential at the CF electrode. Fe^{2+} produced at the electrode reacts there with $[Fe(CN)_6]^{3-}$ provided from the solution to generate PB crystals on the electrode. The stable modification of PB on the surface of CF might be achieved by controlling the Fe^{2+} generation rate, which depends on the applied potential. CVs of $FeCl_3$ and $K_3[Fe(CN)_6]$ in the mixed solution of 0.1 M KCl and 3 mM HCl by a CF electrode are shown in Fig. 1. A redox couple of $[Fe(CN)_6]^{4-/3-}$ appeared near 0.3 V as a sharp peaks. A redox couple of $Fe^{2+/3+}$ were broad, and the oxidative peak was about 0.7 V and the reductive peak was about 0.3 V. The effective potential range for the deposition of PB at the electrode should be limited to be more negative than the reduction potential of Fe^{3+} to Fe^{2+} and to be more positive than the reduction potential

of $[Fe(CN)_6]^{3-}$. At a more negative potential than 0.3 V, $[Fe(CN)_6]^{3-}$ is reduced to $[Fe(CN)_6]^{4-}$ even though Fe^{3+} is more rapidly reduced to Fe^{2+}. Therefore, the formation of PB should mainly occur in the bulk solution. This was confirmed by the color change in the solution (Fig. 2). Figure 2 shows the absorbance of the solution at 710 nm and absorption ratio at 420 nm after potentials applying plotted as a function of the applied potential at the CF electrod. The absorbance at 710 nm is derived from the charge transition between $[Fe^{II}(CN)_6]^{4-}$ and Fe^{III} in PB [15]. Therefore, the increased absorbance at 710 nm indicates the formation of PB in the solution. According to the photograph in Fig. 2, the solution color only minimally changed at a more positive potential than 0.3 V. In addition, the degradation ratio evaluated by using the absorbance at 420 nm was almost the same at the potentials of 0.3 V and 0.35 V. However, a remarkable increase in the absorbance at 710 nm was observed between 0.2 V and 0.35 V, where the reduction of $[Fe(CN)_6]^{3-}$ occurred. The potential range between 0.35 V and 0.5 V was adequate to selectively immobilize PB on CF electrode. This potential is located between the reduction peaks of $[Fe(CN)_6]^{3-}$ and Fe^{3+}. In this potential range, Fe^{3+} was gently reduced to Fe^{2+} and reacted with $[Fe(CN)_6]^{3-}$ at the CF electrode surface to form stable PB crystals on the CF.

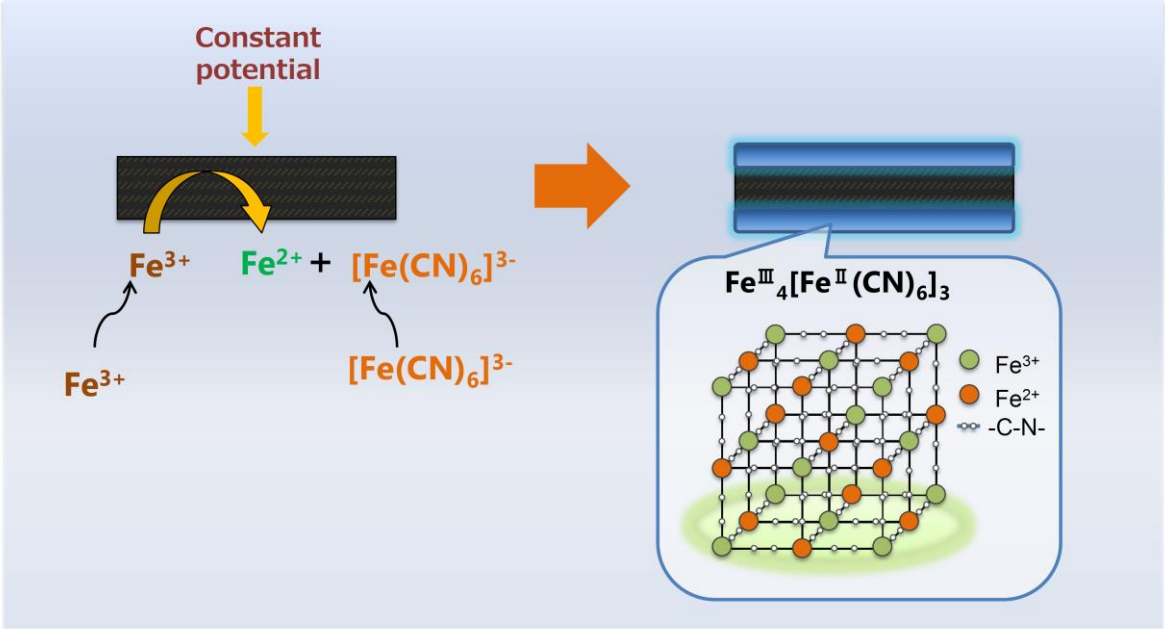

Scheme 1. Electrochemical reaction of Fe^{2+} with $Fe(CN)_6^{3-}$ and preparation of PB.

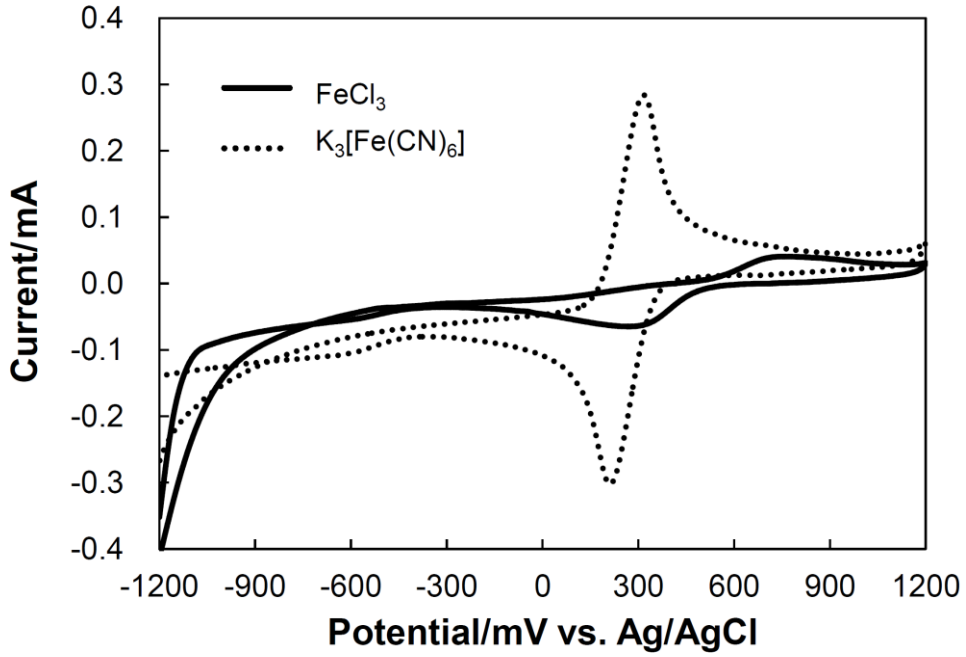

Fig. 1. Cyclic voltammograms (CV) of CF in 2 mM $FeCl_3$ or $K_3[Fe(CN)_6]$ containing 0.1 M KCl and 3 mM HCl. Sweep rate: 50 mV/s.

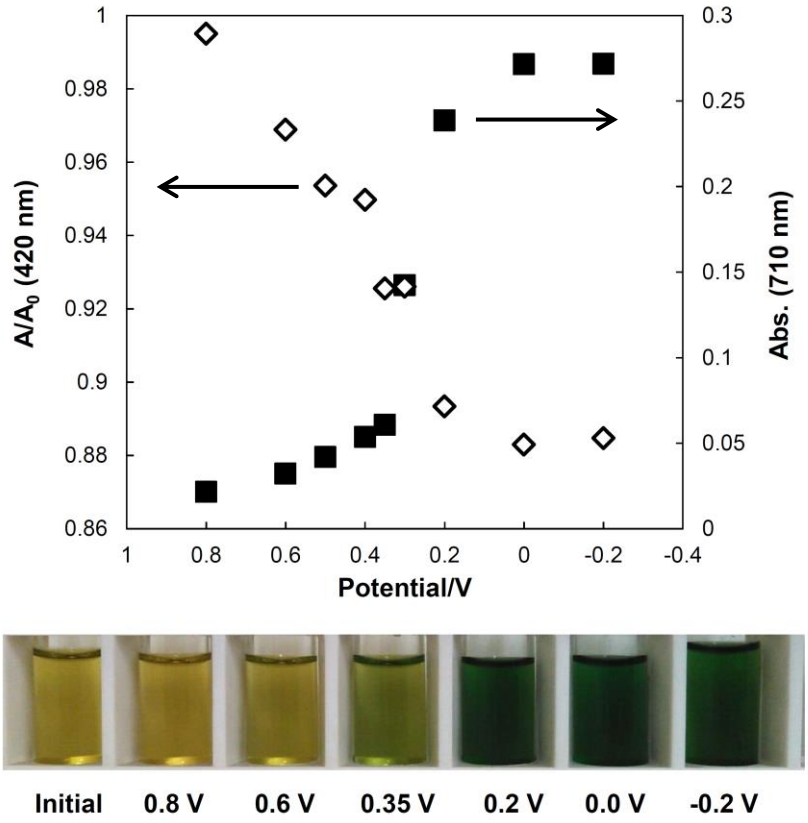

Fig. 2. Absorbance at 710 nm (closed square) and absorption ratio at 420 nm (open diamond) for several modification potentials.

2.3.1.2. Amount of modified PB

The amounts of electrochemically modified PB on CF were estimated by measuring the weight of PB-CF before and after the elution of PB from CF. PB on CF should be dissolved completely in 0.1 M oxalic acid by repeating the immersion until the eluting solution became clear. Table 1 shows the amounts of PB on CF under several modification conditions. PB was not deposited significantly on the CF by just immersing in the mixed solution of $FeCl_3$ and $K_3[Fe(CN)_6]$ without an applied potential. Although the immobilization of PB on CF was observed at potentials of -0.2

V and 0.2 V, PB was also generated in the bulk solution under the conditions in which the reduction of $[Fe(CN)_6]^{3-}$ occurred. The amount of PB on CF was obviously increased at 0.35 V and 0.5 V. At these potentials, the reduction of Fe^{3+} to Fe^{2+} was significantly proceeded to immobilize PB on CF within a short time. When the potential of 0.35 V was applied, the amount of PB modified on the CF surface was twice greater than that prepared at 0.6 V.

2.3.2. Characterization of PB-CF

2.3.2.1. Cyclic voltammograms of PB-CF

The CV of a thread of PB-CF is shown in Fig. 3. When the thread of PB-CF was used as a working electrode in the KCl solution, two pairs of redox peaks were observed around 0.2 V and 1.0 V. According to the paper by Itaya et al., there are two redox reactions of PB; from PB to Berlin green (BG) and from PB to Prussian white (PW). These redox reactions of PB↔PW and PB↔BG correspond to the peaks around 0.2 V and 1.0 V, respectively [1,16]. The two pairs of redox peaks gradually disappeared after adsorption of Cs^+ (Fig. 3B), which is similar to previous observations [3,17].

Table 1. Amount of PB on the surface of CF at several modification times (n=5).

Potential/V	**Modification time/min**	**Weight of PB/mg g^{-1}**	**Standard deviation**
-0.2	30	37.4	8.6
0.2	10	34.0	17.8
	20	36.8	14.4
	30	43.6	13.6
0.35	1	13.1	9.4
	3	23.1	12.6
	5	32.2	5.8
	10	72.6	25.6
	20	64.1	32.7
	30	107.0	13.0
0.5	5	28.5	10.8
	10	55.8	8.7
	20	58.8	12.4
	30	67.0	15.1
0.6	10	32.0	7.7
	20	32.7	6.8
	30	55.9	4.0
	Immersion time/min	**Weight of PB/mg g^{-1}**	**Standard deviation**
without potential	30	1.1	2.6

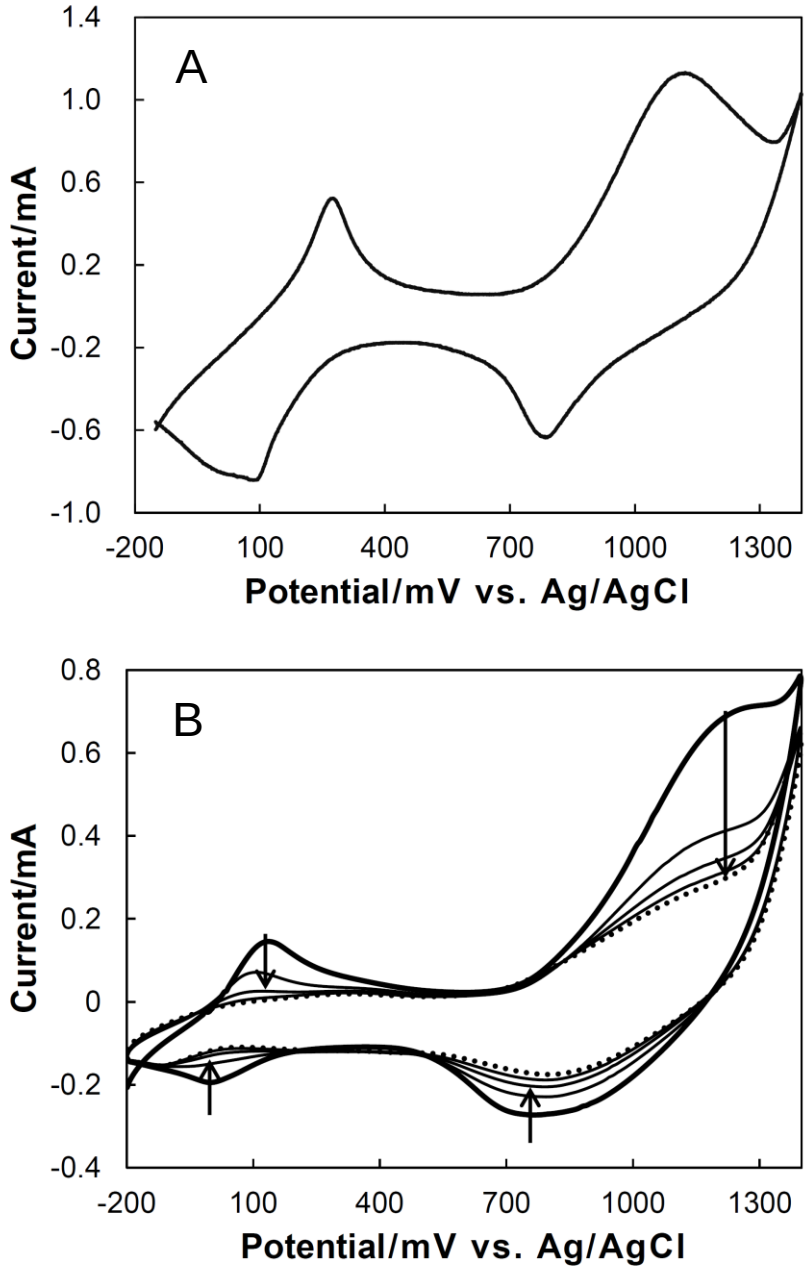

Fig. 3. Cyclic voltammograms of PB-CF (A) in 0.1 M KCl and (B) in 0.1 M CsCl (bold line is first, dotted line is last cycle). Sweep rate: 100 mV/s.

2.3.2.2. SEM and EDS mapping images of PB-CF

The SEM images of bare CF and PB-CF clothes before and after modification at 0.35 V for 10 min are shown in Fig. 4. The surface of the plain CF (A1, A2) is

smooth and any crystals of PB could not be observed. However, many ring-like crystals of PB were observed on the PB-CF (B1, B2). The thickness of the rings was between 1.5 μm and 2 μm. The PB crystals appear as beadwork because of the formation of many cracks on the PB-CF surface, which were caused by the drying treatment of PB-CF or the mechanical weathering. The EDS mapping images of PB-CF prepared at 0.35 V for 10 min (Fig. 5) confirm that Fe was present only on the ring-like structure of PB-CF (Fig. 5 D).

The SEM images of PB on CF prepared under several modification potentials are shown in Fig. 6. When the potential was set at 0.2 V, the PB rings on some parts of CF had a significant thickness of about 5 μm. The thickness become more than twice at 0.35 V. However, the uniformity of the modification was low and many regions of CF were unmodified. When applying 0.5 V or 0.6 V, PB on CF showed an island-type structure, and the uniformity of the modification was higher than at other potentials. Meanwhile, the thickness of PB was less than 1 μm. The ring-like structure of PB was observed only when the modification was carried out at the potential of 0.2 V and 0.35 V. An applied potential of 0.35 V for 1 min produced an island structure similar to that for PB modified at 0.5 V or 0.6 V for 10 min (Fig. 7). When the modification time was 3 min at 0.35 V, the thickness of the PB layer on the surface of CF increased, and the ring-like structure was gradually formed. An applied potential of approximately 0.35 V was required to efficiently immobilize a sufficient amount of PB on CF.

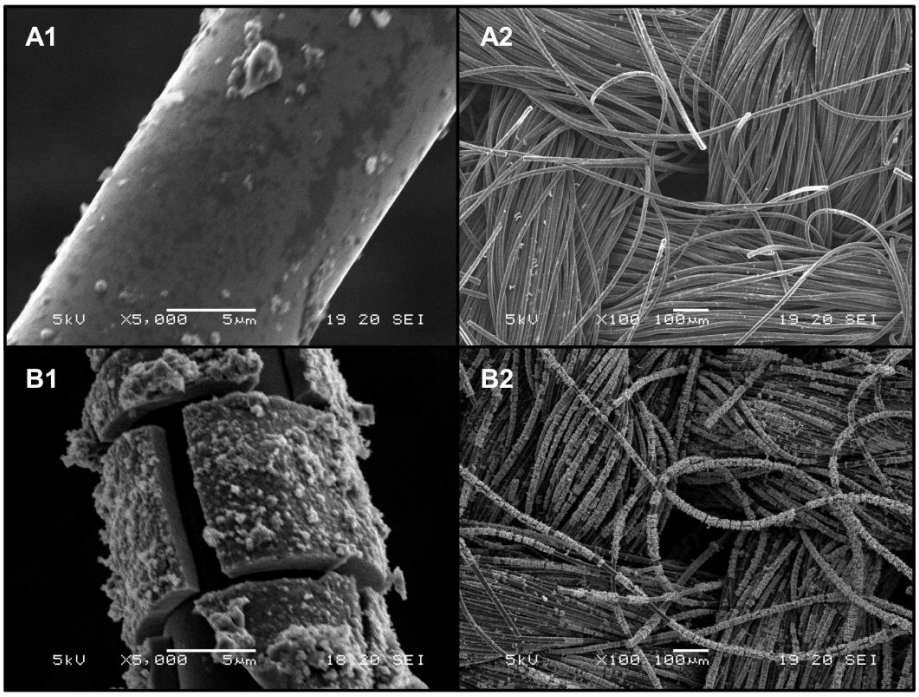

Fig. 4. SEM images of (A1, A2) CF and (B1, B2) PB-CF modified at 0.35 V for 10 min.

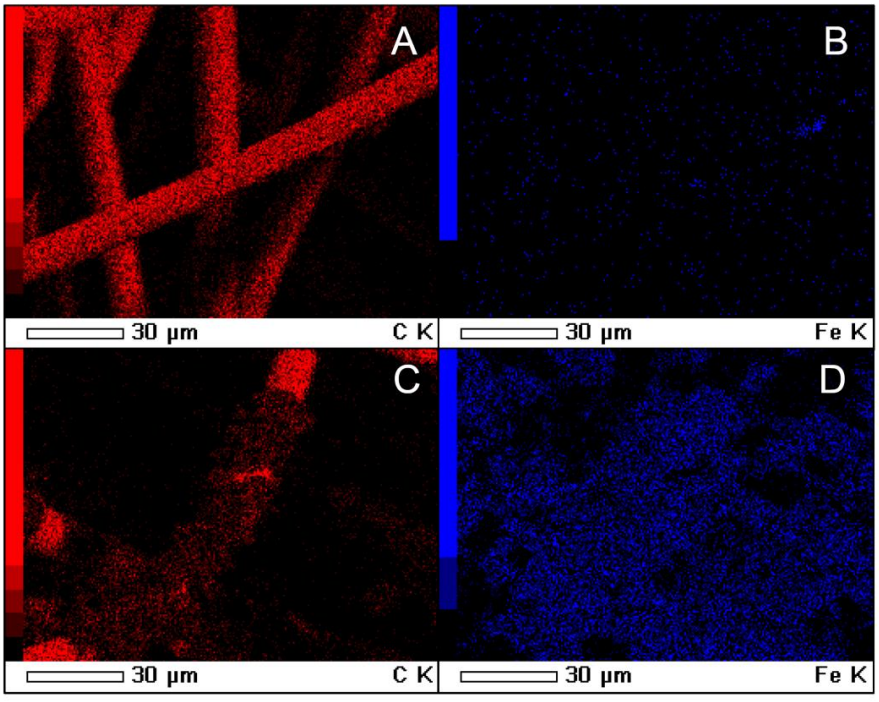

Fig. 5. EDS mapping images of CF and PB-CF surface. (A) C on CF, (B) Fe on CF, (C) C on PB-CF, and (D) Fe on PB-CF.

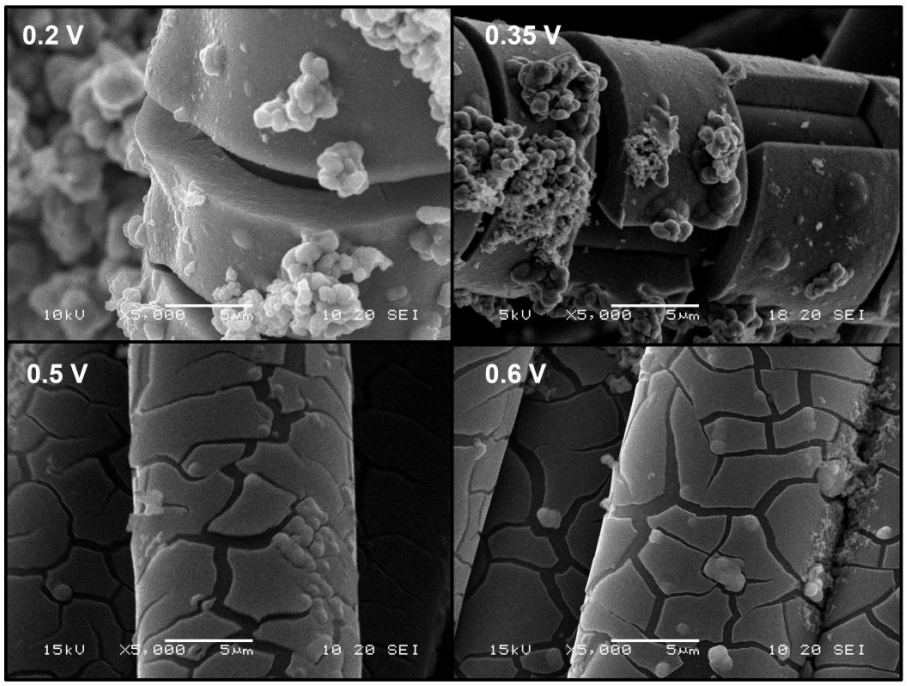

Fig. 6. SEM images of the PB-CF surface modified at different potentials for 10 min.

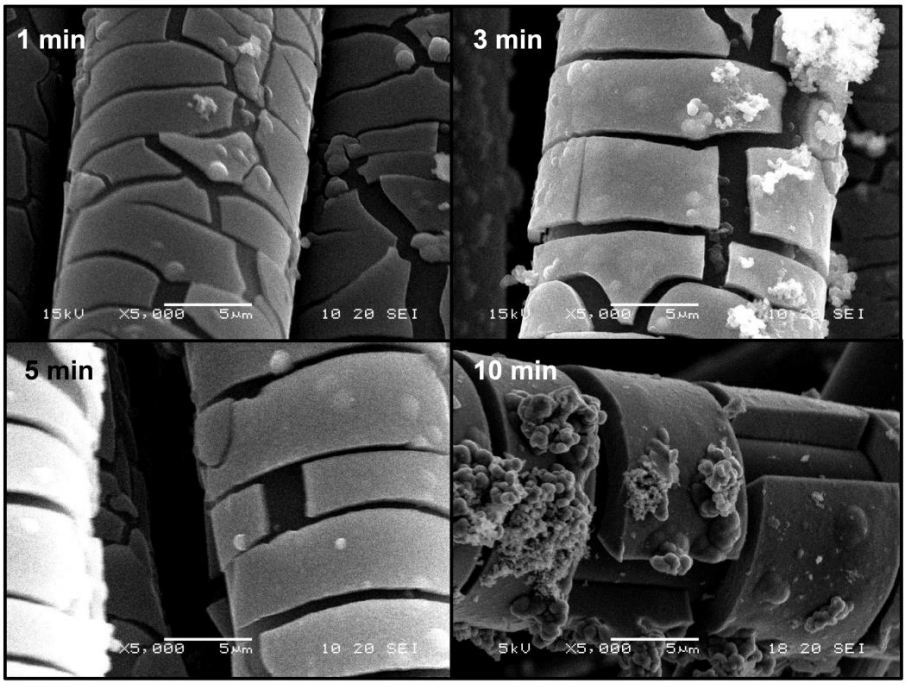

Fig. 7. SEM images of the PB-CF surface modified at 0.35 V for several minutes.

2.3.3. Chemical and physical stability of PB-CF

The observation of PB-CF by SEM showed that the morphology of PB on CF depended on both the applied potential and time. When 0.2 V was selected as the applied potential, a large amount of PB was modified on CF within a short time. However, the modified PB was unstable and could be easily detached from CF. The stability of PB on CF improved, and the amount of PB remarkably increased at an applied potential of 0.35 V. When the applied potential was increased to 0.5 V, the homogeneity of the modified PB became higher and more stable. The modification of PB by dipping was partially limited on the CF, and the PB layer was not stable (Fig. 8). There was a large difference in the physical stability of immobilization of PB on CF between the electrochemical and chemical modification in a short time.

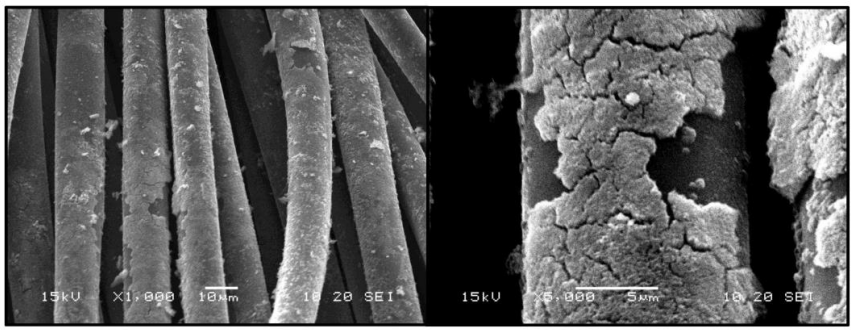

Fig.8. SEM images of the PB-CF surface modified by dipping in $K_3[Fe(CN)_6]$ and $FeCl_2$ for 10 min.

The effect of pH on the stability of PB-CF was investigated using CV. After immersing a thread of the modified PB-CF in the solution (pH 1-11, adjusted by HCl

and NaOH), the PB-CF thread was used as a working electrode, and the CVs were measured in 0.1 M KCl. The stability of PB on CF was estimated from the changes in the oxidation peak current of the oxidation process of PW to PB. The oxidation peak current decreased with increasing pH (Fig. 9). In particular, after immersing in the solution at pH 11 for 30 min, the oxidation peak current decreased to less than 10% of the initial value. PB on CF was comparatively stable at a low pH. Meanwhile, a previous study reported that PB was unstable above pH 7 [18,19]. This instability is due to the reaction between the hydroxyl ions in the solution and the ferric ions from the PB structure. In higher pH solutions, ferric hydroxide was produced from the ferric ions and hydroxyl ions on the surface of PB; consequently, the Fe-CN-Fe bonds in the PB lattice were broken [20,21].

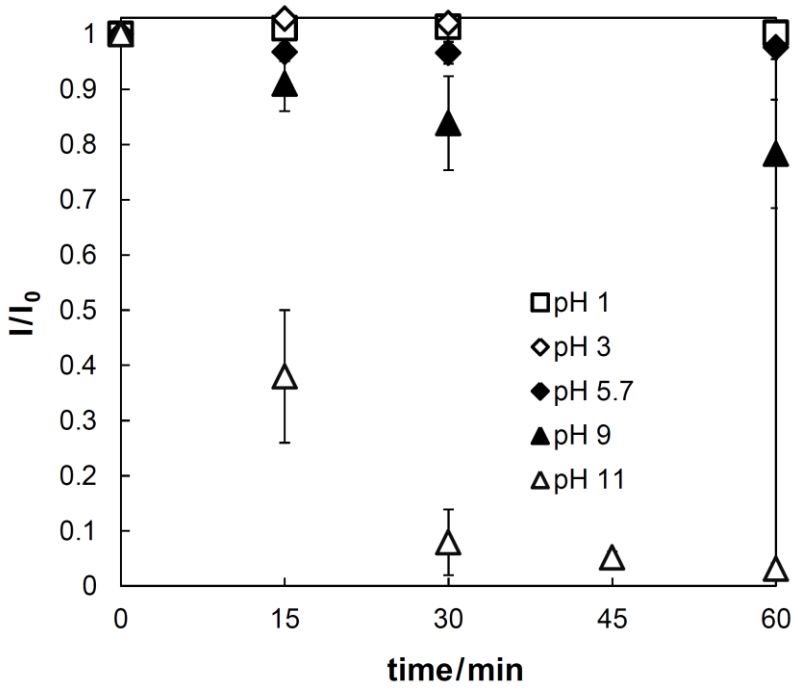

Fig. 9. Changes in the oxidation peak current of the PB-CF at different pH values.

2.3.4. Adsorption of Cs^+ on PB-CF

The adsorption behavior of Cs^+ on PB-CF was investigated using PB-CF prepared at a modification potential at 0.35 V for several modification time from 1 min to 30 min. The adsorption ability for Cs^+ of CF without PB was very low. By using PB-CF, the adsorption ratio of Cs^+ increased with respect to the contact time and reached equilibrium after 48 h. PB has a specific adsorption ability for Cs^+. The monovalent cations can be adsorbed in the crystal lattice of PB by electrostatic interactions, and this process is related to the Stokes radii of the hydrated ions. The hydrated radii of K^+, NH_4^+, Rb^+, and Cs^+ are 1.25, 1.25, 1.18 and 1.19 Å, respectively [22]; the channel diameter of PB is about 3.2 Å [23]. Therefore, these cations can absorb into the PB lattice. In contrast, Li^+ and Na^+ have hydrated radii of 2.37 and 1.83 Å, respectively, and they cannot be captured through the PB lattice [16,23]. The adsorption amount of Cs^+ into PB-CF became constant after 10 min of PB-CF modification at 0.35 V (Fig. 10). The amount of PB prepared by the 30-min modification was about 1.7 times greater than that prepared by the 10-min modification. SEM images (Fig. 7) also show that the thickness of the PB layer increased with respect to the modification time. Although the amount of PB on CF increased, the adsorption amount of Cs^+ did not increase with respect to increasing modification time. The author presume that Cs^+ adsorbed mainly on the outer parts of the PB lattice, and Cs^+ adsorption on the inner part of PB was limited. Studies by Chen et al. using copper hexacyanoferrates modified on an Au electrode showed that the removal efficiency of Cs^+ did not increase above a certain film thickness [24]. Similar

results were obtained in this study.

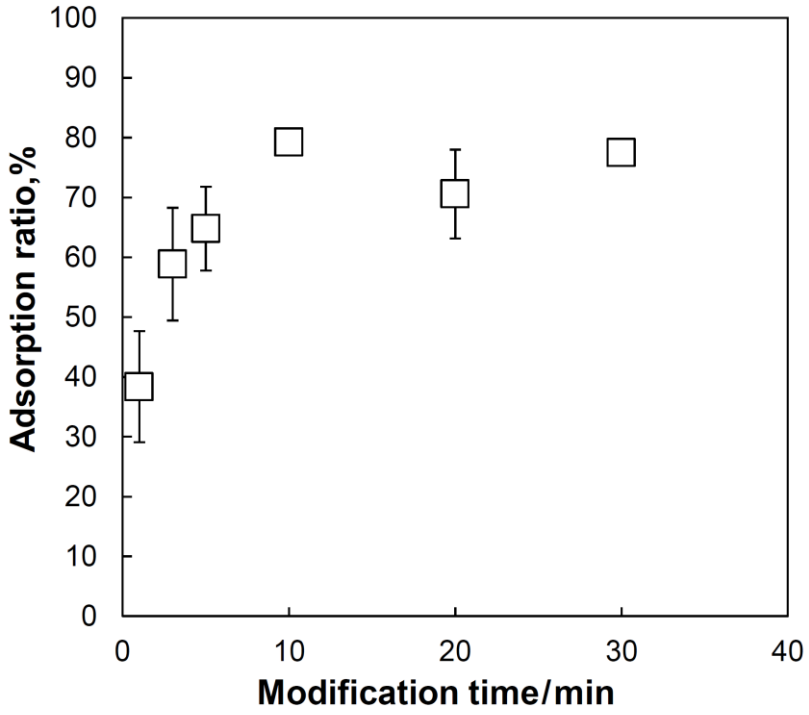

Fig. 10. Adsorption ratios of Cs^+ by PB-CF modified at 0.35 V at different modification times.

2.3.5. Influence of pH on adsorption

The influence of pH on Cs^+ adsorption using three types of PB-CF was investigated, and the results are shown in Fig. 11. Under these conditions, Cs is present as a monovalent ion at all pH values [25,26]. The adsorption ratio at pH 1 for 48 h was about 60%, and the adsorption ratio at pH 5.6 for 48 h was more than 90% using PB-CF modified by a potential of 0.35 V. At pH 11, the adsorption of Cs^+ on PB-CF

was approximately 80%. In contrast, the Cs^+ adsorption ratios after 48 h using PB-CF prepared by potentials of 0.5 V and 0.6 V were about 40% at pH 1 and about 70% at pH 5.6, respectively. These values were lower than that for PB-CF prepared at 0.35 V. The adsorption ratio at pH 1 was lower than that at pH 5.6 because of the competition of Cs^+ with H^+ at a low pH [13]. In spite of the instability of PB-CF at a high pH, which was presumed by the degradation of the oxidation peak current, a higher adsorption ratio was obtained at pH 11 than in acidic conditions when PB-CF was modified at 0.35 V and 0.5 V. In general, PB was unstable under basic conditions. The changes in the oxidation current show the possibility that the reaction between hydroxyl ions and ferric ions occurred at pH 11. However, the pH change by the reaction was not large (11 to 10.4 after 24 h). Therefore, the effect of OH^- on PB-CF was limited to the partial formation of $Fe(OH)_3$ on the surface of PB, which did not interfere with the adsorption reaction of Cs^+ into the internal lattice of PB. Fig. 12 shows the surface of PB-CF and the EDS mapping images after the adsorption experiment at pH 11 for 48 h. Fig. 12 B and C indicates that Cs^+ exists at the position of PB crystals on CF. As a result, it was confirmed that Cs^+ adsorbed inside the lattice structure of PB under the condition of pH 11.

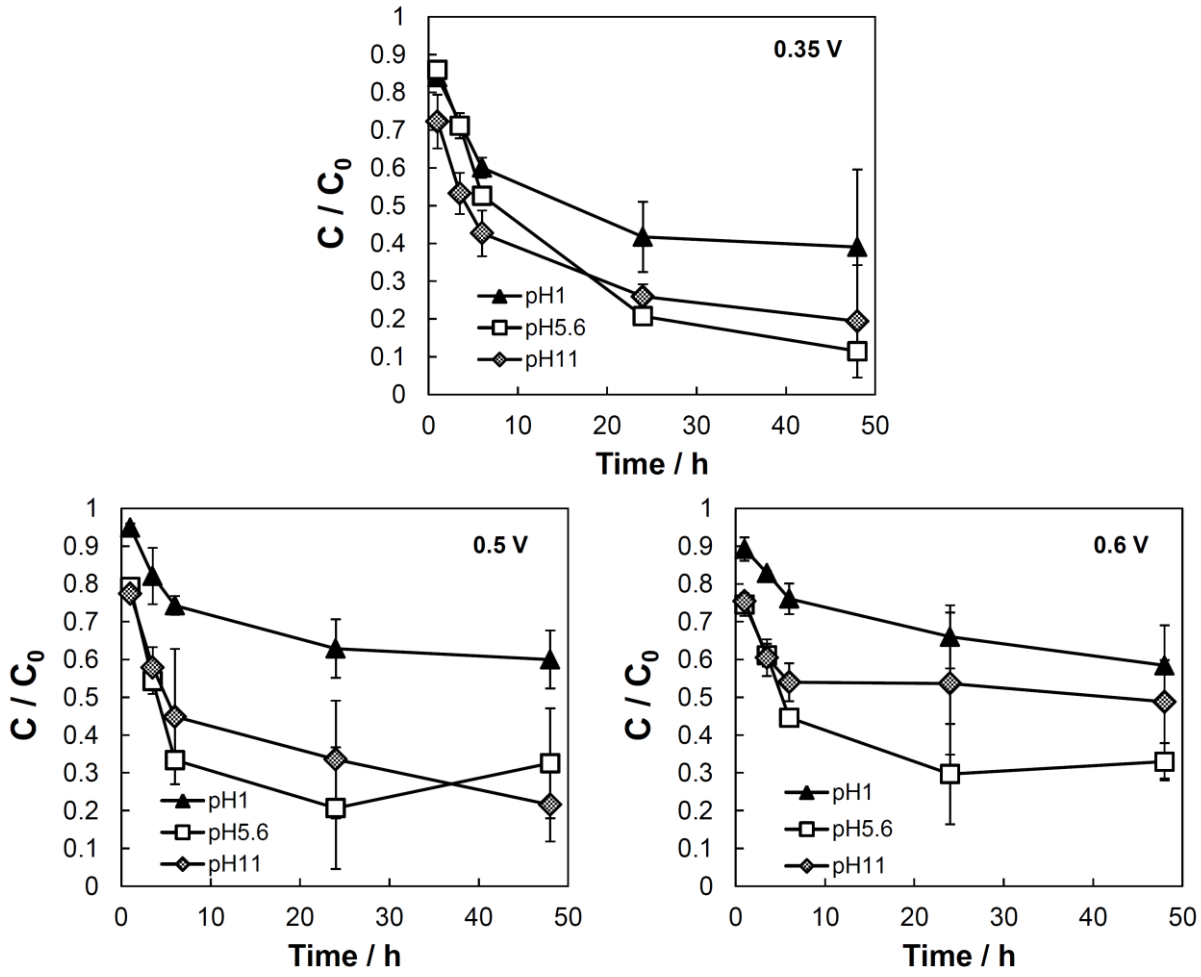

Fig. 11. Adsorption of Cs^+ using PB-CF (modification potential: 0.35 V, 0.5 V, and 0.6 V, modification time: 10 min) in CsCl solutions.

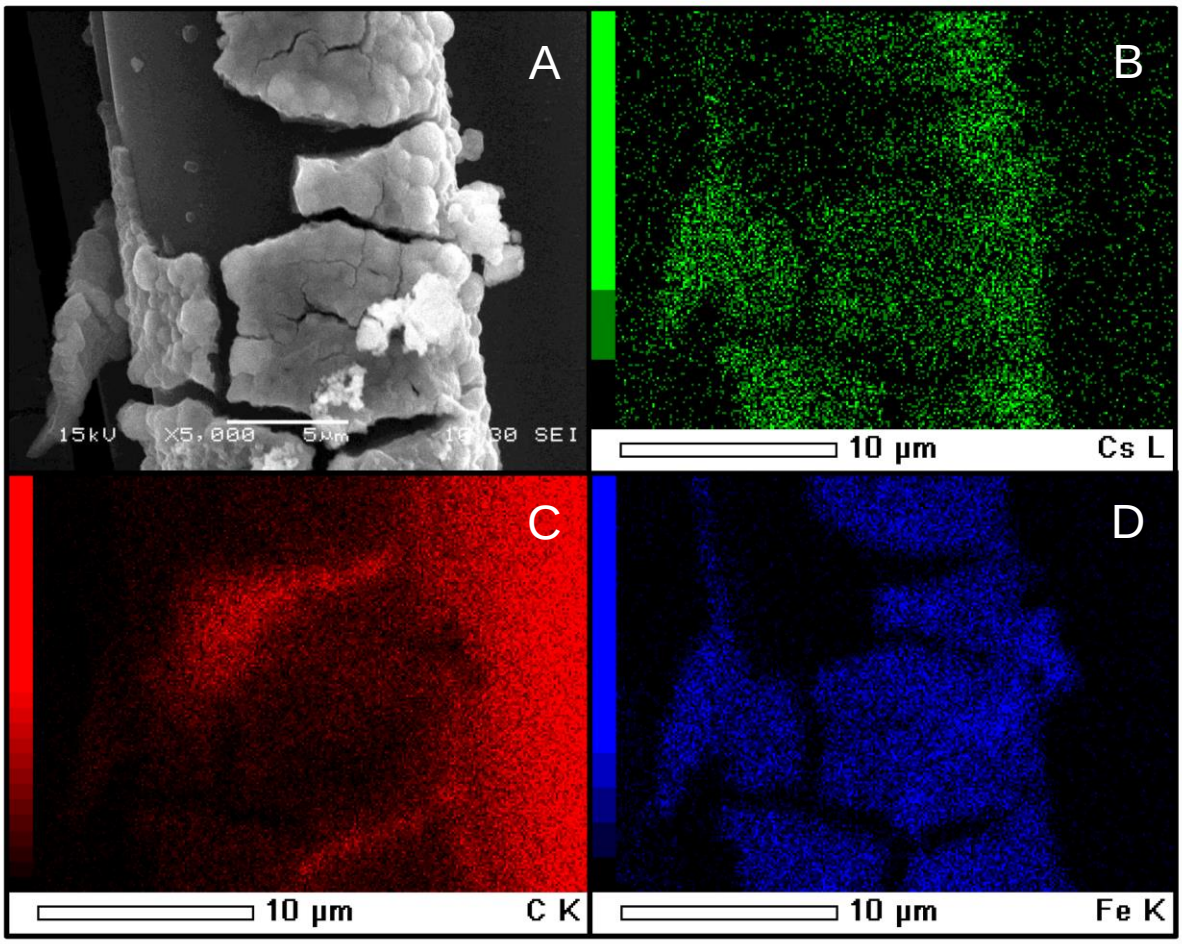

Fig. 12. EDS mapping images of PB-CF surface after 48 h of Cs^+ adsorption in the solution of pH 11. (A) SEM image of PB-CF, (B) Cs on PB-CF, (C) C on PB-CF, and (D) Fe on PB-CF.

2.3.6. Comparison with other PB based adsorbents

The adsorption performance of PB-CF was evaluated from the distribution coefficient (K_d, mL/g) for Cs^+ adsorption. K_d is used as an indicator for the adsorption ability of the adsorbent, and is calculated as:

$$K_d = \frac{(C_0 - C_f)}{C_f} \times \frac{V}{M}$$

where C_0 and C_f are the initial and final concentrations of Cs^+, respectively, after adsorption, V is the volume of the solution (L), and M is the mass of the adsorbent (g). The relationship between the Cs^+ concentration and K_d in the case of PB-CF is shown in Fig. 13. In the concentration of Cs^+ at 5 ppm, the K_d was 22,100 mL/g. This value is lower than that of the other adsorbents using PB: 38,000 mL/g (PB modified magnetic nanoparticles) [27], 8.7×10^5 mL/g (PB modified indium tin oxide) [3], and 73,000 mL/g (insoluble PB) [28]. In addition, the maximum amount of adsorption of PB-CF prepared by applying 0.35 V for 10 min was 6.8 mg/g. This is one-tenth of that for the PB powder [29]. This result is due to the different surface areas of PB and low mass ratio of PB versus CF. However, the K_d of PB-CF was much higher than 5,000 mL/g, which is considered to be a good ability as adsorbents [28,30]. Thus, PB-CF can be used as a sufficient adsorbent for Cs^+.

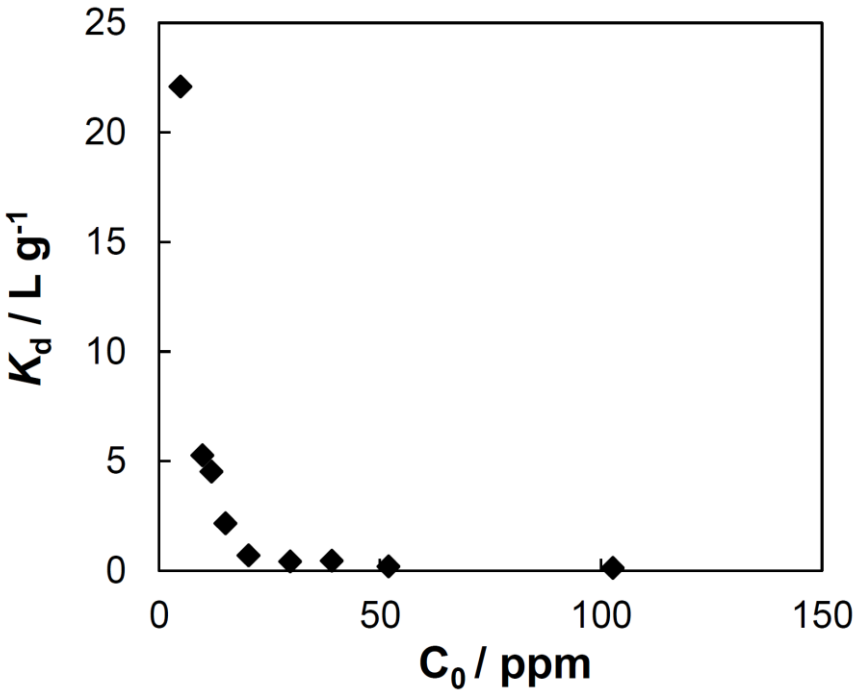

Fig. 13. Distribution coefficient (K_d) of PB-CF for Cs^+ in various initial concentrations (5-100 ppm).

2.4. Conclusions

The modification of PB crystals on carbon materials was demonstrated using an electrochemical method in a mixed solution of $[Fe(CN)_6]^{3-}$ and Fe^{3+}. The shape and amount of modified PB could be controlled by the applied potential and modification time. PB was stably immobilized onto CF in the range of 0.35 V to 0.5 V. The SEM images showed the beadwork pattern of PB rings on the CF surface. The beadwork structure of PB was formed on the CF by applying potentials of 0.2 V or 0.35 V for 10 min. In contrast, PB was deposited as a thin layer with an island structure using potentials of 0.5 V or 0.6 V for 10 min. Adsorption of Cs^+ on PB-CF was achieved, even under basic conditions. Electrochemically modified PB-CF can be applied for Cs^+ removal, and it is useful as an adsorbent over a wide range of pH values, including basic conditions.

Acknowledgements

We would like to thank Open Facility (Hokkaido University, Sousei Hall) for allowing us to use a low vacuum-SEM (JSM-6360LA, JEOL, Japan) to obtain SEM images.

References

[1] K. Itaya, H. Akahoshi, S. Toshima, Electrochemistry of Prussian Blue modified electrodes: an electrochemical preparation method, *J. Electrochem. Soc*. 129 (1982) 1498–1500.

[2] V.D. Neff, Electrochemical Oxidation and Reduction of Thin Films of Prussian Blue, *J. Electrochem. Soc.* 125 (1978) 886–887.

[3] T. Tatsuma, Y. Kuroiwa, K. Ishii, K. Kudo, A. Sakoda, Uptake and electrochemical ejection of cesium ion by a Prussian blue-modified electrode, *Chem. Lett.* 43 (2014) 1281–1283.

[4] X. Zhang, J. Wang, B. Ogorevc, U.S. Spichiger, Glucose nanosensor based on Prussian-Blue modified carbon-fiber cone nanoelectrode and an integrated reference electrode, *Electroanalysis*. 11 (1999) 945–949.

[5] P. Salazar, M. Martín, R. Roche, J.L. González-Mora, R.D. O'Neill, Microbiosensors for glucose based on Prussian Blue modified carbon fiber electrodes for in vivo monitoring in the central nervous system, *Biosens. Bioelectron.* 26 (2010) 748–753.

[6] A.A. Karyakin, O.V. Gitelmacher, E.E. Karyakina, Prussian Blue-based first-generation biosensor. A sensitive amperometric electrode for glucose, *Anal. Chem.* 67 (1995) 2419–2423.

[7] A.A. Karyakin, E.E. Karyakina, L. Gorton, Prussian-Blue based amperometric biosensors in flow-injection analysis, *Talanta*. 43 (1996) 1597–1606.

[8] N. Sonoyama, T. Sakata, Electrochemical continuous decomposition of chloroform and other volatile chlorinated hydrocarbons in water using a column type metal impregnated carbon fiber electrode, *Environ. Sci. Technol.* 33 (1999) 3438–3442.

[9] H. Kuramitz, M. Matsushita, S. Tanaka, Electrochemical removal of bisphenol A based on the anodic polymerization using a column type carbon fiber electrode, *Water. Res.* 38 (2004) 2331–2338.

[10] M. Matsushita, H. Kuramitz, S. Tanaka, Electrochemical Oxidation for Low Concentration of Aniline in Neutral pH Medium: Application to the Removal of Aniline Based on the Electrochemical Polymerization on a Carbon Fiber, *Environ. Sci. Technol*. 39 (2005) 3805–3810.

[11] F. Ricci, A. Amine, G. Palleschi, D. Moscone, Prussian Blue based screen printed biosensors with improved characteristics of long-term lifetime and pH stability, *Biosens. Bioelectron.* 18 (2003) 165–174.

[12] A.A. Karyakin, E.E. Karyakina, Prussian Blue-based `artificial peroxidase' as a transducer for hydrogen peroxide detection. Application to biosensors, *Sens. Actuat. B.* 57 (1999) 268–273.

[13] B. Sun, X.G. Hao, Z.D. Wang, G.Q. Guan, Z.L. Zhang, Y.B. Li, S.B. Liu, Separation of low concentration of cesium ion from wastewater by electrochemically switched ion exchange method: experimental adsorption kinetics analysis, *J. Hazard. Mater*. 233-234 (2012) 177–183.

[14] P. Nie, L. Shen, G. Pang, Y. Zhu, G. Xu, Y. Qing, H. Dou, X. Zhang, Flexible metal–organic frameworks as superior cathodes for rechargeable sodium-ion batteries, *J. Mater. Chem. A.* 3 (2015) 16590–16597.

[15] M.B. Robin, The Color and Electronic Configurations of Prussian Blue, *Inorg. Chem.* 1 (1962) 337–342.

[16] K. Itaya, T. Ataka, S. Toshima, Spectroelectrochemistry and electrochemical preparation method of Prussian blue modified electrodes, *J. Am. Chem. Soc.* 104 (1982) 4767–4772.

[17] J. Garcia-Jareno, J. Navarro-Laboulais, A. Sanmatias, F. Vicente, The correlation between electrochemical impedance spectra and voltammograms of PB films in aqueous NH_4Cl and CsCl, *Electrochim. Acta*. 43 (1998) 1045–1052.

[18] K. Itaya, N. Shoji, I. Uchida, Catalysis of the reduction of molecular oxygen to water at Prussian Blue modified electrodes, *J. Am. Chem. Soc.* 106 (1984) 3423–3429.

[19] R. Garjonyte, A. Malinauskas, Operational stability of amperometric hydrogen peroxide sensors, based on ferrous and copper hexacyanoferrates, *Sens. Actuators B.* 56 (1999) 93–97.

[20] R. Koncki, O.S. Wolfbeis, Composite films of Prussian blue and N-substituted polypyrroles: fabrication and application to optical determination of pH, *Anal. Chem.* 70 (1998) 2544–2550.

[21] A.A. Karyakin, E.E. Karyakina, L. Gorton, On the mechanism of H_2O_2 reduction at Prussian Blue modified electrodes, *Electrochem. Commun.* 1 (1999) 78–82.

[22] E.R. Nightingale, Jr., Phenomenological Theory of Ion Solvation. Effective Radii of Hydrated Ions, *J. Phys. Chem.* 63 (1959) 1381–1387.

[23] K. Itaya, I. Uchida, V.D. Neff, Electrochemistry of polynuclear transition metal cyanides: Prussian Blue and its analogues, *Acc. Chem. Res.* 19 (1986) 162–168.

[24] R. Chen, H. Tanaka, T. Kawamoto, M. Asai, C. Fukushima, H. Na, M. Kurihara, M. Watanabe, M. Arisaka, T. Nankawa, Selective removal of cesium ions from wastewater using copper hexacyanoferrate nanofilms in an electrochemical system, *Electrochimica Acta*, 87 (2013) 119–125.

[25] N.L. Hakem, I. Al Mahamid, J.A. Apps, G.J. Moridis, Sorption of Cesium and Strontium on Hanford Soil, *J. Radioanal. Nucl. Chem.* 246 (2000) 275–278.

[26] M.M. Hamed, M. Holiel, I.M. Ahmed, Sorption behavior of cesium, cobalt and europium radionuclides onto hydroxyl magnesium silicate, *Radiochim. Acta*. 104 (2016) 873–890.

[27] C. Thammawong, P. Opaprakasit, P. Tangboriboonrat, P. Sreearunothai, Prussian blue-coated magnetic nanoparticles for removal of cesium from contaminated environment, *J. Nanopart. Res.* 15 (2013) 1689–1698.

[28] T. Sangvanich, V. Sukwarotwat, R.J. Wiacek, R.M. Grudzien, G.E. Fryxell, R.S. Addleman, C. Timchalk, W. Yantasee, Selective capture of cesium and thallium from natural waters and simulated wastes with copper ferrocyanide functionalized mesoporous silica, *J. Hazard. Mat.* 182 (2010) 225–231.

[29] Y. Mihara, M.T. Sikder, H. Yamagishi, T. Sasaki, M. Kurasaki, S. Itoh, S. Tanaka, Adsorption kinetic model of alginate gel beads synthesized micro particle-Prussian blue to remove cesium ions from water, *J. Water Process Eng.* 10 (2016) 9–19.

[30] G.E. Fryxell, Y. Lin, S. Fiskum, J.C. Birnbaum, H. Wu, K. Kemner, S. Kelly, Actinide Sequestration Using Self-Assembled Monolayers on Mesoporous Supports, *Environ. Sci. Technol.* 39 (2005) 1324–1331.

Chapter 3

Application of Electrochemical Immobilized Prussian Blue on Carbon Fiber for Removal of Cesium

3.1. Introduction

In chapter 2, PB-modified CF (PB-CF) showed a high adsorption ability for Cs^+ in wide pH ranges. On the other hand, PB-CF has a low tolerance against attacks by some chemicals. Therefore, for the actual use of PB-CF, the protection of the surface of PB-CF should be considered. PB/polymer composites and polymer-covered PB-modified electrodes have been often reported [1–3]. However, these studies were performed for the development of electrochromical or sensor materials, and there are few studies on protecting of the surface of the adsorbent.

In this chapter, we evaluated the adsorption ability and stability of PB-CF, which was prepared by electrochemically modifying CF. The adsorption behavior of Cs^+ at PB-CF was compared using the isotherm curves of adsorption and a kinetic analysis. Furthermore, in order to protect the PB surface and to improve the stability in solution, PB-CF coated with polyaniline was prepared by electrochemical polymerization. Then the adsorption ability for Cs^+ and stability of PB-CF covered with polyaniline were investigated.

3.2. Materials and methods

3.2.1. Materials

Iron(III) chloride hexahydrate and potassium hexacyanoferrate(III) used for the preparation of PB-CF were purchased from Wako Pure Chemical Industries, Ltd. (Osaka, Japan). Sodium dihydrogen phosphate and disodium hydrogen phosphate dodecahydrate used to prepare buffer solutions were purchased from Wako Pure Chemical Industries, Ltd., and Junsei Chemical Co., Ltd. (Tokyo, Japan), respectively. Ethanol for the hydrophilization of CF was purchased from Junsei Chemical Co., Ltd. For the alkali metal salts used in the adsorption experiment, a cesium standard solution (1000 mg/L) was purchased from Junsei Chemical Co., Ltd. Sodium chloride and ammonium chloride were purchased from Wako Pure Chemical Industries, Ltd. Hydrochloric acid and sodium hydroxide for pH adjustment were purchased from Kanto Chemical Co., Inc. (Tokyo, Japan) and Junsei Chemical Co., Ltd., respectively. Potassium chloride used for an electrolyte, adsorption experiments, and Cs^+ analysis by atomic adsorption spectroscopy (AAS) was purchased from Junsei Chemical Co., Ltd. Aniline and Nafion® perfluorinated resin solution used for polymer coating were purchased from Wako Pure Chemical Industries, Ltd., and Sigma-Aldrich Co., LLC. (USA), respectively. Oxalic acid was purchased from Wako Pure Chemical Industries, Ltd. The 28% ammonia solution and ethylenediamine-N,N,N',N'-tetraacetic acid for the preparation of the solution after adsorption of Cs^+ in oxalic acid solution were purchased from Junsei Chemical Co., Ltd., and Dojindo Molecular Technologies, Inc. (Kumamoto, Japan), respectively. Iron(II) sulfate heptahydrate and Sulfuric acid 95%

used for the detection of ferrocyanide were purchased from Wako Pure Chemical Industries, Ltd. All reagents were of analytical grade and were used without any prior treatment.

3.2.2. Electrochemical modification of Prussian blue

PB immobilized CF (PB-CF) were prepared by the methods described in Chapter 2.2.2.

3.2.3. Preparation of polymer-coated PB-CF

Polyaniline-coated PB-CF (PAn-PB-CF) was prepared by repeating the cycle scans between -0.2 V and 1.0 V at a scan rate of 100 mV/s for 20 times in 10 mM aniline, 0.1 M KCl and, 6 mM HCl by using the PB-CF as a working electrode. In this process, aniline was polymerized on the PB-CF surface. Nafion®-coated PB-CF (Naf-PB-CF) was prepared by immersing PB-CF in 5 wt% Nafion® dispersed solution, and then dried in air. These prepared polymer-coated PB-CFs were stored in the dark at room temperature.

3.2.4. Characterization of PB-CF and PAn-PB-CF

The characterization of PB-CF and PAn-PB-CF was carried out by cyclic voltammetry (CV), scanning electron microscopy (SEM), and X-ray photoelectron spectroscopy (XPS). The morphological structure of the PB-CF was observed by a low vacuum-SEM (JSM-6360LA, JEOL, Japan). A fully automatic X-Ray photoelectron

spectroscopy XPS-7000 (Rigaku Denki, Japan) was used for XPS analysis.

3.2.5. Adsorption study

All adsorption experiments were performed using the batch method. one cm × one cm PB-CF sheet was immersed in 10 mL of Cs^+ solution and slowly shaken for a constant time at room temperature. After adsorption, the PB-CF was removed from the solution, and Cs^+ remaining in the solution was measured by AAS (A-2000 Hitachi, Japan) at 852.11 nm with air-acetylene gas. In order to prevent the ionization of Cs, 1000 ppm of K^+ was added to the sample solutions before the measurement. Kinetic studies were performed by using PB-CF prepared at the potentials of 0.35, 0.5, and 0.6 V. These adsorbents were immersed in 10, 20, and 30 ppm of Cs^+ solution without any pH adjustment and shaken for 1−48 h. Equilibrium adsorption experiments were carried out using the PB-CF prepared at the potential of 0.35 V. The initial concentrations of Cs^+ solution ranged from 5 ppm to 100 ppm, and the shaking time was 72 h at room temperature. The amount of adsorbed Cs^+ was calculated by Eq. (1).

$$Q = \frac{(C_0 - C_e)V}{W} \quad (1)$$

where Q is the amount of adsorbed Cs^+ (mg g^{-1}); C_0 and C_e are the initial and equilibrium concentrations of Cs^+ in the solution (mg L^{-1}), respectively; V is the volume of Cs^+ solution (L); and W is the weight of the PB-CF (g). The equilibrium times were 48 h for PB-CF prepared at 0.5 V and 0.6 V, 72 h for PB-CF prepared at

0.35 V, respectively. The effect of coexisting cations on Cs^+ adsorption was also investigated. An adsorption test in the presence of coexisting cations was carried out using 5 ppm of Cs^+ solution containing 50, 500, and 5000 ppm of Na^+, K^+, and NH_4^+, respectively, for 24 h.

3.2.6. Adsorption behavior of PAn-PB-CF in the presence of oxalic acid

An adsorption experiment in the presence of oxalic acid was also carried out. PAn-PB-CF was immersed in Cs^+ solution during a constant time at room temperature. After that, the PAn-PB-CF was taken away from the solution, and 2 mM of ethylenediamine-N,N,N',N'-tetraacetic acid solution (adjusted to pH 11.4 with NH_4OH solution) was added and PB particle detached from PAn-PB-CF was decomposed. The remaining amount of Cs^+ in the solution was measured by AAS.

3.2.7. Suppression of elution of ferrocyanide ion using PAn-PB-CF

An eluted ferrocyanide ion by decomposition of PB was measured by the official method. Iron sulfate(II) (0.2 M, containing about 1% sulfuric acid) was added to a solution after the Cs^+ adsorption experiment, followed by the reaction of Fe^{2+} with free ferrocyanide ion in the solution. After that, the absorbance after 30 minutes was measured at the wavelength of 720 nm.

3.3. Results and discussion

3.3.1. Adsorption study using PB-CF

3.3.1.1. Adsorption behavior of Cs^+ and kinetic study

In Chapter 2, the electrochemical immobilization of PB on CF was carried out at several modification potentials, and the adsorption property of PB-CF for Cs^+ was investigated. In this Chapter, PB-CFs prepared by applying the potentials of 0.35, 0.5, and 0.6 V for 10 min were used to investigate the adsorption behavior of Cs^+ in more detail. SEM images of the PB-CF are shown in Fig. 1. As shown in Chapter 2, the surface of the CF without modification was smooth but the layer of PB on CF was observed after modification by applying a constant potential. The thickness of the PB layer and the morphology were remarkably different between 0.35 V and 0.5, 0.6 V of the modification potential. The differences affected the adsorption ability of Cs^+ and the stability of PB-CF. When one cm × one cm PB-CF sheet was immersed in 10 mL of the 5-ppm Cs^+ solution and shaken at room temperature, the adsorption efficiency of Cs^+ on PB-CF from water at three different pHs are listed in Table 1. At pH 5.6, the removal of more than 70% of Cs^+ was achieved by the PB-CFs modified by every potential. The high adsorption efficiency was achieved by using the PB-CF prepared by the potentials of 0.35 V and 0.5 V even at pH 11.

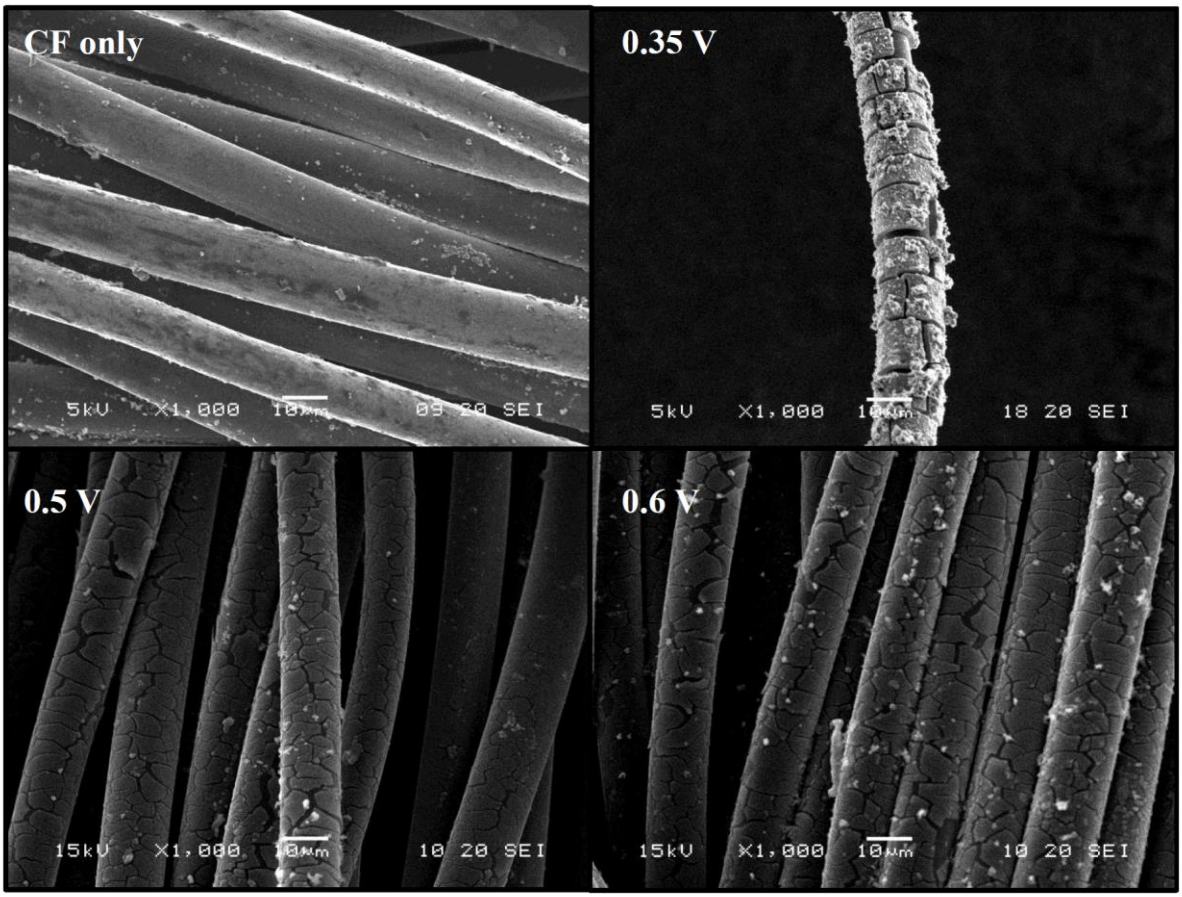

Fig. 1. SEM images of CF and PB-CF modified at 0.35, 0.5, and 0.6 V for 10 min.

Table 1. Amounts of PB on PB-CF modified by different potentials and Cs^+ adsorption ratio at several pH values.

Modification potential/V	Weight of PB/mg g^{-1}	Cs^+ adsorption raito		
		pH 1	pH 5.6	pH 11
0.35	72.6	61.0%	88.5%	80.6%
0.5	55.8	40.0%	79.4%	78.5%
0.6	32.0	41.6%	70.4%	51.2%

A kinetics study was performed in order to analyze the adsorption behavior of Cs^+ on the PB-CF. The adsorption behavior of Cs^+ was compared in 10, 20, and 30 ppm of Cs^+ solution for 1–48 h. The pseudo-first-order equation of Lagergren is widely used, and this equation is given as follows:

$$\ln(Q_e - Q_t) = \ln Q_e - k_1 t \quad (2)$$

where Q_e and Q_t are the amounts of adsorbed Cs^+ at the equilibrium and t min (mg g^{-1}), respectively, and k_1 is the constant of the pseudo first order (min^{-1}) [4,5]. A pseudo-second-order model was also applied to analyze the experimental data. This model has some advantages in that it can evaluate not only the rate constant but also the adsorption capacity of the adsorbents and the initial adsorption rate. It can be expressed as follows:

$$\frac{t}{Q_t} = \frac{1}{k_2 Q_e^2} + \frac{1}{Q_e} t \quad (3)$$

When t approaches 0, the initial adsorption rate h (mg g^{-1} min) can be expressed as

$$h = k_2 Q_e^2 \quad (4)$$

The half time $t_{1/2}$ can be obtained by substituting half of Q_e for Q_t, and it is given as

$$t_{1/2} = \frac{1}{k_2 Q_e} \quad (5)$$

where Q_e and Q_t are the amounts of adsorbed Cs^+ (mg g^{-1}) at equilibrium and at t min, respectively, and k_2 is the constant of the pseudo second order (g mg^{-1} min^{-1}) [5,6]. The adsorption behavior for Cs^+ at several initial concentrations fitted well for the pseudo-second-order model, as shown in Fig. 2. These results of the adsorption amount of Cs^+ per unit weight (Fig. 2A, B, C) and the adsorption ratio (Fig. 2D) indicated that the PB-CF prepared at 0.35 V had the highest adsorption capacity for Cs^+. For the Cs^+ concentration of 10 ppm, more than 90% of Cs^+ was adsorbed. The adsorption rate increased in the order of PB-CFs prepared at 0.35 V, 0.5 V, and 0.6 V. It is suggested that the adsorption rate increased depending on the amount of PB layer on CF and the immobilization amount of PB. The parameters of the pseudo first order and pseudo-second-order are shown in Table 2. The R_2 values (the square of the correlation coefficient) of the pseudo-second-order model were 0.968–0.998. The R_2 values of the pseudo first order were exceptionally low compared with those of the pseudo-second-order model.

The half time $t_{1/2}$ and initial adsorption rate h in 20 and 30 ppm of Cs^+ concentration using the PB-CF prepared at 0.35 V were slightly smaller than those of the other potentials. On the other hand, the Q_e value of PB-CF prepared at 0.35 V was higher than those of the others. Similarly, the k_2 value of the PB-CF modified at 0.35 V showed lower values of 0.82–1.15 × 10^{-3} compared with the other PB-CFs modified at 0.5 V or 0.6 V. This indicated that the thicker PB layer on CF prepared at 0.35 V has a

larger adsorption capacity but a slower adsorption rate for Cs^+ into the internal layer. Meanwhile, for the PB-CFs modified at 0.5 V and 0.6 V, the CF surface is covered with a thin layer of PB. Therefore, the adsorption rate is increased but the adsorption capacity is smaller compared with that prepared at 0.35 V. In these results, the large variations were observed regardless of the initial concentration and modification potential. From the above results, the high adsorption capacity of PB-CF prepared at 0.35 V is suited for the removal of Cs^+ from water.

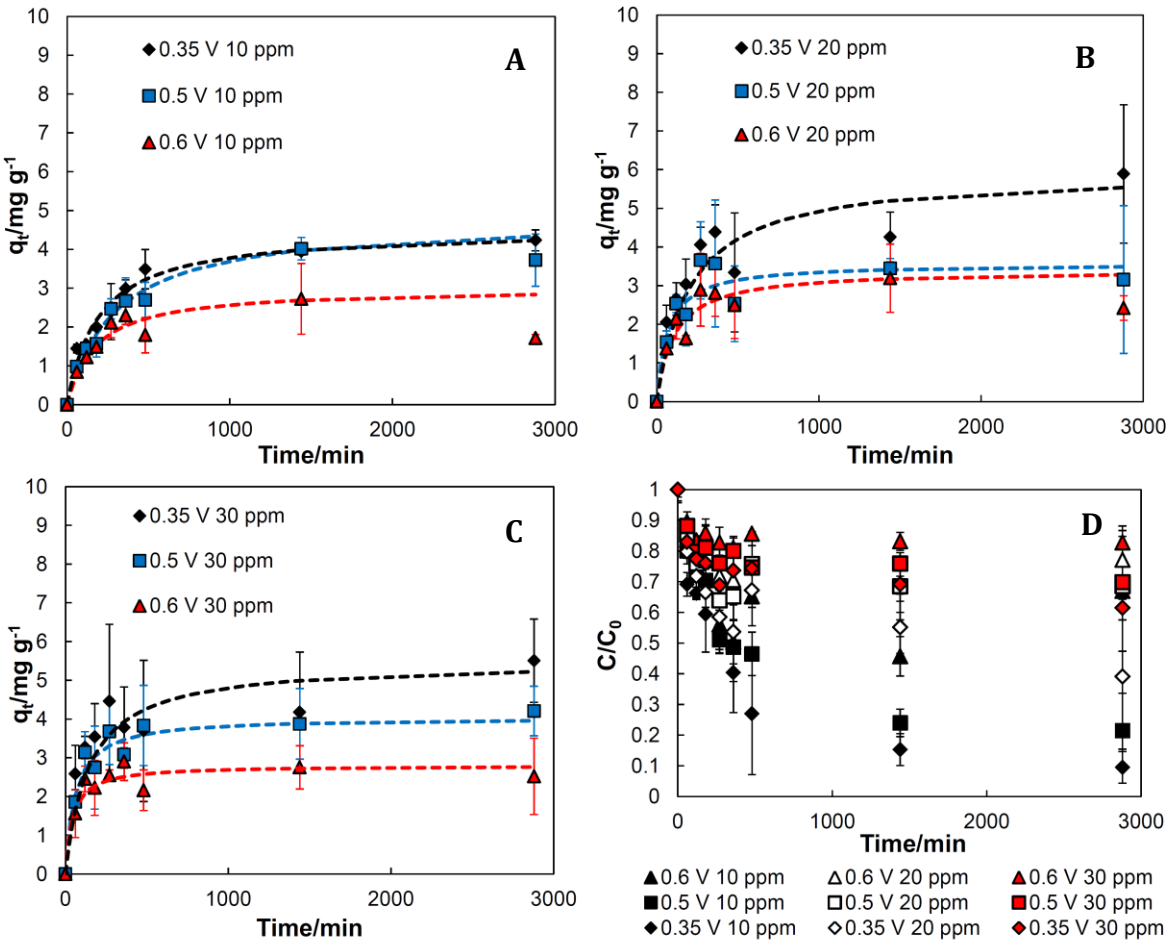

Fig. 2. Adsorption behaviors for Cs^+ on PB-CFs at several initial concentrations (diamond: PB-CF modified by potential of 0.35 V, square: PB-CF modified by potential of 0.5 V, triangle: PB-CF modified by potential of 0.6 V, dashed line: fitting for pseudo second order).

Table 2. Pseudo-first-order and pseudo-second-order kinetics parameters for adsorption of Cs^+.

Modification potential/V	Cs^+/ppm	Pseudo first order			Pseudo second order				
		k_1/min^{-1}	Qe/mg g^{-1}	R^2	k_2/g mg^{-1} min^{-1}	$t_{1/2}$/h	h/mg g^{-1} min^{-1}	Qe/mg g^{-1}	R^2
0.35	10	2.17×10^{-3}	4.23	0.8325	1.15×10^{-3}	3.22	2.33×10^{-2}	4.51	0.9982
	20	1.28×10^{-3}	5.89	0.3674	0.82×10^{-3}	3.43	2.88×10^{-2}	5.93	0.9681
	30	1.48×10^{-3}	5.50	0.2590	1.11×10^{-3}	2.73	3.34×10^{-2}	5.48	0.9788
0.5	10	2.78×10^{-3}	4.02	0.8978	0.71×10^{-3}	4.91	1.62×10^{-2}	4.78	0.9871
	20	3.65×10^{-3}	3.44	0.3667	4.11×10^{-3}	1.14	5.24×10^{-2}	3.57	0.9790
	30	8.31×10^{-3}	3.87	0.6769	4.15×10^{-3}	0.99	6.78×10^{-2}	4.04	0.9953
0.6	10	3.77×10^{-3}	2.72	0.4901	1.92×10^{-3}	2.89	1.73×10^{-2}	3.01	0.9772
	20	5.02×10^{-3}	3.19	0.4114	2.74×10^{-3}	1.79	3.18×10^{-2}	3.40	0.9864
	30	5.82×10^{-3}	2.75	0.0409	8.48×10^{-3}	0.70	6.65×10^{-2}	2.80	0.9896

3.3.1.2 Isothermal curves of PB-CF for Cs^+

The isothermal curves of PB-CF prepared at 0.35 V were measured. The Langmuir isotherm model is calculated as follows:

$$Q_{\mathrm{e}} = \frac{(Q_{\mathrm{m}} K_{\mathrm{L}} C_{\mathrm{e}})}{1 + (\mathrm{K_L} C_{\mathrm{e}})} \tag{6}$$

where Q_e and Q_m are the amount of adsorbed Cs^+ at the equilibrium and the maximum adsorption amount of Cs^+ (mg g^{-1}), respectively; K_L is a constant of the Langmuir isotherm model and relates to the affinity of the binding sites; and C_e is the equilibrium concentration of Cs^+ after adsorption (mg L^{-1}). Two types of linearization patterns were used for the experimental data. Type 1 is linearized as

$$\frac{C_{\mathrm{e}}}{Q_{\mathrm{e}}} = \frac{1}{Q_{\mathrm{m}}} C_{\mathrm{e}} + \frac{1}{K_{\mathrm{L}} Q_{\mathrm{m}}} \tag{7}$$

and type 2 is linearized as:

$$\frac{1}{Q_{\mathrm{e}}} = \left(\frac{1}{K_{\mathrm{L}} Q_{\mathrm{m}}}\right) \frac{1}{C_{\mathrm{e}}} + \frac{1}{Q_{\mathrm{m}}} \tag{8}$$

The Freundlich isotherm model is represented as follows:

$$Q_{\mathrm{e}} = \mathrm{K_F} (C_{\mathrm{e}})^{1/n} \tag{9}$$

where Q_e is the amount of adsorbed Cs^+ at equilibrium (mg g^{-1}); K_F is the constant of the Freundlich isotherm model and relates to the adsorption capacity; C_e is the concentration of Cs^+ in the solution after adsorption (mg L^{-1}); and $1/n$ shows the intensity of adsorption. The adsorption isotherm curves of Cs^+ on PB-CF are shown in Fig. 3, and the parameters are listed in Table 3. The result shows that the adsorption by PB-CF was fitted for the Langmuir model better than the Freundlich model. The Langmuir model corresponds to the monolayer adsorption model. The PB-CF prepared at 0.35 V has a thick layer of PB on the fiber. Only the outer layer and internal layer close to the surface of PB-CF might be available for the strong adsorption of Cs^+. The maximum adsorption amount of Cs^+ calculated by the type-1 Langmuir model was 7.44 mg g^{-1}, and that for the type-2 model was 6.52 mg g^{-1}. The maximum adsorption capacity (Q_m) and distribution coefficient (K_d) for Cs^+ adsorption were compared with other reported adsorbents (Table 4). K_d is calculated as

$$K_d = \frac{(C_0 - C_f)}{C_f} \times \frac{V}{M} \quad (10)$$

where C_0 is the initial concentration of Cs^+ in solution, and C_f is the final concentration of Cs^+ after adsorption (mg L^{-1}). V is the volume of the solution (L), and M is the mass of the adsorbent (g). In Table 4, the values of K_d and Q_m of various types of adsorbent modified with many substances are listed. K_d of PB-CF was on the same order of magnitude as other PB-modified materials. However, the Q_m value of PB-CF was lower than that of other PB-based adsorbents. The Q_m value of PB powder was 10 times

higher than that of PB-CF [7]. This is because of the difference in the surface area. The PB-CF prepared electrochemically has a thick layer of PB-CF, and the contact area for Cs^+ is smaller than that for fine particles of PB.

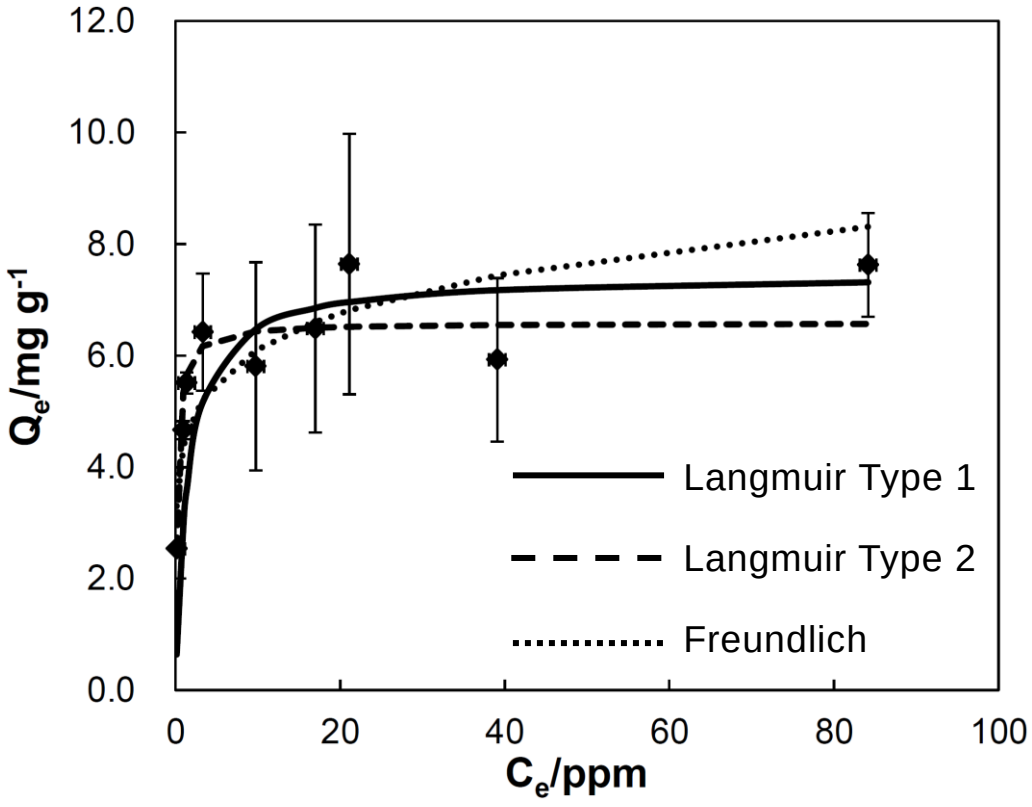

Fig. 3. Adsorption isotherms of PB-CF(modification potential: 0.35 V) for adsorption of Cs^+.

Table 3. Parameters of Langmuir and Freundlich models for adsorption of Cs^+ into PB-CF.

Langmuir 1		Langmuir 2		Freundlich		
Q_m/mg g^{-1}	R^2	Q_m/mg g^{-1}	R^2	K_F	n	R^2
7.44	0.9844	6.52	0.9566	4.37	7.07	0.7495

Table 4. Comparison of distribution coefficient (K_d) and maximum adsorption capacity (Q_m) of PB-CF with other reported adsorbents.

Adsorbent	Substances	K_d/mL g^{-1}	Q_m/mg g^{-1}	Ref.
PB powder			53.2	[7]
PB	Magnetic nanoparticle	38000	96	[8]
PB	Fe_3O_4,	1.2×10^4	46.2963	[9]
PB	Fe_3O_4/GO	5.14×10^4	55.5556	[9]
PB	Fe_3O_4		16.2	[10]
Nickel hexacyanoferrate	Walnut shell	171.4	4.94	[11]
sericite			6.68	[12]
PB	Carbon fiber	22100	7.44	This study

3.3.2. Effect of coexisting cations

To remove Cs^+ by using adsorbents, we have to consider the effect of the coexisting cations. In particular, when removing Cs^+ from wastewater or burned ash, a large amount of salt often exists. Therefore, high selectivity in the adsorption of Cs^+ is required. Cations having a small hydrated radii significantly affect Cs^+ adsorption. Therefore, the adsorption behaviors of PB-CF in the presence of Na^+, K^+, and NH_4^+ were investigated (Fig. 4). A total of 50 ppm, 500 ppm, and 5000 ppm of Na^+, K^+, and NH_4^+ were added to 5 ppm of Cs^+ solution, and the adsorption ratios were compared. The channel radius of PB is about 1.6 Å and the hydrated radii of Na^+, K^+, NH_4^+, and Cs^+ are 1.83, 1.25, 1.25, and 1.19 Å, respectively [13–15]. These results in Fig. 4 indicated that the 5000 ppm of Na^+ and K^+ did not affect the Cs^+ adsorption. In the presence of 5000 ppm of NH_4^+, the adsorption ratio was decreased to half the adsorption ratio without NH_4^+. While Na^+ cannot enter into the lattice of PB owing to

the large hydrated size, both K^+ and NH_4^+ are able to enter into the PB lattice. It is indicated that the NH_4^+ interfered with the adsorption of Cs^+ into the PB lattice more than K^+. A total of 500 ppm of NH_4^+, which is significantly higher than the concentration of NH_4^+ in wastewater and sea water, did not affect the adsorption of Cs^+. These results indicate that PB-CF can be used for the selective adsorption of Cs^+ in the presence of coexisting cations.

On the basis of the result of Cs^+ adsorption behavior in the presence of coexisting ions, the desorption behavior after Cs^+ adsorption and the regeneration of PB-CF were investigated. The detachment of Cs^+ after adsorption was attempted by using NH_4^+, which had the largest effect on the removal of Cs^+ from PB-CF. The results are shown in Fig. 5. By using 0.5 M NH_4Cl as the eluent, in all of PB-CF prepared at three kinds of potentials, about 40% of desorption ratio for Cs^+ could be achieved in 3 h. These results suggested that ion exchange might happen between Cs^+ and NH_4^+.

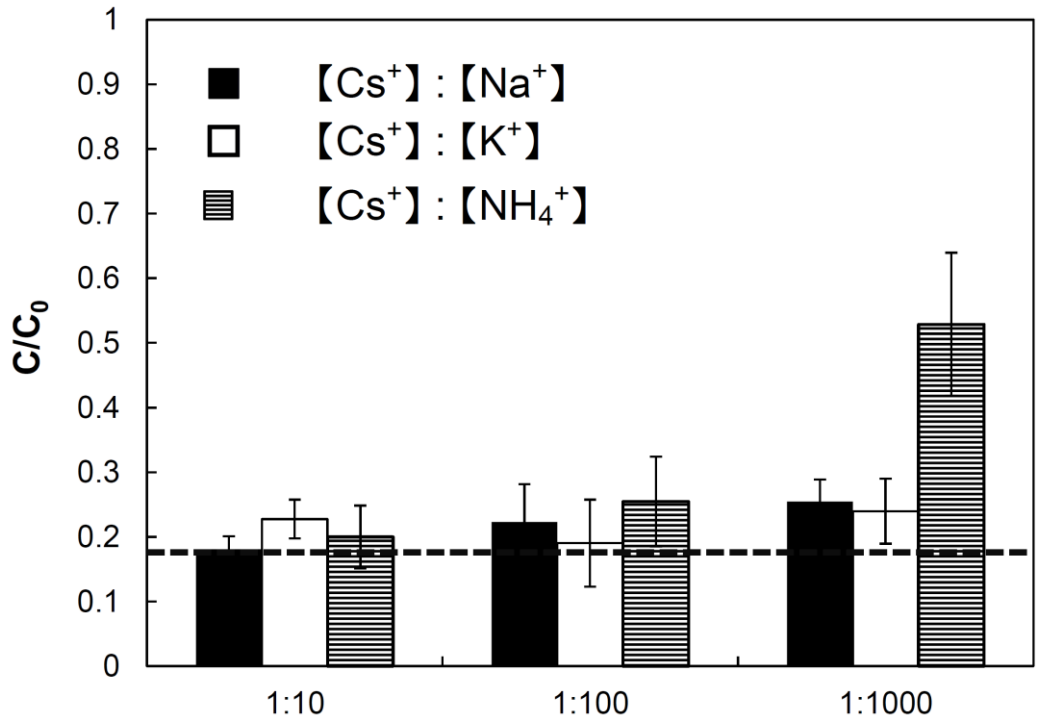

Fig. 4. Cs^+ adsorption with PB-CF in NaCl, KCl, and NH_4Cl solution (dashed line is adsorption ratio of Cs^+ without coexisting cation; ratio was calculated in units of mg/L).

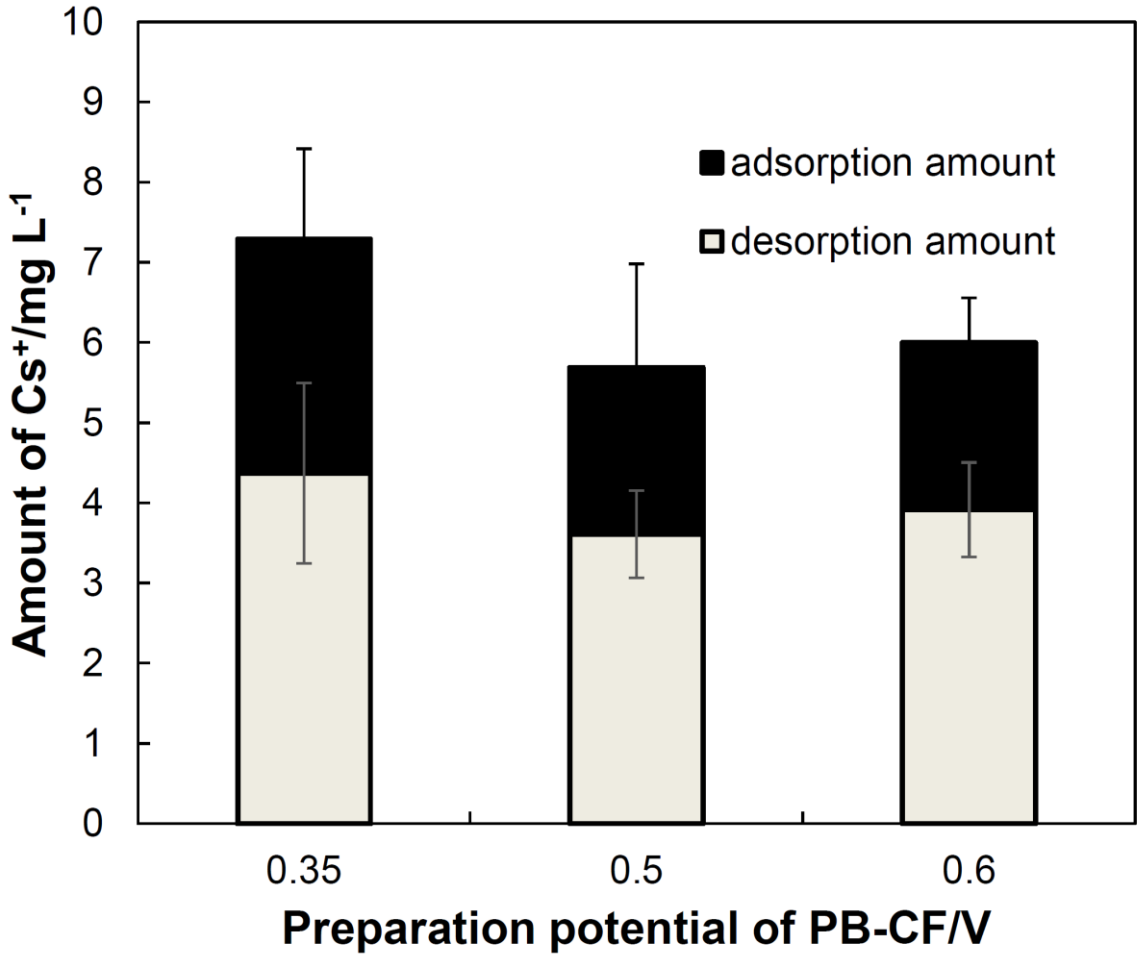

Fig. 5. Adsorption and desorption amount of Cs^+ from PB-CF prepared at several potentials. (Adsorption was performed in 10 mL of 10 ppm Cs^+ solution for 24 h, and desorption was performed in 10 mL of 0.5 M NH_4Cl solution for 3 h)

3.3.3. Characterizations of PB-CF and polyaniline coated PB-CF

For the elution of Cs^+ from fly ash and soil, oxalic acid solution was used in some cases [16–18]. However, it is known that oxalic acid dissolves PB to form a colloidal solution. Therefore, a polyaniline film was coated on the surface of PB-CF by using PB-CF as a working electrode in order to improve the stability. Furthermore, the effect of coating of the PB-CF electrode with polyaniline on the adsorption of Cs^+ and the durability against oxalic acid was investigated. Cyclic voltammograms were recorded using the PB-CF in 10 mM aniline solution. The results are shown in Fig. 6. It is known that the aniline was polymerized by the electrochemical oxidation to form a polyaniline film on the electrode surface [19]. Cycle scans of the CF electrode without PB showed that the oxidation peak near 0.7 V drastically decreased and new redox peaks around 0.2 and 0.4 V appeared (Fig. 6A). These peaks were characteristic responses in the electropolymerization of aniline [20]. A similar result was obtained in cycle scans using PB-CF. The oxidation peak near 0.7 V was decreased, and new peaks appeared around 0.4 V (Fig. 6B). This redox peak overlapped the peaks derived from the redox reaction of PB. These peaks did not disappear even after the cycle scans continued for 10 min. On the other hand, when the concentration of aniline solution was increased to 100 mM, the peaks disappeared after three cycles of scans (Fig. 6C).

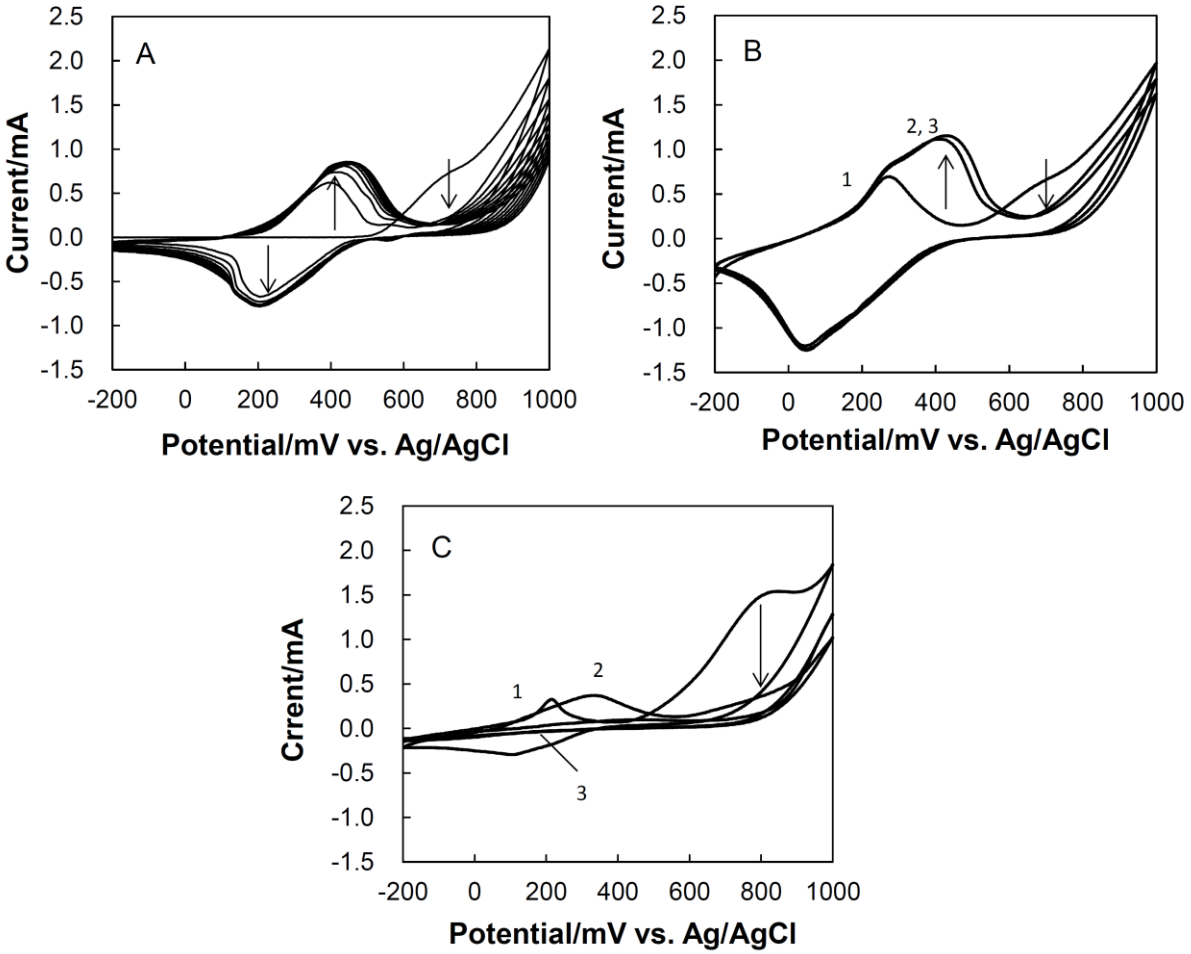

Fig. 6. Cyclic voltammogram of (A) a thread of CF and (B) PB-CF in 10-mM aniline solution, and (C) a thread of PB-CF in 100-mM aniline solution containing 6 mM of HCl and 0.1 M of KCl. Sweep rate: 100 mV/s

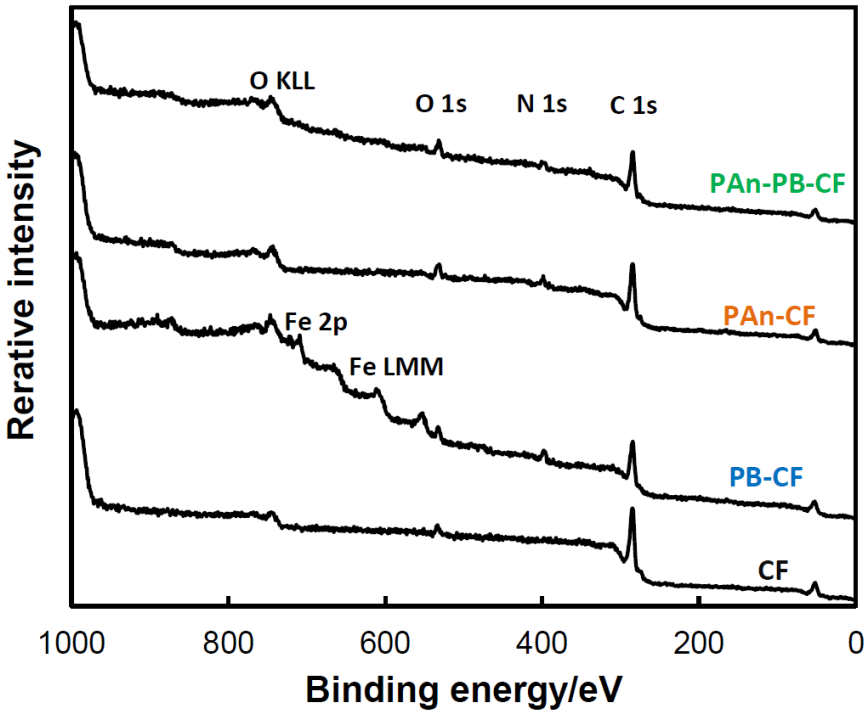

Fig. 7. Wide-range X-ray photoelectron spectra of CF, PB-CF, PAn-CF, and PAn-PB-CF.

Furthermore, the chemical compositions of PB-CF and the PAn-PB-CF surface were observed by an XPS analysis (Fig. 7). The XPS spectra of PB-CF showed Fe peaks (Fe2p and Fe LMM) derived from the component of the PB lattice immobilized on CF. The peaks of 713 eV and 721 eV corresponded to the binding energies of $Fe2p_{3/2}$ and $Fe2p_{1/2}$ in Fe^{3+}, respectively [21]. The peak at 709 eV was derived from $Fe2p_{3/2}$ in $[Fe(CN)_6]^{4-}$ [22,23]. These peaks did not appear clearly in the wide-range spectra of PAn-PB-CF owing to coating with polyaniline. Nevertheless, by comparing the XPS spectra of PAn-PB-CF with polyaniline-coated CF (PAn-CF), an increase in energy intensity was observed in the ranges where the Fe peaks appeared. A N_{1s} peak was observed for all of the adsorbents except for CF. These peaks corresponded to the

peak of C-N as the component of both polyaniline and the PB lattice. From these results, the immobilization of PB on CF and the modification of polyaniline by electrochemical polymerization were confirmed.

3.3.4. Adsorption of Cs in several pH and the stability in the presence of oxalic acid

Polyaniline film coated by the electrochemical polymerization of aniline on PB-CF improved the stability of PB-CF. The effect of polyaniline coating on the adsorption of Cs^+ was investigated. CF, PB-CF, and PAn-PB-CF were immersed in Cs^+ solution, and the amount of Cs^+ adsorption on three kinds of adsorbents for 24 h was compared. This is shown in Fig. 8. The large change in the adsorption ability for 5 ppm of Cs^+ was not observed with the polyaniline coating. The polyaniline film on the PB surface did not interrupt the adsorption of Cs^+ into PB.

Fig. 9 shows the results when Nafion®-coated PB-CF (Naf-PB-CF) and PAn-PB-CF were immersed in 0.1 M and 0.01 M oxalic acid. In 0.1 M oxalic acid solution, PB eluted from the surface of PB-CF and Naf-PB-CF just after being immersed in solution for 1 h. Then the solution immediately changed to a blue color. By contrast, the elution of PB was hardly observed in the case of PAn-PB-CF, and the quantity of elution of PB 1 h later was lower than in the other two kinds. In 0.01 M oxalic acid solution, coloration by the elution of PB from PAn-PB-CF was not observed.

The results of an adsorption experiment for Cs^+ in 0.01, 0.1, and 0.5 M oxalic

acid solution are shown in Fig. 10. The PB was eluted in 0.1 M and 0.5 M oxalic acid solution with time, and 75% and 95% of Cs^+ remained in the solution, respectively. However, in 0.01 M oxalic acid solution, 85% of the Cs^+ in solution was removed after 24 h. From these results, it was clarified that coating with polyaniline on PB-CF improved the stability and maintained the adsorption ability for Cs^+ in the 0.01 M oxalic acid solution. Polyaniline has positive charges in strongly acidic conditions of oxalic acid solution [24,25]. Therefore, it is considered that the electrostatic interaction between the positive charge of the polyaniline film and oxalate ions having a negative charge prevented oxalic acids from entering into the polyaniline film and reacting with PB. Another hypothesis is due to physical blocking by polyaniline film formed on PB-CF. The invasion of oxalate ions into the inside of the polyaniline may be inhibited by the polyaniline film uniformly formed on the PB-CF surface by cyclic scan of potentials. Therefore, the application of PAn-PB-CF to Cs^+ removal in the presence of organic acids such as oxalic acid was suggested to be possible.

The effect of polyaniline coating on Cs^+ adsorption in oxalic acid solution was investigated under different conditions for coating. PAn-PB-CF was prepared by 20 cycles of repeated potential sweeping between -0.2 V and 1.0 V in 10 mM and 100 mM aniline solution (Fig. 11 A and B), and prepared by applying a constant potential of 0.8 V in a 10 mM aniline solution for 8 min (Fig. 11C). These were used for the adsorption experiments of Cs^+. As a result, PAn-PB-CF prepared by potential sweep (Fig. 11 A and B) showed the same rate of Cs^+ adsorption after 24 h. On the other hand, PAn-PB-CF prepared by a constant potential of 0.8 V showed a Cs^+ adsorption rate of

about 20% lower than that of the PAn-PB-CF prepared by potential sweeping in the 0.01 M oxalic acid solution. From these results, it is considered that a more stable polyaniline film was formed by sweeping the potential.

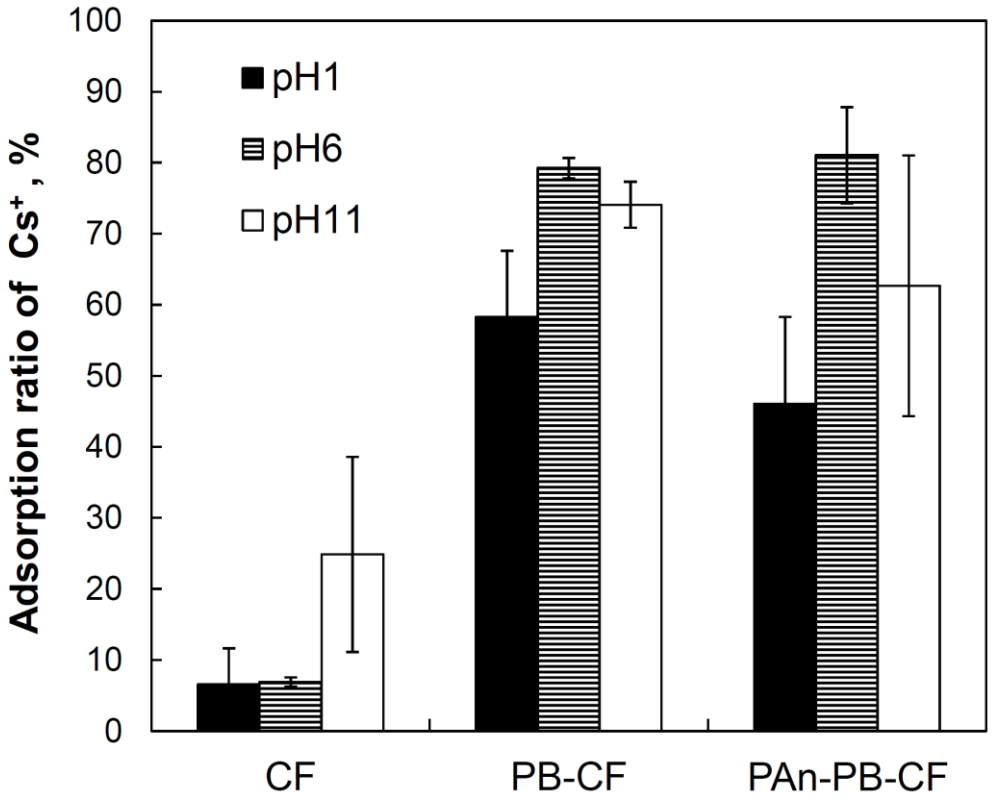

Fig. 8. Adsorption of Cs^+ using CF, PB-CF (PB modification potential: 0.35 V), and PAn-PB-CF in 5 ppm of CsCl solution.

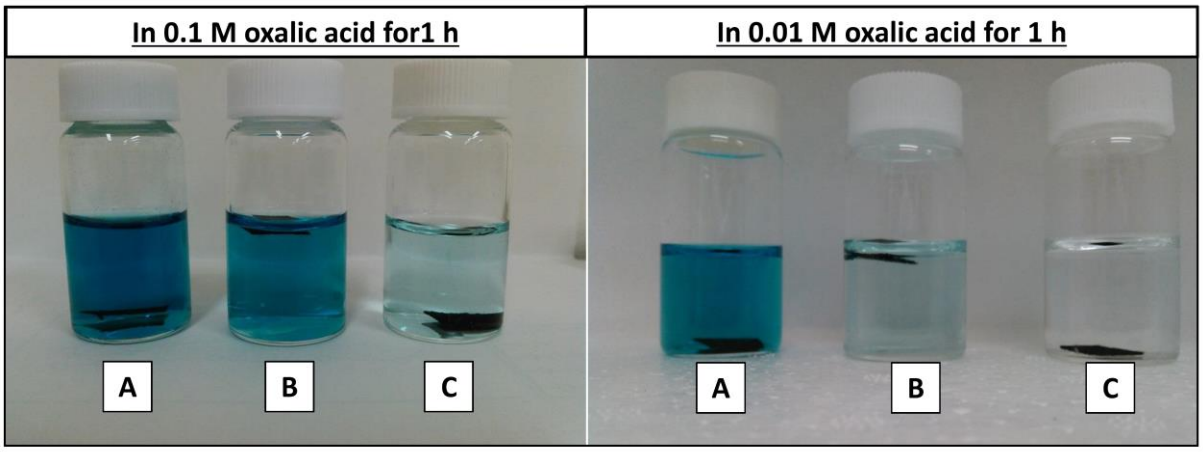

Fig. 9. Stability of PB on surface of (A) PB-CF, (B) Naf-PB-CF and (C) PAn-PB-CF in 0.1 M and 0.01 M oxalic acid.

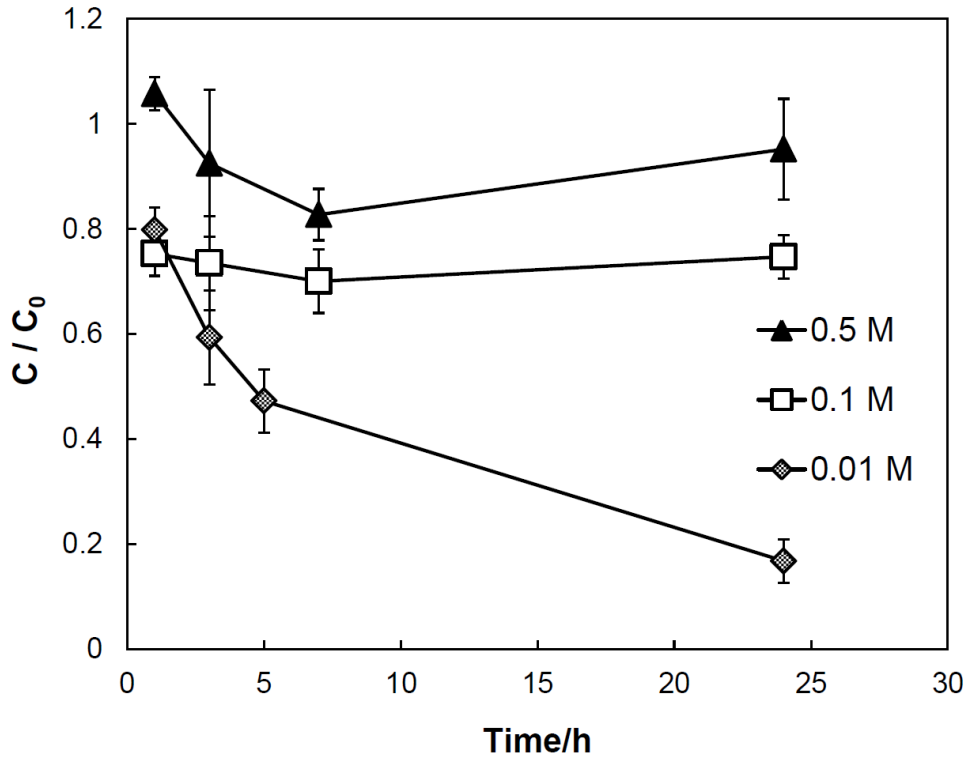

Fig. 10. Adsorption of 5 ppm Cs^+ using PAn-PB-CF containing 0.01, 0.1, and 0.5-M oxalic acid solutions.

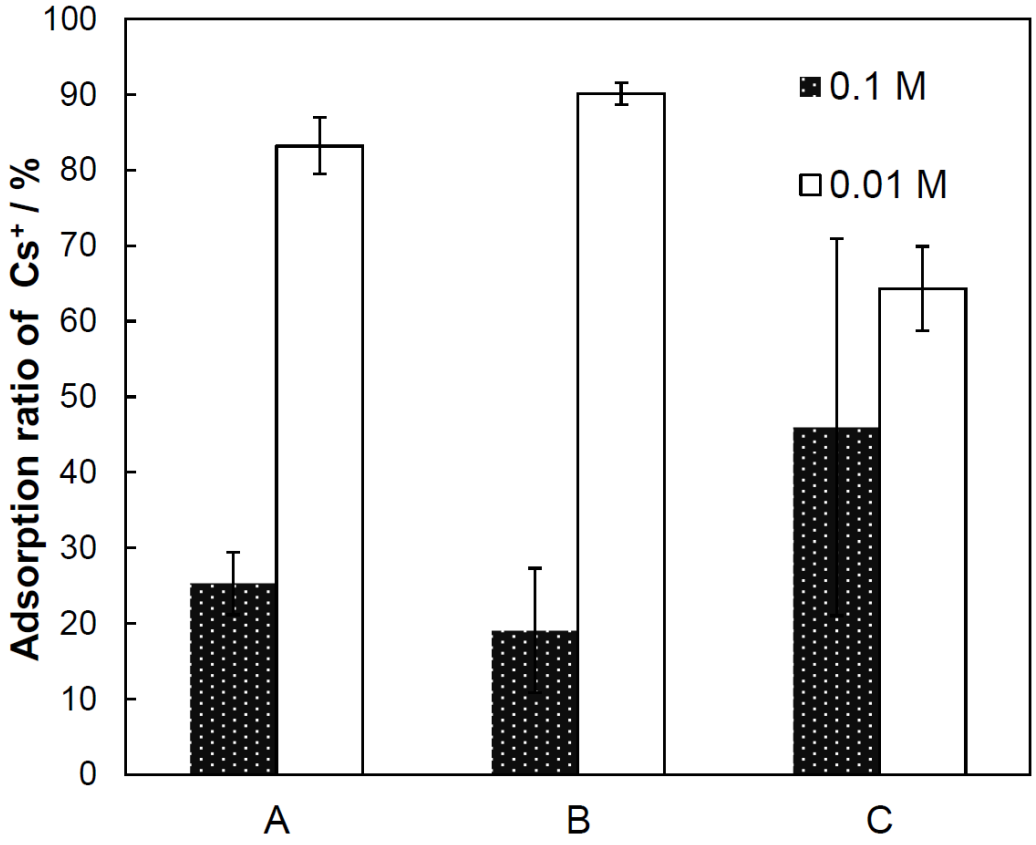

	Coting method	Concentration of Aniline
A	CV	10 mM
B	CV	100 mM
C	Constant potential	10 mM

Fig. 11. Adsorption of 5 ppm Cs^+ from 0.1-M and 0.01-M oxalic acid solution for 24 h using (A) PAn-PB-CF prepared by cycle scans (between -0.2 V and 1.0 V) in 10-mM aniline solution, (B) PAn-PB-CF prepared by cycle scans (between -0.2 V and 1.0 V) in 100-mM aniline solution, and (C) PAn-PB-CF prepared by constant potential of 0.8 V in 10-mM aniline solution.

3.3.5. Elution of PB component during Cs^+ adsorption and suppression of ferrocyanide by polyaniline coating

The amount of eluted iron and ferrocyanide ion after Cs^+ adsorption was shown in Fig. 12 and Fig. 13. The eluted iron ions were less than 1 ppm at pH 1 and pH 5.6 and 3-7 ppm at pH 11. Consequently, the elution amount of iron ions in any pH region was below the Japanese wastewater standard for soluble iron (10 mg/L). However, the elution amount of ferrocyanide ions after the adsorption test was very high over pH 11. Because the ferrocyanide ion contains cyanide in the structure, it is a subject to control the total amount as total cyanide compounds. Therefore, the suppression of dissolution of ferrocyanide ion from PB-CF by polyaniline coating was investigated (Fig. 14). As a result, it was confirmed that the elution amount of ferrocyanide from PB-CF decreased in accordance with the aniline concentration at the preparation of PAn-PB-CF. When PAn-PB-CF prepared in 100 mM aniline solution was used, the elution amount of ferrocyanide ion was reduced to about a half when PB-CF was used. Since the polyaniline film is neutral under basic conditions, suppression of elution of this ferrocyanide is considered to be due to containment for ferrocyanide to inside of the film of the polyaniline film. From this result, it seems that it becomes possible to prevent a secondary contamination due to the decomposition of the adsorbent.

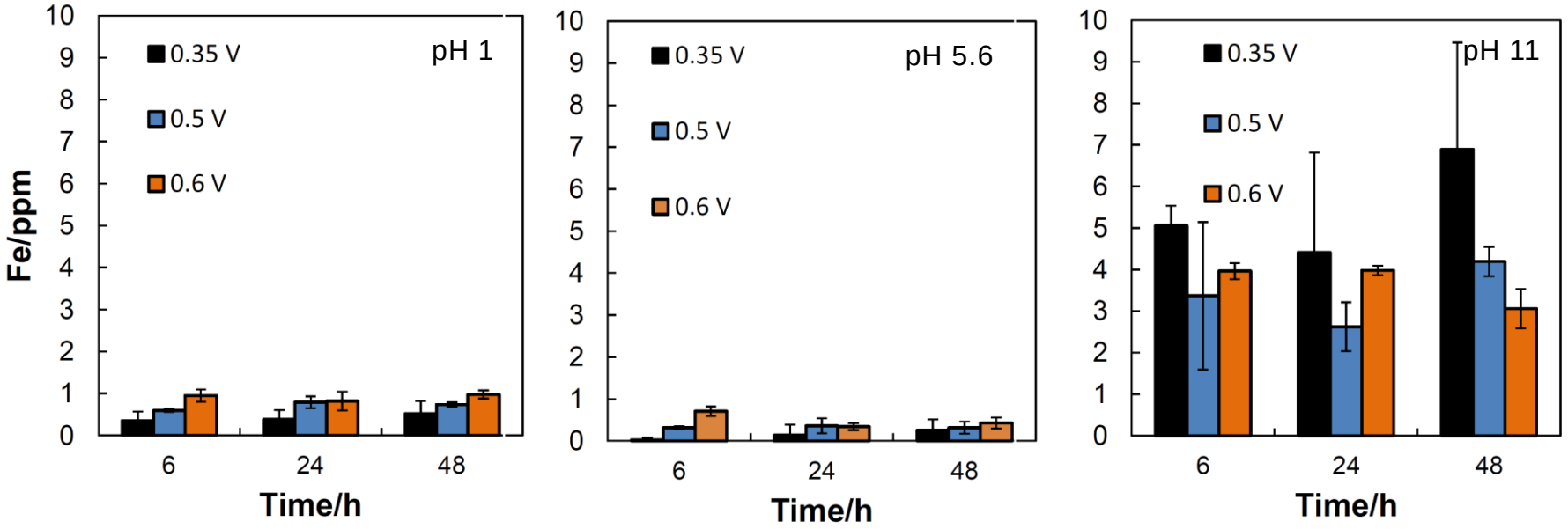

Fig. 12. Elution amount of iron ion from PB-CF after adsorption of Cs^{+} in pH 1, 5.6, and 11.

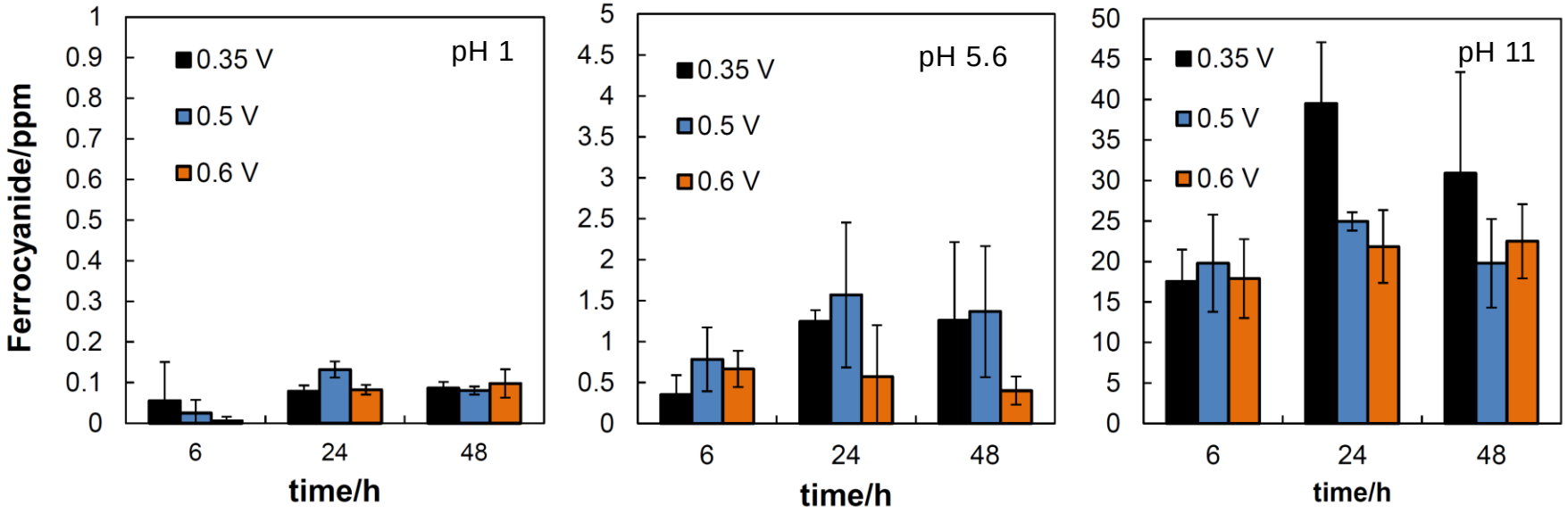

Fig. 13. Elution amount of ferrocyanide ion from PB-CF after adsorption of Cs^+ in pH 1, 5.6, and 11.

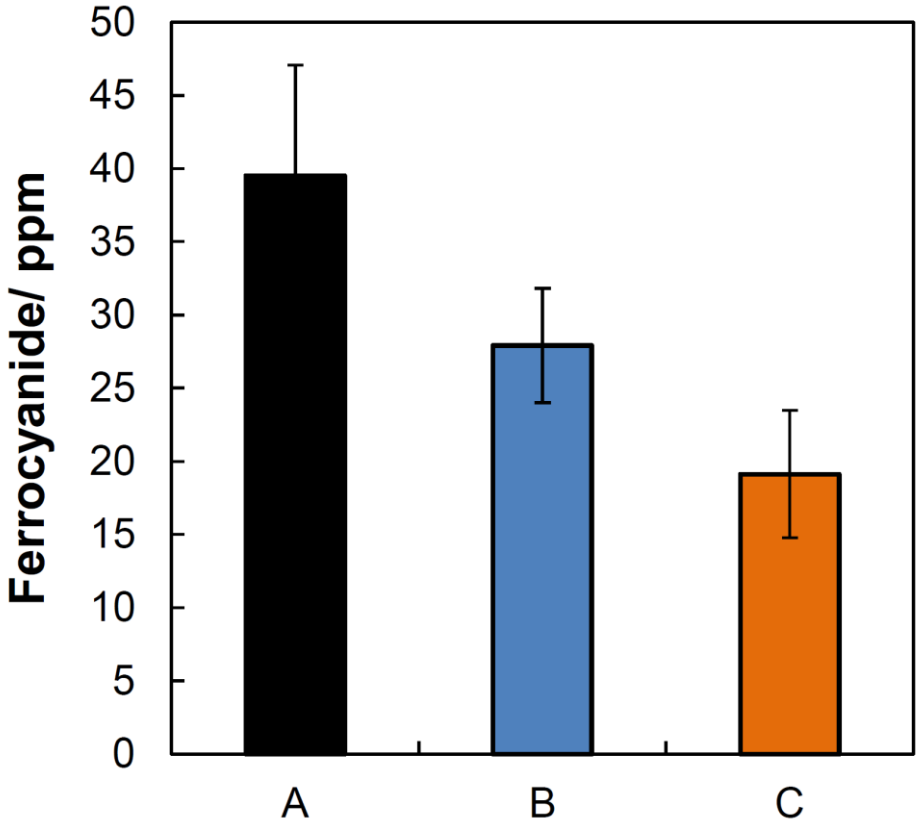

Fig. 14. Elution amount of ferrocyanide ion at pH 11 (containing 5 ppm of Cs^+). (A) PB-CF prepared at 0.35 V, (B) PAn-PB-CF prepared by 10 mM aniline solution, and (C) PAn-PB-CF prepared by 100 mM aniline solution.

3.4. Conclusion

Prussian blue on carbon fiber was prepared by the electrochemical method, and the its usage as an adsorbent of Cs^+ was examined. All of the PB-CF prepared at the potentials of 0.35, 0.5, and 0.6 V showed good adsorption performance for Cs^+, and the PB-CF prepared at 0.35 V had the highest adsorption capacity among the three types of PB-CF. A pseudo-second-order kinetics model and Langmuir isotherm were fitted well for the adsorption experimental data. The value of the maximum adsorption capacity of PB-CF prepared at 0.35 V was 6.89 mg/g. Furthermore, the PB-modified carbon material was coated with a polyaniline film, and the influence on stability was examined under various kinds of conditions. A change in stability was not observed in PAn-PB-CF in a wide pH region, but the stability in an oxalic acid solution was improved. In addition, the elution of ferrocyanide accompanying decomposition of PB could be suppressed by coating with polyaniline The application of PB-CF to Cs^+ adsorption under a variety of conditions was suggested by coating it with polyaniline.

Acknowledgements

We would like to thank the Open Facility (Hokkaido University, Sousei Hall) for allowing us to use a low vacuum-SEM (JSM-6360LA, JEOL, Japan) to obtain SEM images.

References

[1] D.M. DeLongchamp, P.T. Hammond, High-Contrast Electrochromism and Controllable Dissolution ofAssembled Prussian Blue/Polymer Nanocomposites, *Adv. Funct. Mater.* 14 (2004) 224–232.

[2] D.M. DeLongchamp, P.T. Hammond, Multiple-color electrochromism from layer-by-layer-assembled polyaniline/Prussian blue nanocomposite thin films, *Chem. Mater.* 16 (2004) 4799–4805.

[3] W. Zhao, J.J. Xu, C.G. Shi, H.Y. Chen, Multilayer membranes via layer-by-layer deposition of organic polymer protected Prussian blue nanoparticles and glucose oxidase for glucose biosensing, *Langmuir.* 21 (2005) 9630–9634.

[4] S. Lagergren, About the theory of so-called adsorption of soluble substance, *K. Sven. Vetenskapsakad. Handl*. 24 (1898) 1–39.

[5] Y.S. Ho, G. McKay, Pseudo-second order model for sorption processes, *Process Biochem.* 34 (1999) 451–465.

[6] Y.S. Ho, G. McKay, The kinetics of sorption of divalent metal ions onto sphagnum moss peat, *Water Res.* 34 (2000) 735–742.

[7] Y. Mihara, M.T. Sikder, H. Yamagishi, T. Sasaki, M. Kurasaki, S. Itoh, S. Tanaka, Adsorption kinetic model of alginate gel beads synthesized micro particle-Prussian blue to remove cesium ions from water, *J. Water Process Eng.* 10 (2016) 9–19.

[8] C. Thammawong, P. Opaprakasit, P. Tangboriboonrat, P. Sreearunothai, Prussian blue-coated magnetic nanoparticles for removal of cesium from contaminated environment, *J. Nanopart. Res.* 15 (2013) 1689–1698.

[9] H. Yang, L. Sun, J. Zhai, H. Li, Y. Zhao, H. Yu, In situ controllable synthesis of magnetic Prussian blue/graphene oxide nanocomposites for removal of radioactive cesium in water, *J. Mater. Chem. A.* 2 (2014) 326–332.

[10] T. Sasaki, S. Tanaka, Magnetic separation of cesium ion using Prussian blue modified magnetite, *Chem. Lett*. 41 (2012) 32-34.

[11] D. Ding, Y. Zhao, S. Yang, W. Shi, Z. Zhang, Z. Lei, Y. Yang, Adsorption of cesium from aqueous solution using agricultural residue – Walnut shell: Equilibrium, kinetic and thermodynamic modeling studies, *Water. Res.* 47 (2013) 2563–2571.

[12] J.O. Kim, S.M. Lee, C. Jeon, Adsorption characteristics of sericite for cesium ions from an aqueous solution, *Chem. Eng. Res. Des*. 92 (2014) 368–374.

[13] K. Itaya, T. Ataka, S. Toshima, Spectroelectrochemistry and electrochemical preparation method of Prussian blue modified electrodes, *J. Am. Chem. Soc*. 104 (1982) 4767–4772.

[14] E.R. Nightingale, Jr., Phenomenological theory of ion solvation. Effective radii of hydrated ions, *J. Phys. Chem.* 63 (1959) 1381–1387.

[15] K. Itaya, I. Uchida, V.D. Neff, Electrochemistry of polynuclear transition metal cyanides: Prussian blue and its analogues, *Acc. Chem. Res.* 19 (1986) 162–168.

[16] Y. Fujikawa, H. Ozaki, X. Chen, S. Taniguchi, R. Takanami, A. Fujinaga, S. Sakurai, P. Lewtas, Extractability and chemical forms of radioactive cesium in designated wastes investigated in an on-site test, In: Takahashi T. (eds) Radiological Issues for Fukushima's Revitalized Future. Springer (2016), pp 89–107.

[17] N. Kozai, S. Suzuki, N. Aoyagi, F. Sakamoto, T. Ohnuki, Radioactive fallout cesium in sewage sludge ash produced after the Fukushima Daiichi nuclear accident, *Water Res.* 19 (1986) 162–168.

[18] Japan Atomic Energy Agency, Sector of Fukushima Research and Development, Japan (2012) Report of the Results of the Decontamination Model Projects. Decontamination Technology Demonstration Test Project 2, Available at: http://fukushima.jaea.go.jp/english/decontamination/pdf/3-2%20Decontamination_Technology_Demonstration_Test_Project-2.pdf. Accessed 30 August 2017.

[19] E.M. Genies, C. Tsintavis, Redox mechanism and electrochemical behaviour or polyaniline deposits, *J. Electroanal. Chem.* 195 (1985) 109–128.

[20] H. Yang, A.J. Bard, The application of fast scan cyclic voltammetry. Mechanistic study of the initial stage of electropolymerization of aniline in aqueous solutions, *J. Electroanal. Chem.* 339 (1992) 423–449.

[21] L. Zhang, A. Zhang, D. Du, Y. Lin, Biosensor based on Prussian blue nanocubes/reduced graphene oxide nanocomposite for detection of organophosphorus pesticides, *Nanoscale.* 4 (2012) 4674–4679.

[22] K.B.Yatsimirskii, V.V. Nemoshkalenko, Yu.P. Nazarenko. V.G. Aleshin, V.V. Zhilinskaya, N.A. Tomashevsky, Use of X-ray photoelectron and Mössbauer spectroscopies in the study of iron pentacyanide complexes, *J. Electron. Spectros. Relat. Phenom.* 10 (1977) 239–245.

[23] L. Cao, Y. Liu, B. Zhang, L. Lu, In situ controllable growth of Prussian blue nanocubes on reduced graphene oxide: Facile synthesis and their application as enhanced nanoelectrocatalyst for H_2O_2 reduction, *ACS Appl. Mater. Interfaces.* 2 (2010) 2339–2346.

[24] X. Zhang, B. Ogorevc, J. Wang, Solid-state pH nanoelectrode based on polyaniline thin film electrodeposited onto ion-beam etched carbon fiber, *Anal Chim. Acta.* 452 (2002) 1–10.

[25] M. Hassan, K.R. Reddy, E. Haque, S.N. Faisal, S. Ghasemi, A.I. Minett, V.G. Gomes, Hierarchical assembly of graphene/polyaniline nanostructures to synthesize free-standing supercapacitor electrode, *Compos. Sci. Technol*. 98 (2014) 1–8.

Chapter 4

A Simple Colloidal Prussian Blue Solution Based Optical Detection Method for Cesium

4.1. Introduction

In chapter 2 and 3, the high Cs^+ selectivity and adsorption property of PB-CF was demonstrated. Cs^+ is selectively adsorbed into the PB structure due to the slightly smaller hydrated ion radius of Cs^+ compared to the channel radius of the PB lattice [1]. Therefore, Cs^+ can penetrate the inner side of the PB lattice and is strongly intercalated. Because of these unique structural features, PB and PB analogs (PBAs) are widely used as Cs^+ adsorbents. In addition, PB and PBAs have been used for sensing alkali cations [2], hydrogen peroxide [3], glucose [4], ascorbic acid [5], and pH [6,7]. A number of studies have been published regarding detection methods of glucose and hydrogen peroxide using PB or PBAs as an electrode material. In these reports, the target molecules were detected based on the redox reactions of PB or PBAs. Moreover, pH and ascorbic acid could be optically detected by the color change of PB. Although PB selectively adsorbs Cs^+, reports on the application of PB to Cs^+ sensing are scarce, with the exception of electrochemical detection method [8].

Considering the selective adsorption of Cs^+ by PB, the following characteristic behavior was observed. When adsorption experiments of Cs^+ on PB-CF were performed under basic conditions, the color of PB changed in response to Cs^+. In the presence of Cs^+, the color of PB remained stable, whereas, in the absence of Cs^+, the color changed from dark blue to brown due to the formation of iron hydroxide. Previously, it has been reported that the presence of Cs^+ suppresses the elution of iron from PB [9]. According to this report, when Cs^+ is adsorbed by PB, the elution of iron from PB is suppressed with higher Cs^+ concentrations. However, this phenomenon

remains somewhat unclear. In this study, the decomposition behavior of PB in the presence of Cs^+ was examined in detail. In addition, a simple detection method for Cs^+ using this phenomenon was developed.

4.2. Materials and methods

4.2.1. Materials

Iron(III) chloride hexahydrate and potassium hexacyanoferrate(II) trihydrate used for the preparation of PB were purchased from Wako Pure Chemical Industries, Ltd. (Osaka, Japan) and Kanto Chemical Co., Inc. (Tokyo, Japan), respectively. The cesium standard solution (1000 mg L^{-1}), ammonium standard solution (1000 mg L^{-1}), and 0.01 mol/L sodium hydroxide were purchased from Junsei Chemical Co., Ltd. Cesium chloride, potassium chloride, sodium chloride, ammonium chloride, and calcium chloride were purchased from Wako Pure Chemical Industries, Ltd. All reagents were of analytical grade and used without further purification.

4.2.2. Preparation of colloidal Prussian blue solution

The PB colloidal solution was prepared by mixing $FeCl_3$ and $K_4[Fe(CN)_6]$ in equimolar concentration. The PB colloidal solution was stored at room temperature, and 2 mM of this solution was used for the colorimetric detection of Cs^+ after 2 days of storage.

4.2.3. Measuring color changes of the Prussian blue solution

4.2.3.1. Color change of PB solutions in the presence of several cations

The degradation and color change of PB solutions containing various cations were observed. First, 0.5 mL of the 2 mM PB solution was mixed with 10 mL each of 10 mM CsCl, KCl, NaCl, NH_4Cl, and $CaCl_2$ solutions. Subsequently, 0.5 mL of 0.01 M

NaOH was added to the prepared solutions (Fig. 1).

4.2.3.2. Decomposition of PB at different concentrations

First, 0.5 mL of 2, 5, and 10 mM PB solutions were added to 5 mL of a Cs^+ solution containing 1 mM NaOH. Subsequently, the color changes of mixtures were observed after 10 min (Fig. 2).

4.2.3.3. Decomposition of PB by NaOH

First, 0.5 mL of 2 mM PB solution was mixed with 10 mL of various Cs^+ solutions. Subsequently, 0.2 or 0.5 mL of 0.01 M NaOH solution was added to the mixtures and color changes of the mixtures were observed (Fig. 3).

4.2.3.4. Colorimetric detection of Cs^+ using PB and NaOH

Initially, 0.5 mL of 2 mM PB solution was added to 10 mL of Cs^+ solution and shaken for 60 min. Subsequently, 0.2 or 0.5 mL of 0.01 M NaOH solution was added to the mixture, and the absorbance of the solution was measured after 60 min using a UV-Vis spectrophotometer (V-550 and V-650DS, JASCO, Japan).

4.2.3.5. Decomposition of PB and colorimetric detection of NH_4^+

The decomposition of PB with NH_4^+ was carried out by the similar method to that for Cs^+. First, 0.5 mL of 2 mM PB solution was mixed with 10 mL of various NH_4^+ solutions. Subsequently, 0.2-0.5 mL of 0.01 M NaOH solution was added to the

mixtures and color changes of the mixtures were observed (Fig. 11–13).

Colorimetric detection was also carried out by a similar method to that for Cs^+. Initially, 0.5 mL of 2 mM PB solution was added to 10 mL of Cs^+ solution. Subsequently, 0.3 mL of 0.01 M NaOH solution was added to the mixture, and the absorbance of the solution was measured after 10 min using a UV-Vis spectrophotometer.

4.3. Results and discussion

4.3.1. Decomposition behavior of Prussian blue in the presence of cations

PB is known to decompose by the reaction of its constituent ferric ions and hydroxide ion under basic conditions [10,11]. The decomposition behavior of PB varies depending on its concentration and form. Upon adsorption of Cs^+, the amount of Fe eluted from PB decreases, especially for solutions containing a large amount of Cs^+ [9]. This behavior was not observed in the presence of other ions such as K^+, Na^+, and Ca^{2+}. The detailed decomposition behavior of PB under basic conditions in the presence of various cations (Cs^+, K^+, Na^+, NH_4^+, and Ca^{2+}) is shown in Fig. 1. As indicated by the color change of the solution, PB immediately decomposed in the presence of K^+, Na^+, and Ca^{2+} ions after the addition of NaOH. However, in the presence of NH_4^+, the blue color of PB was maintained for several tens of minutes, but finally decomposed. In contrast, in the presence of Cs^+, the PB solution retained its blue color even after 20 h, indicating that the PB structure was maintained only in the presence of Cs^+.

Based on these results, the colorimetric detection of Cs^+ was further investigated. A PB colloidal dispersion was prepared to simplify the treatment and observation of color changes. The decomposition of PB was largely suppressed with higher Cs^+ concentrations (Fig. 2). For the test with a 2 mM initial concentration of PB, color change was observed to depend on the concentration of Cs^+. On the other hand, for the 10 mM PB solution, color change could not be observed visually. After adsorption of Cs^+ in the 2 mM PB solution, 0.2 or 0.5 mL of 0.01 M NaOH solution

was added, and changes in the color as a function of time are shown in Fig. 3. The decomposition of PB was significantly dependent on the amount of NaOH added. Upon addition of 0.2 mL of 0.01 M NaOH, the blue color of the PB solution was maintained, and the degradation of the blue color was monitored in the presence of 0.1–5 ppm Cs^+. After adding 0.5 mL of 0.01 M NaOH, the blue color disappeared between 0.1 and 1 ppm Cs^+, but changed only gradually when the Cs^+ concentration was greater than 2 ppm.

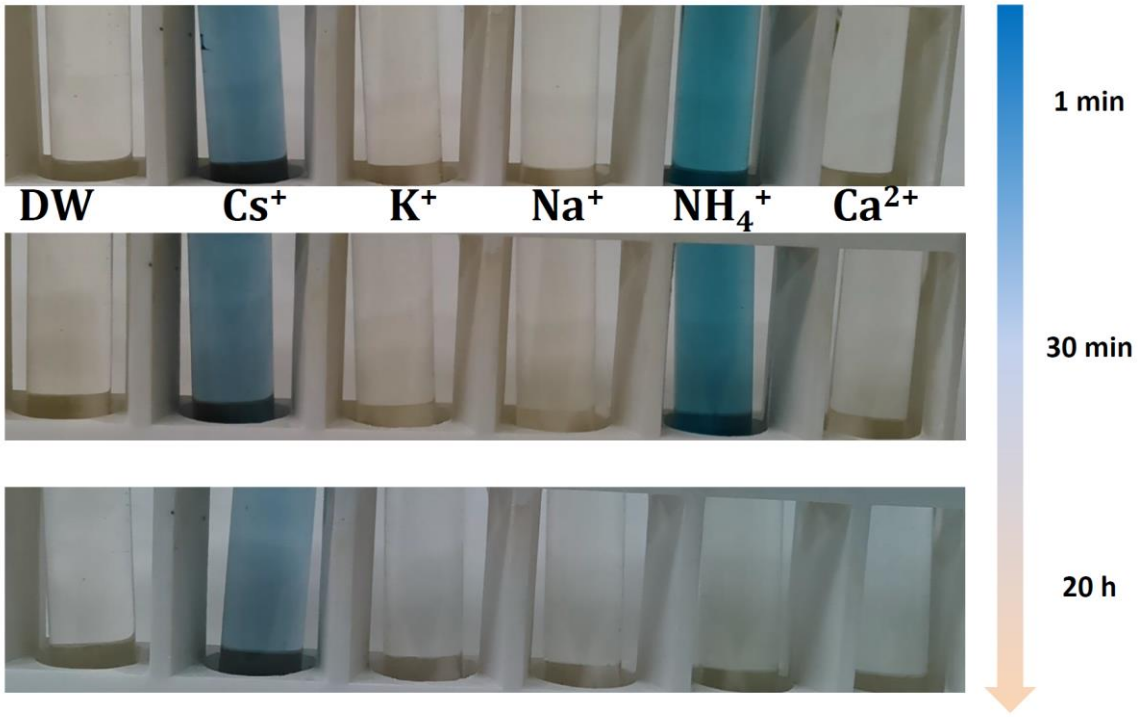

Fig. 1. Color changes upon decomposition of PB in the presence of various cations.

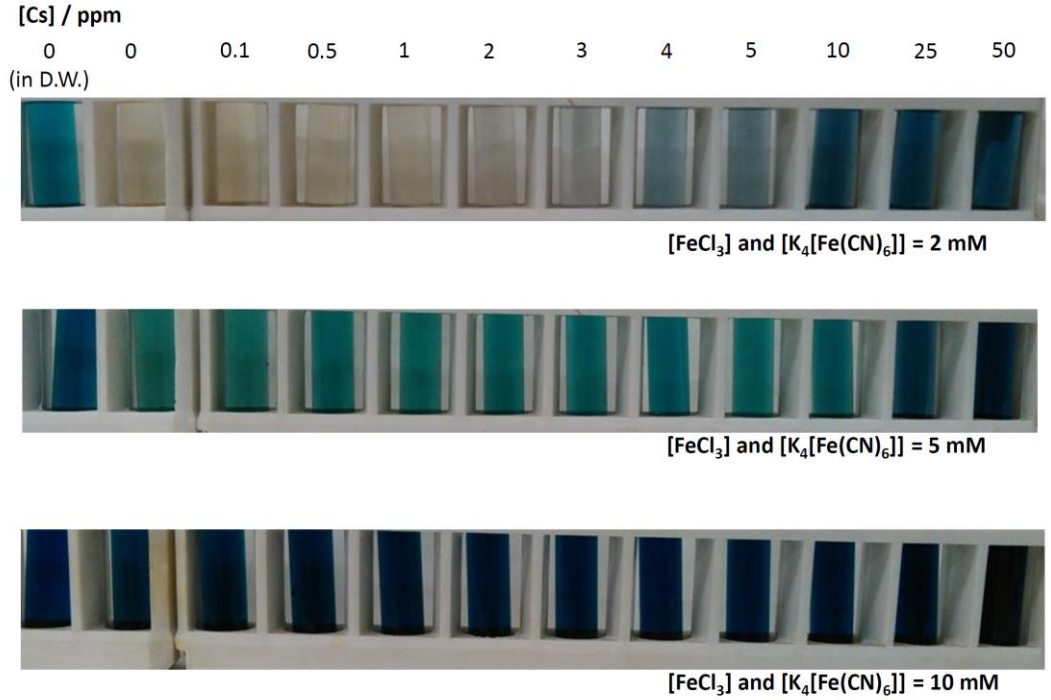

Fig. 2. Decomposition behavior of different concentrations of PB and Cs^+.

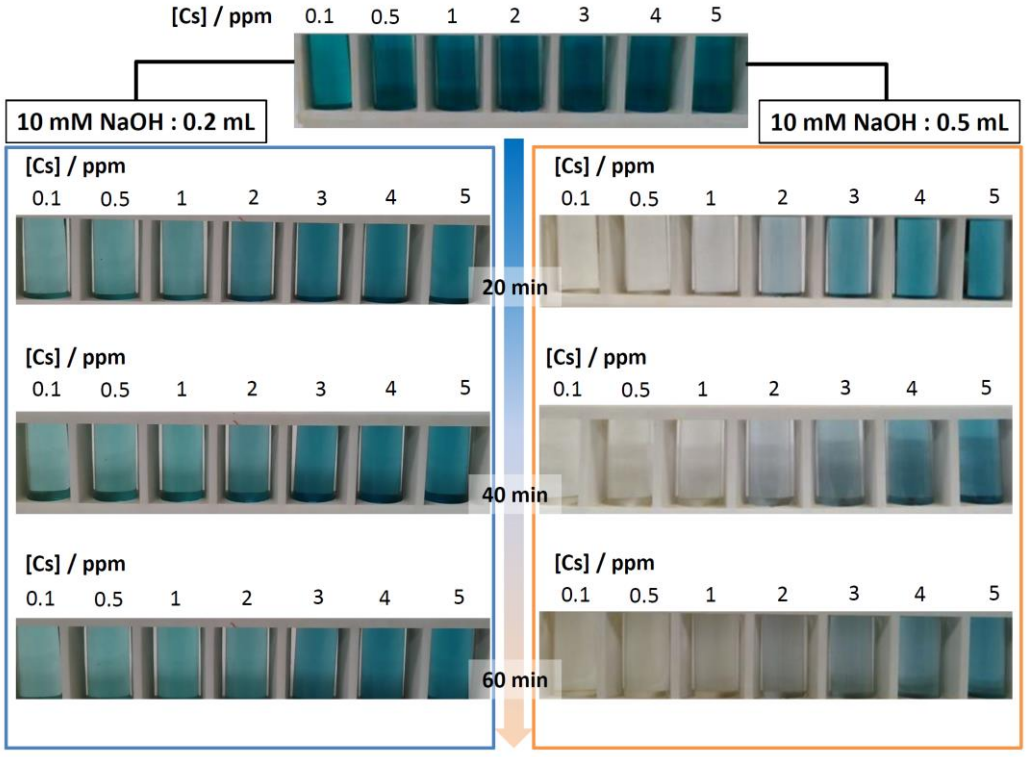

Fig. 3. Colorimetric response of PB decomposition in the presence of various Cs^+ concentrations.

4.3.2. Changes in the degradation behavior of PB

4.3.2.1. Effect of Cs^+ adsorption time on the absorbance of Prussian blue

The effect of adsorption time with Cs^+ on the decomposition behavior of PB was investigated (Fig. 4). First, 0.5 mL of 2 mM PB solution was added in 10 mL of Cs^+ solution. After the solution was left to certain period, 0.2 mL of 0.01 M NaOH was added, and then the maximum absorbance of the solution was measured. The decomposition behavior did not significantly change. Hence, it is likely that Cs^+ was rapidly adsorbed by PB, which stabilized the compound. The addition of 0.5 mL of 0.01 M NaOH yielded similar results, with a relatively constant maximum absorbance.

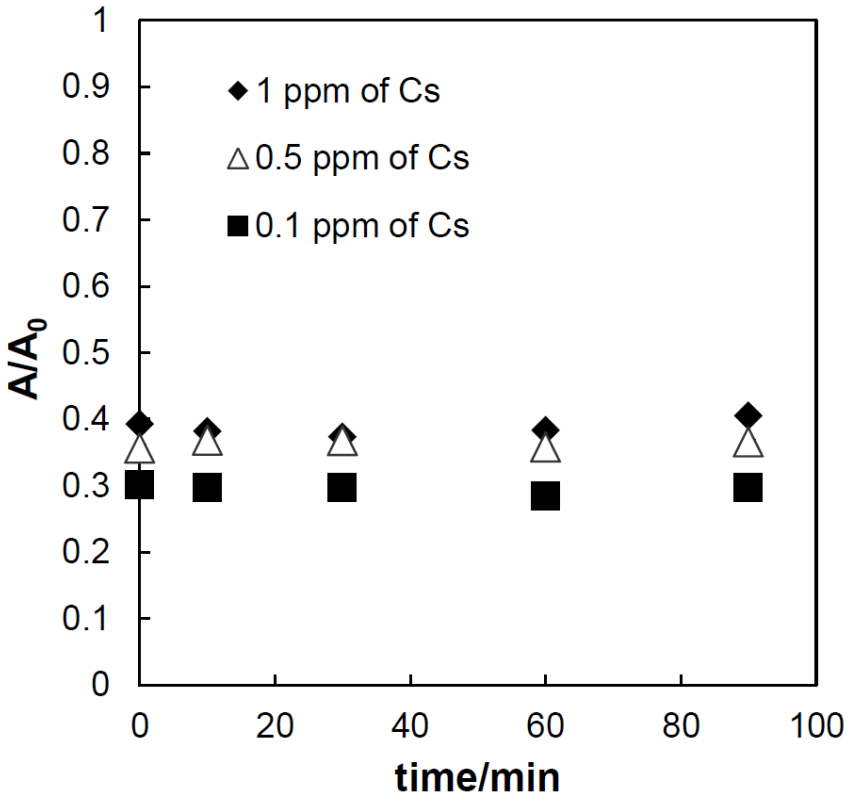

Fig. 4. Iinfluence of contact times of several concentrations of Cs^+ on the degradation of PB.

4.3.2.2 Changes in the maximum absorbance and absorption wavelength

The decomposition behavior of PB was monitored by adding 0.5 mL of 2 mM PB solution to 0.1–5 ppm of Cs^+ solutions with shaking for 60 min. After adding 0.2 mL of 0.01 M NaOH, the absorbance in the 500–800 nm range was measured at regular time intervals. As shown in Fig. 5, PB quickly decomposed in the presence of 0.1 ppm Cs^+, and the absorbance became constant after 10 min. The presence of 5 ppm of Cs^+ significantly suppressed PB decomposition. The maximum absorption wavelength at 0.1 and 1 ppm Cs^+ red-shifted as the decomposition reaction progressed (Fig. 5B). Ferric hydroxide was generated by the decomposition of PB, and it is likely that the shift in the maximum absorption wavelength was caused by the mixing of PB and ferric hydroxide colors. For a small amount of decomposed PB, the final color of the solution was bluish purple, indicating a shift to a shorter maximum absorption wavelength. With increasing amounts of decomposed PB, the color changes from blue to green, and subsequently from green to yellow. For incomplete decomposition of PB, the blue-green color was retained, indicating a shift to a longer maximum absorption wavelength and increasingly yellow color. For the 1 ppm Cs^+ solution, the maximum absorption wavelength initially shifted to a slightly shorter wavelength and then shifted again to a longer wavelength after 5 min. The color of the solution changed to blue-violet, following which PB gradually decomposed. This decomposition caused the color of the solution to change and the maximum absorption wavelength to shift to a longer wavelength. In the presence of 5 ppm Cs^+, the maximum absorption wavelength shifted to a shorter wavelength immediately after the addition of NaOH, reaching an

equilibrium maximum at approximately 673 nm. The peak was stable due to the slight decomposition of PB, which was not enough to change the blue coloration. Another reason may be the change of PB from “insoluble” PB to “soluble” PB. It is known that the maximum absorption wavelength shifts to shorter wavelengths with the conversion from “insoluble PB” to “soluble PB” [12]. The “insoluble” PB is represented by the structural formula $Fe_4[Fe(CN)_6]_3$, and “soluble” PB is represented as $KFe[Fe(CN)_6]$. When excess Fe is present, PB precipitated as the “insoluble” form. Conversely, “soluble” PB exists mainly as a colloidal dispersion when equimolar Fe^{3+} and $Fe(CN)_6^{4-}$ are mixed. The “insoluble” PB possesses lattice defect sites in its structure, whereas “soluble” PB adopts an ideal crystal lattice structure (Fig. 6). The precise control of the formation of a lattice defect site in PB is difficult. Therefore, the PB colloidal dispersion consists of both an ideal lattice structure and lattice defect sites. After adding NaOH, the Fe^{3+} near the lattice defect site reacted with OH^-, but OH^- attack of the ideal crystal lattice of PB may be prevented by the presence of Cs^+ in the lattice. Thus, it is likely that the PB lattice structure was changed by decomposition and the maximum absorption wavelength shifted to a shorter wavelength (Fig. 7).

The decomposition of PB upon addition of 0.5 mL of 0.01 M NaOH is shown in Fig. 8. The decomposition reaction proceeded to a greater extent compared to when 0.2 mL of the NaOH solution was added. The absorbance rapidly decreased and the solution color turned to light yellow in the 1 ppm Cs^+ solution. For the 5 and 10 ppm Cs^+ solutions, the absorbance decreased rapidly until 5 min, after which it decreased only gradually. The maximum absorption wavelength shifted to a shorter value after

the addition of NaOH. The peak shifts of 5 and 10 ppm Cs^+ solutions likely followed the same mechanism as when 0.2 mL of the NaOH solution was added to the 5 ppm Cs^+ solution. On the other hand, the peak of the 1 ppm Cs^+ solution completely disappeared due to the extensive decomposition of PB.

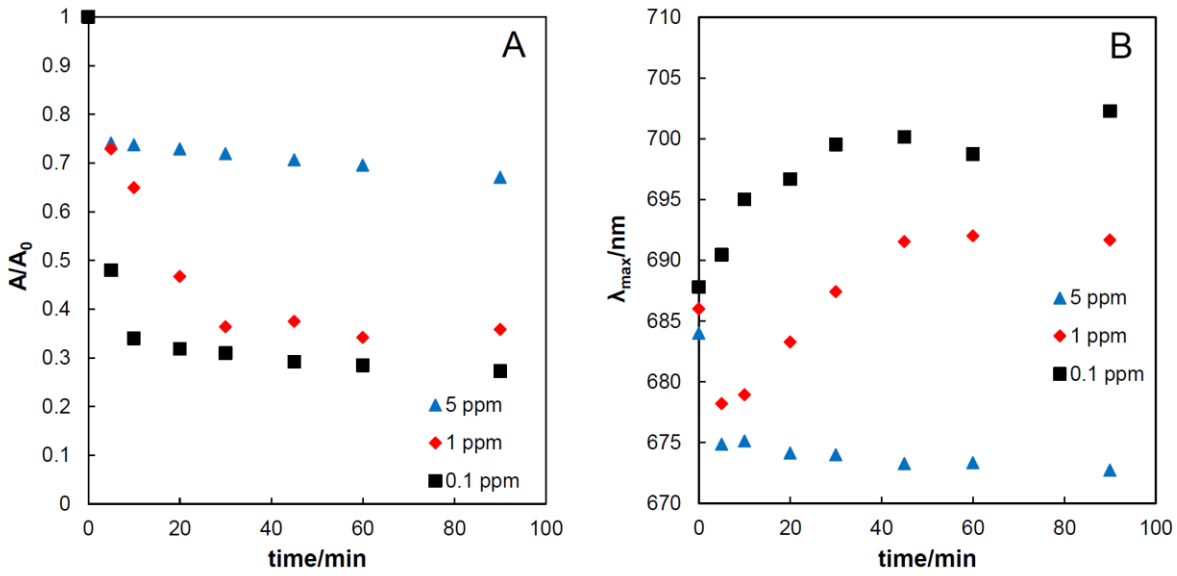

Fig. 5. Change of (A) maximum absorbance ratio, (B) maximum absorption wavelength, as a function of time after addition of 0.2 mL of 0.01 M NaOH in the presence of several Cs^+ concentrations.

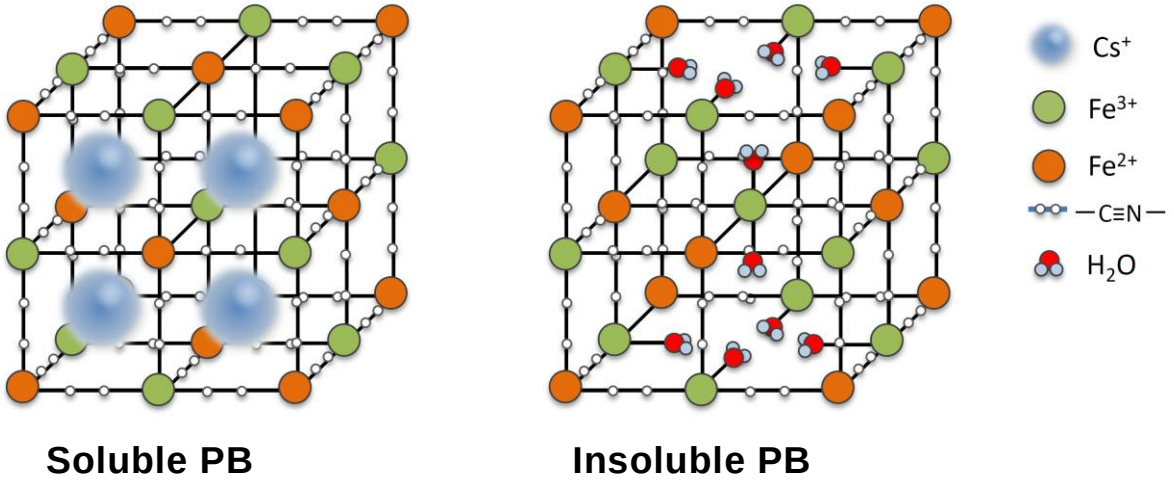

Fig. 6. Schematic of the “soluble” and “insoluble” PB crystal lattices.

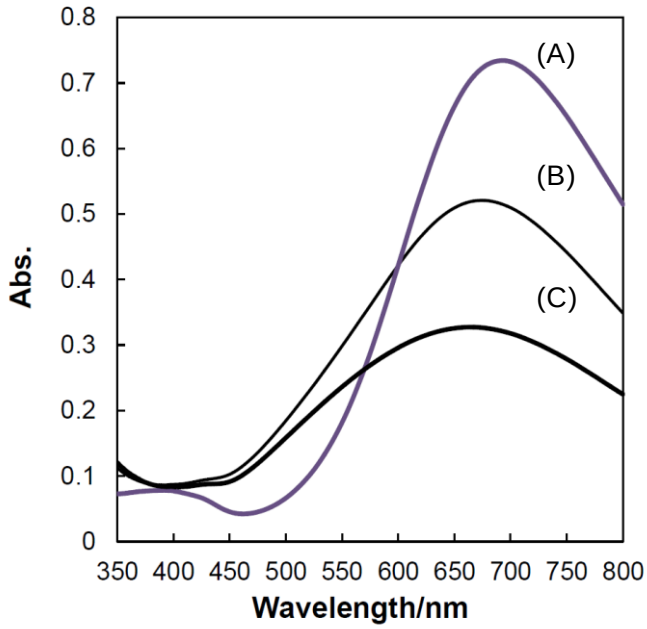

Fig. 7. Absorption spectrum of (A) 2 mM PB solution, (B) after the addition of 0.2 mL of 0.01 M NaOH in 5 ppm Cs^+, and (C) after addition of 0.5 mL of 0.01 M NaOH in 5 ppm Cs^+.

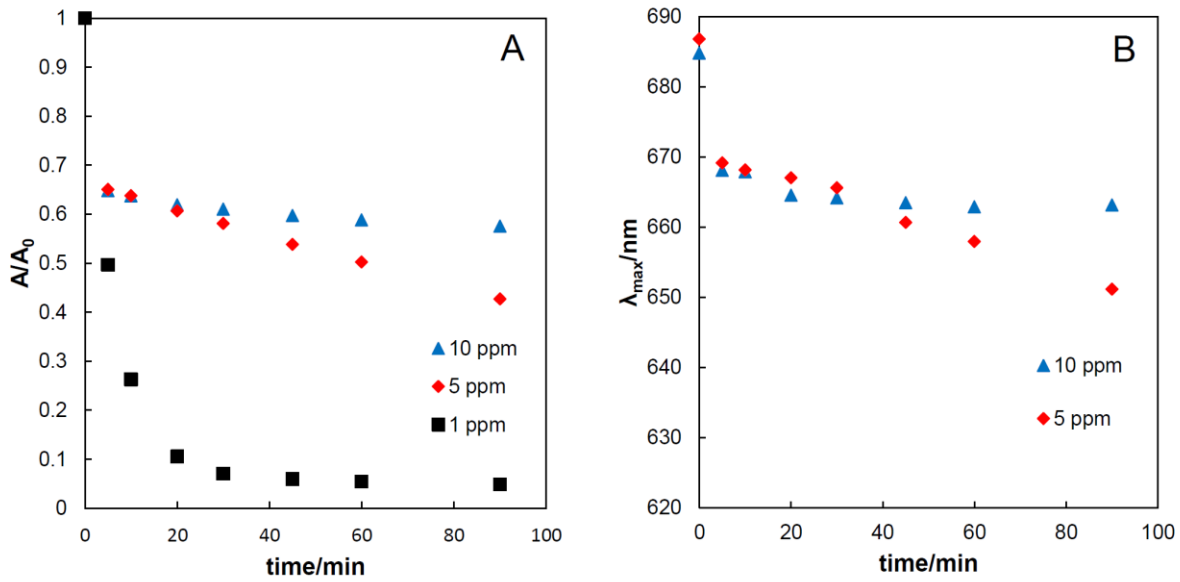

Fig. 8. Change of (A) maximum absorbance ratio, (B) maximum absorption wavelength as a function of time after the addition of 0.5 mL of 0.01 M NaOH at several Cs^+ concentrations.

4.3.3. Colorimetric detection of Cs^+ using a colloidal Prussian blue solution

The degradation behavior of PB in the presence of Cs^+ suggested that Cs^+ could be determined by the color change of PB. The linearity of the absorbance calibration curve, maximum absorption wavelength, and ratio of absorbance at two wavelengths (Abs_{676}/Abs_{700}) were compared. As shown in Fig. 9A, the absorbance and maximum absorption wavelength changed gradually with increasing Cs^+ concentration. The maximum absorbance wavelength was approximately constant when the concentration of Cs^+ was higher than 3 ppm (Fig. 9C). The maximum absorption wavelength changed when the Cs^+ concentration was less than 4 ppm and became nearly constant at approximately 675 nm (Fig. 9D). By considering the ratio of the maximum absorption wavelength before and after the peak shift, good linearity was

obtained from 0.01 to 1 ppm Cs^+ (Fig. 9B). The ratio of the absorbance at 676 and 700 nm in the low-concentration Cs^+ solutions showed the highest linearity. As shown in Fig. 3, this linearity is derived from the retention of the blue color of PB even with low Cs^+ concentrations. The absorption spectrum of PB when 0.5 mL of 10 mM NaOH solution was added is shown in Fig. 10. A large increase in absorbance at approximately 650 nm was observed at Cs^+ concentrations above 2 ppm. On the other hand, negligible changes in absorbance were observed at lower Cs^+ concentrations (less than 1 ppm, Fig. 10A). The maximum absorption wavelength was slightly red-shifted with increasing Cs^+ concentration, and poor linearity was observed due to the decomposition of PB (Fig. 10C and D). However, good linearity was observed in the change in the maximum absorbance in the range of 1–5 ppm Cs^+ (Fig. 10B). Based on the results presented herein, it is clear that the decomposition reaction of PB with OH^- was dependent on the concentrations of Cs^+ and OH^-.

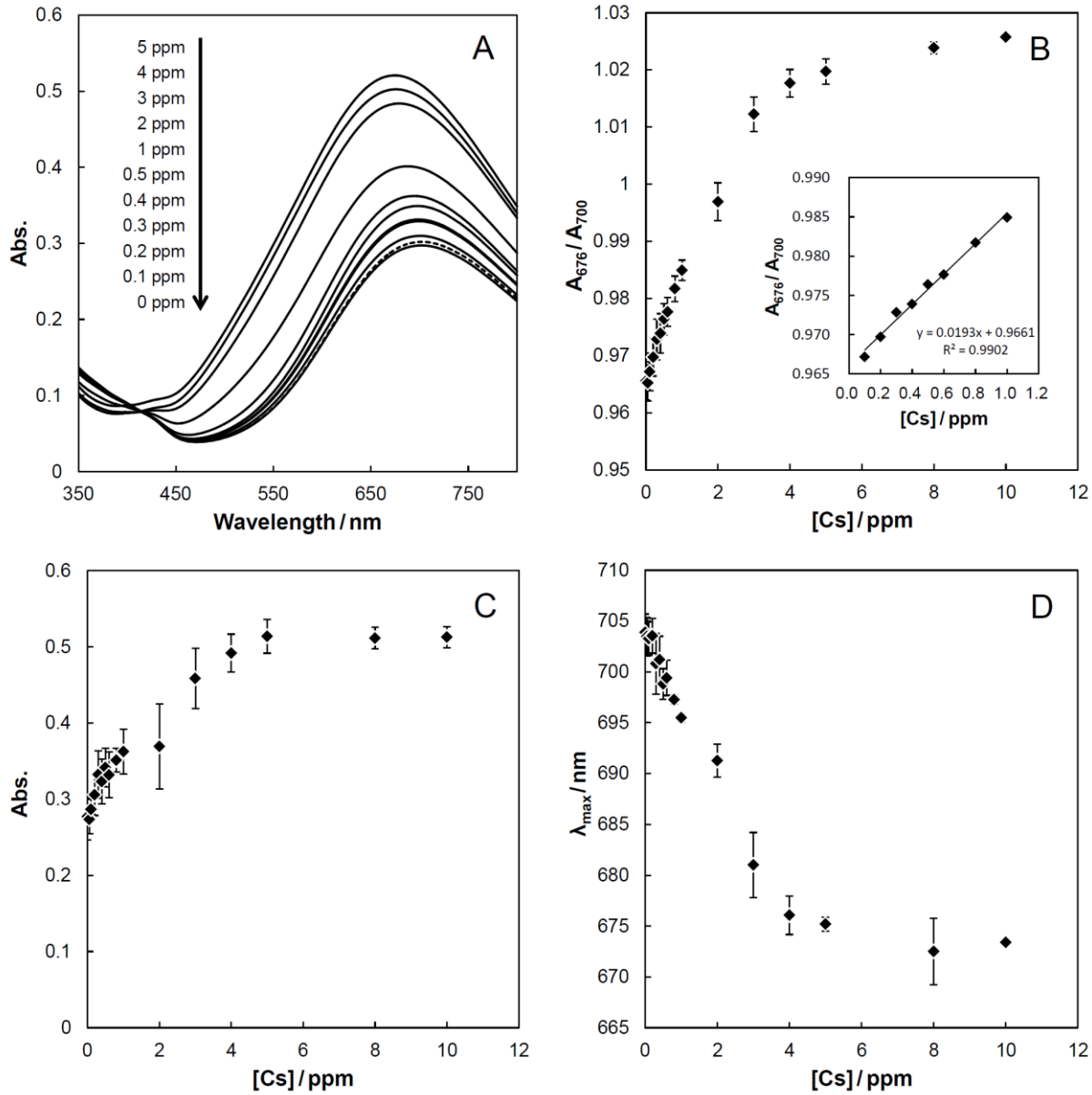

Fig. 9. (A) UV-Vis spectra, (B) ratio of the absorbance at 676 and 700 nm, (C) maximum absorbance, and (D) maximum absorption wavelength of the PB solution after the addition of 0.2 mL of 0.01 M NaOH in the presence of different concentration of Cs^{+}.

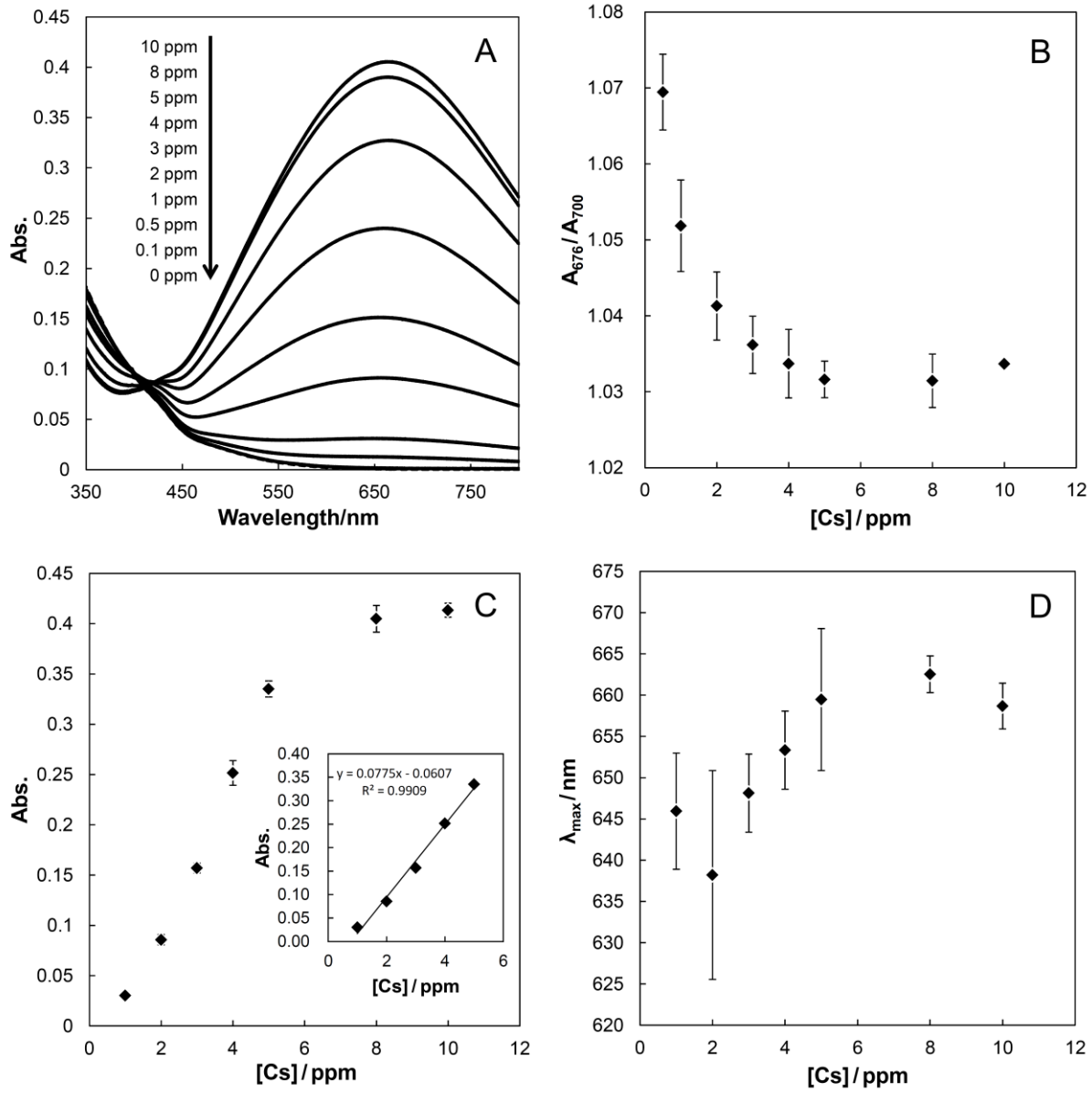

Fig. 10. (A) UV-Vis spectra, (B) ratio of the absorbance at 676 and 700 nm, (C) maximum absorbance, and (D) maximum absorption wavelength of the PB solution after the addition of 0.5 mL of 0.01 M NaOH in the presence of different concentration of Cs^+.

4.3.4. Colorimetric detection of NH_4^+ using a colloidal Prussian blue solution

Based on the investigation of the decomposition behavior of PB in the presence of Cs^+, the decomposition behavior of PB in the presence of NH_4^+ was similarly investigated. As shown in Fig. 1, NH_4^+ shows an effect for suppressing the decomposition of PB under basic conditions in a short time of about several tens minutes. Therefore, using the 0.2 to 10 ppm NH_4^+ solution, the decomposition behavior of PB was compared (Fig. 11–13). The suppression effect of PB decomposition by NH_4^+ was lower than Cs^+, and the decomposition of PB proceeded in a shorter time. Therefore, in other words, there is a possibility that it can be applied to the detection of NH_4^+ in a shorter time. When 0.5 mL of 10 mM NaOH was added, it was difficult to compare because PB was decomposed rapidly at a 5 ppm or less of NH_4^+ concentration. Similarly, when 0.2 mL of 10 mM NaOH was added, the color difference was very small, and then colorimetric detection is considered to be difficult. Therefore, 0.3 mL of 10 mM NaOH was added and absorption analysis was performed using the solution after 10 minutes. This result was shown in Fig. 14. Similarly to the case of Cs^+, the absorbance after 10 min was retained with the concentration of NH_4^+. In addition, the maximum absorption wavelength shifted to the shorter wavelength side. In the range of 0.2-3 ppm, the maximum absorption wavelength and absorbance showed a good linearity dependent on the concentration. On the other hand, although the concentration dependence was observed in the ratio of absorption wavelength (665 nm/700 nm), the linearity could not be obtained.

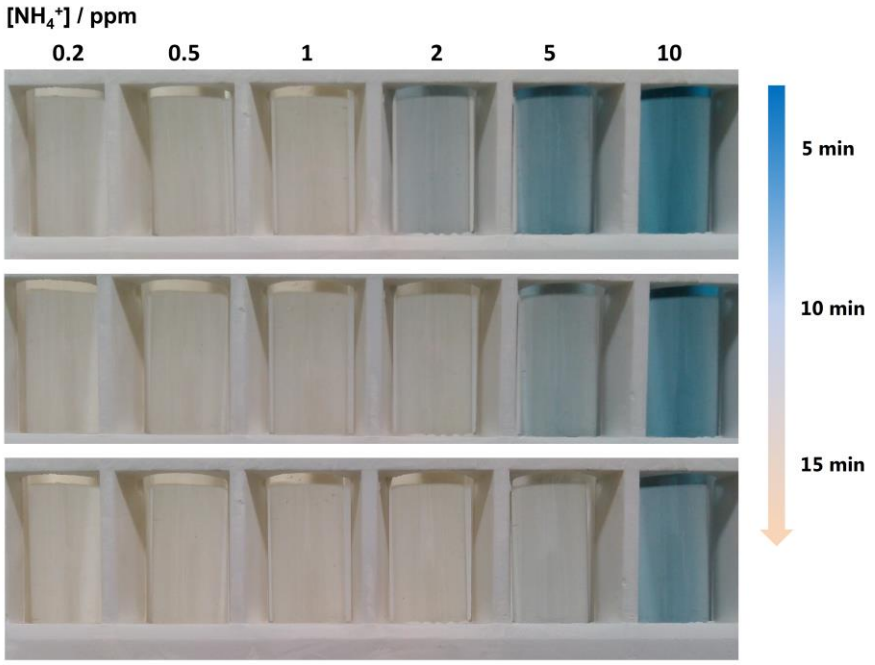

Fig. 11. Colorimetric response of PB decomposition after adding 0.5 mL of 10 mM NaOH in the presence of various NH_4^+ concentrations.

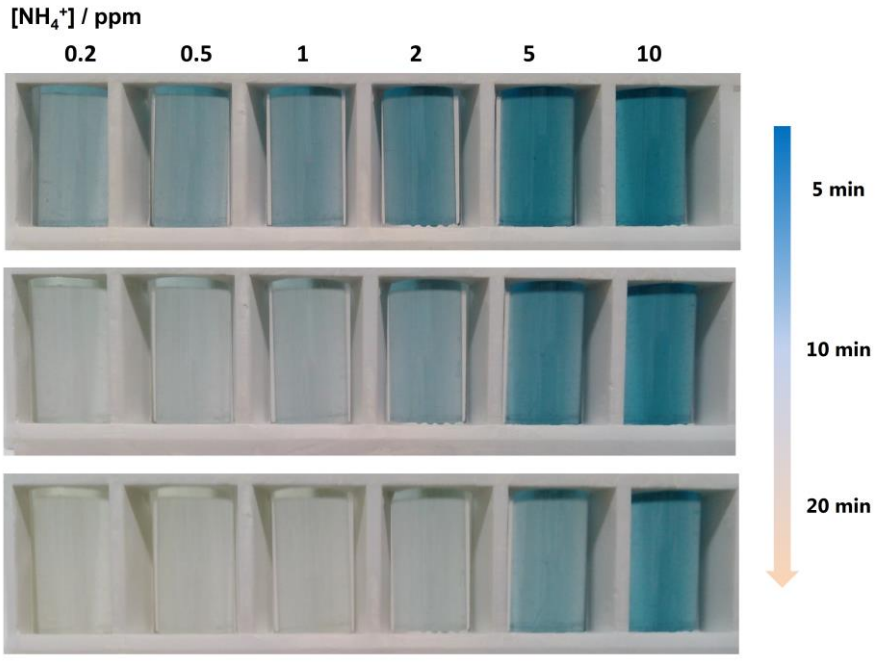

Fig. 12. Colorimetric response of PB decomposition after adding 0.3 mL of 10 mM NaOH in the presence of various NH_4^+ concentrations.

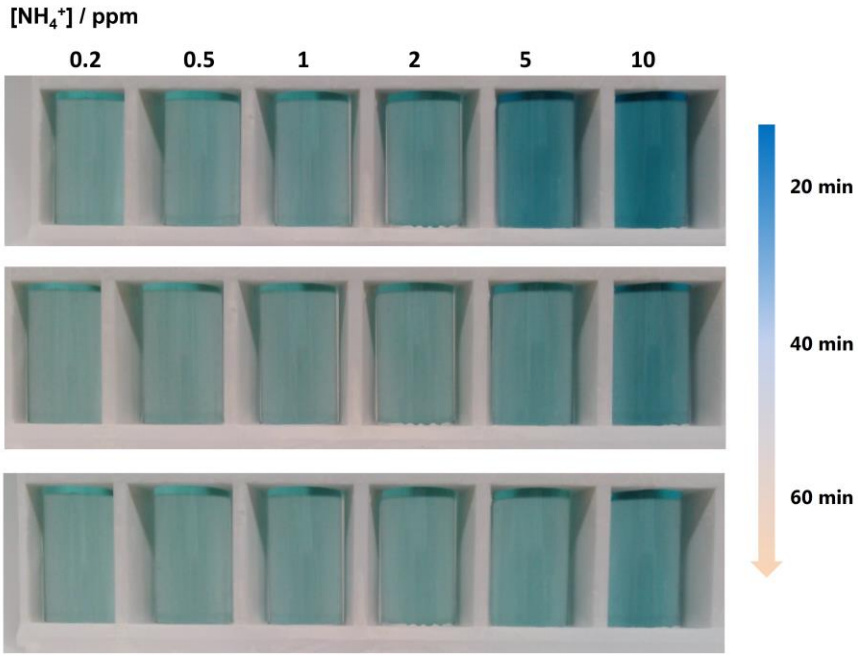

Fig. 13. Colorimetric response of PB decomposition after adding 0.2 mL of 10 mM NaOH in the presence of various NH_4^+ concentrations.

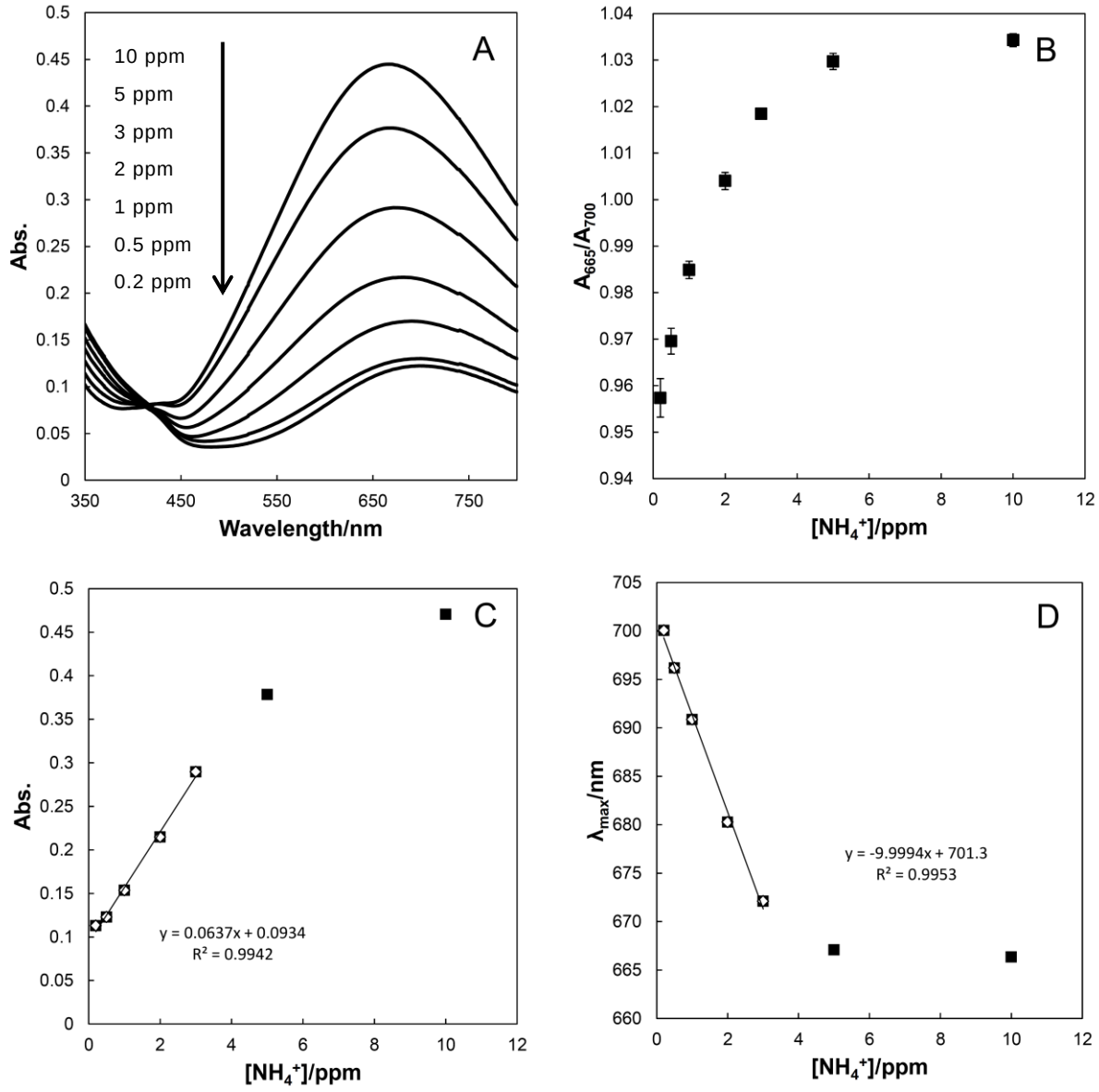

Fig. 14. (A) UV-Vis spectra, (B) ratio of the absorbance at 665 and 700 nm, (C) maximum absorbance, and (D) maximum absorption wavelength of the PB solution after the addition of 0.3 mL of 0.01 M NaOH in the presence of different concentration of NH_4^+.

4.4. Conclusion

In this study, colorimetric detection of Cs^+ was investigated using the suppression of PB decomposition in the presence of Cs^+. When a colloidal PB solution was added to Cs^+ solutions of various concentrations followed by the addition of 0.01 M NaOH, the color change associated with the decomposition of PB could be observed depending on the concentration of Cs^+.

The formation of ferric hydroxide due to the decomposition of PB caused a color change. Although there was no absorbance at 670–700 nm in the absence of Cs^+, the absorbance showed a linear increase with Cs^+ concentration. This indicates that the decomposition of PB was largely suppressed by Cs^+, and was highly dependent on the Cs^+ concentration. The maximum absorption wavelength was red-shifted due to the decomposition of PB.

From the quantification of Cs^+, good correlation was observed between the absorbance and the 676/700 nm absorbance ratio with Cs^+ concentration. Thus, Cs^+ can be detected by visual observation, and the approximate concentration of Cs^+ can be determined in the 0.5–5 ppm range. In addition, similar results were obtained for NH_4^+. It is suggested that the colorimetric detection in the concentration range of 0.2-10 ppm can be used for quantification of NH_4^+.

References

[1] E.R. Nightingale, Jr., Phenomenological theory of ion solvation. Effective radii of hydrated ions, *J. Phys. Chem.* 63 (1959) 1381–1387.

[2] A.A. Karyakin, Prussian Blue and its analogues: electrochemistry and analytical applications, *Electroanal.* 13 (2001) 813–819.

[3] A.A. Karyakin, O.V. Gitelmacher, E.E. Karyakina, Prussian Blue-based first-generation biosensor. A sensitive amperometric electrode for glucose, *Anal. Chem.* 67 (1995) 2419–2423.

[4] A.A. Karyakin, E.E. Karyakina, L. Gorton, Prussian-Blue based amperometric biosensors in flow-injection analysis, *Talanta*. 43 (1996) 1597–1606.

[5] S.S.L. Castro, V.R. Balbo, P.J.S. Barbeira, N.R. Stradiotto, Flow injection amperometric detection of ascorbic acid using a Prussian Blue film-modified electrode, *Talanta*. 55 (2001) 249–254.

[6] M. Yamada, N. Ohnishi, M. Watanabe, Prussian blue nanoparticles protected by the water-soluble π-conjugated polymer PEDOT-S: synthesis and multiple-color pH-sensing with a redox reaction, *Chem. Commun.* (2009) 7203–7205.

[7] R. Koncki, O.S. Wolfbeis, Composite film of Prussian Blue and N-substituted polypyrroles: fabrication and application to optical determination of pH, *Anal. Chem.* 70 (1998) 2544–2550.

[8] C.Y. Chang, L.K. Chau, W.P. Hu, C.Y. Wang, J.H Liao, Nickel hexacyanoferrate multilayers on functionalized mesoporous silica supports for selective sorption and sensing of cesium, *Micropor. Mesopor. Mater*. 109 (2008) 505–512.

[9] H. Hiraoka, D. Kamiya, Toagosei Co., Ltd., Japan (2013) Cesium adsorbent using iron ferrocyanide, annual studies of Toagosei group. 16 (2013) 31–36, Available at: http://www.toagosei.co.jp/develop/theses/detail/pdf/no16_05.pdf. (in Japanese) Accessed 23 November 2017.

[10] K. Itaya, N. Shoji, I. Uchida, Catalysis of the reduction of molecular oxygen to water at Prussian Blue modified electrodes, *J. Am. Chem. Soc.* 106 (1984) 3423–3429.

[11] R. Garjonyte, A. Malinauskas, Operational stability of amperometric hydrogen peroxide sensors, based on ferrous and copper hexacyanoferrates, *Sens. Actuators B*. 56 (1999) 93–97.

[12] R.J. Mortimer, D.R. Rosseinsky, Iron hexacyanoferrate films: Spectroelectrochemical distinction and electrodeposition sequence of ‘soluble’ (K^+-containing) and ‘insoluble’ (K^+-free) Prussian blue, and composition changes in polyelectrochromic switching, *J. Chem. Soc., Dalton Trans*. (1984) 2059–2061.

Chapter 5

General Conclusion

This thesis describes the preparation of a simple and practical adsorbent based on Prussian blue for the purpose of removing Cs^+ from water. The physical and chemical properties and adsorption ability were evaluated, and also a simple quantitative method for Cs^+ using the properties of PB was developed during this study.

In Chapter 2, PB was immobilized on CF by the electrochemical synthesis, and the control of the modification and the Cs^+ adsorption behavior were investigated. The method of synthesizing PB by applying a constant potential in mixed solution of Fe^{3+} and $[Fe(CN)_6]^{3-}$ is widely used. However, most of them are mainly used for biosensors, and not for development of the adsorbents. Therefore, PB was immobilized on CF for the preparation of the selective adsorbent for Cs^+. The morphology and amount of modified PB could be controlled by the applied potential and modification time. The lower limit of the potential for the stable immobilization of PB is 0.35 V, and it is located around the oxidation peak of $[Fe(CN)_6]^{4-/3-}$. At this time, PB immobilized on the CF surface showed the structure like a beadwork. On the other hand, when the modification potential was 0.5 V or 0.6 V, an island-like thin layer was formed on the surface of CF. In addition, a gradual increasing in film thickness was observed depending on the application time at the modification potential. The adsorption performance of Cs^+ was investigated using the prepared PB-CF. As a result, well adsorption of Cs^+ to PB-CF by immobilization at 0.35 V was achieved even under basic conditions of pH 11. This suggested that electrochemical prepared PB-CF can be applied to the removal of Cs^+ and is useful as an adsorbent over a wide pH range

including basic conditions.

In Chapter 3, the adsorption performance of Cs^+ was examined in more detail by using PB-CF prepared in Chapter 2. All of PB-CFs prepared by three potential of 0.35 V, 0.5 V and 0.6 V showed Cs^+ adsorption ability. In particular, PB-CF modified by 0.35 V had the thick film and showed the largest adsorption capacity among the three types of PB-CF. The maximum adsorption capacity of the PB-CF was 7.44 mg/g. For the surface of this PB-CF, coating with polyaniline was attempted for further improvement of the stability. There was no significant change in the adsorption performance of coated PAn-PB-CF for Cs^+ and in its stability for pH. The improvement of the stability against oxalic acid having the property of dispersing PB particle was confirmed. For the removal of Cs^+ from fly ash and soil, oxalic acid was often used as eluate. The PAn-PB-CF adsorbed Cs^+ well even in the 0.01 M oxalic acid solution. From these results, the application of PAn-PB-CF to the Cs^+ removal in the presence of oxalic acid was suggested. And the applicability of this adsorbent to a wide range of environments has been demonstrated.

Cs^+ has a high affinity with PB compared with other alkali metal ions and binds tightly inside the lattice of PB. Some evidences that PB seems to stabilize by Cs^+ adsorption have been confirmed during the experiment. In Chapter 4, a colorimetric detection of Cs^+ using this behavior of PB was developed. PB exists as a soluble form in the equimolar mixture of ferric ion and ferrocyanide. In the absence of Cs^+, PB decomposed immediately by addition of the alkaline solution, while the suppression of decomposition of PB was confirmed in the presence of Cs^+. The decomposition

behavior depended on the concentration of Cs^+, clear color change due to the decomposition of PB was observed visually according to the Cs^+ concentration. The absorbance, the waveform of the absorption spectrum, and the maximum absorption wavelength also changed corresponding to the Cs^+ concentration. Since the decomposition reaction of PB would be controlled by the amount of added NaOH, we can choose the adequate quantitative range. From the correlation between Cs^+ concentration and absorbance or maximum absorption wavelength, it was possible to visually detect the Cs^+ concentration in the range of about 1 to 5 ppm and 0.1 ppm to 1 ppm by using UV-vis spectrometer.

The conclusion obtained by this study is as follows. Firstly, PB immobilized CF could be prepared by a simple preparation method by controlling the potential and time in a mixed solution of ferric ion and ferricyanide. By this method, PB could be efficiently deposited and applied as an adsorbent for Cs^+. The second, the Cs^+ adsorption ability and the stability of PB-CF in the basic pH region was improved by the layer form of PB. Third, the electrically polyaniline coating on PB-CF improved the stability even in the presence of oxalic acid. It was concluded that polyaniline coating on PB surface could block the attack of low molecular weight compounds such as oxalic acid. Fourthly, the coating of polyaniline makes it possible to suppress the desorption of ferrocyanide ions generated by PB decomposition under basic conditions. By this property, it is thought that secondary contamination during Cs^+ adsorption using PB-CF can be reduced. Finally, using the behavior of PB confirmed during the development of these adsorbents, a colorimetric detection method of Cs^+ using PB

colloidal solution was developed. It would be greatly believed that the findings obtained in this study could serve as the knowledge for the development of effective adsorbents for Cs^+ and the establishment of new detection method for Cs^+.

Acknowledgments

The present thesis is the summary of the author's study from 2013 to 2018 at the Division of Material Science, Graduate School of Environmental Science, Hokkaido University.

I would like to express my grateful heartfelt gratitude to Prof. Shunitz Tanaka for his long-term support and for enormous help throughout my study. I would also like to express my grateful acknowledgement to Prof. Sakairi (Division of Material Science, Graduate School of Environmental Science, Hokkaido University) and Prof. Yagi (Division of Material Science, Graduate School of Environmental Science, Hokkaido University) for provided helpful comments and valuable suggestions. I am deeply grateful to Dr. Sasaki (Faculty of Pharmaceutical Sciences, Health Sciences University of Hokkaido) who provided helpful comments and suggestions. My deep gratitude goes to Prof. Kan (Hokkaido University of Education Sapporo) and Prof. Taguchi (Hokkaido University of Education Sapporo) for their continuing support.

Finally, I would like to express my gratitude to my mother for their moral support and warm encouragement.